Inauguraldissertation

submitted to the

Combined Faculties of Natural Sciences and for Mathematics

of the

Ruperto-Carola University of Heidelberg, Germany

for the degreee of

Doctor of Natural Sciences

Presented by

Diplom-Biologe Marc August Willaredt

born in Emmendingen, Germany

Day of oral examination: _____

Analsysis of the ENU-generated mouse mutant *cbs*: Primary cilia play a crucial role in cortical development

Referees
Prof. Dr. Thomas Holstein
PD Dr. Dr. Ralph Nawrotzki

Acknowledgements

This PhD thesis was undertaken in the lab of PD Dr. Kerry L. Tucker within the Interdisciplinary Center for Neuroscience (IZN) at the Institute of Anatomy and Cell Biology at the University of Heidelberg, Germany. The project belonged to the Teilprojekt B7 of the Sonderforschungsbereich 488 of the German Research Foundation (DFG) “Molecular and cellular bases of neural development”.

I would like to thank PD Dr. Kerry L. Tucker for giving me the possibility to join his research group and providing the interesting and challenging project. He always supported and motivated me in my ongoing work with valuable advice and lively discussions. I had in his lab the opportunity to work independently and to acquire a broad range of methods. I want also to thank Prof. Dr. Thomas Holstein for being my first referee, for his helpful feedback and to make it possible for me to conduct my thesis.

I want also to thank PD Dr. Dr. Ralph Nawrotzki for being my second referee. He had always an open ear for my questions and for his input to my project.

My thanks to all the people of the whole department for support, advice and protocols whenever I needed them. I will miss the kind and friendly atmosphere of the fourth floor.

Special thanks to Prof. Dr. Karin Gorgas, to whom I am very grateful for sharing her vast knowledge of anatomy and methods with me. A special thank also to Xiao-Rui, the best HiWi ever; his tireless assignment was always a great help for me. I would also like to thank Barbara for office equipment, candies and funny and serious conversations. Many thanks to Ingeborg, Michaela, Claudia, Inge, Gabie and Andrea for protcols, advice, talks and everything else. They made life in the lab thus much easier.

Many, many thanks to my parents, my sister and her husband and all my friends for love, sympathy, constant support and for standing by my side during my whole life! Without you, this thesis would have never had a chance to be completed.

Summary

I analysed in the following study the mouse mutant *cobblestone (cbs)* concerning the development of the forebrain. The *cbs* mutation was uncovered by an ethyl-nitroso-urea (ENU) genetic screen, using a mouseline called *tauGFP* was used for the screen, which e expresses the green fluorescent protein (GFP) under the promotor of the microtubule binding protein Tau The Tau protein is specific for the nervous system (NS) and thus the whole developing NS can be visualized by using ultraviolet (UV) light.

….When I started analyzing the cbs mutation, the phenotype of the cbs/cbs mouse mutant was already known, but because of the mutagenic ability of ENU, which causes random mutations, the affected gene was unclear. By applying the method of positional cloning I was able to achieve the identification of intraflagellar transport 88 (Ift88) as the candidate gene.

At the same time the observed phenotypes exhibited in the forebrain of *cbs/cbs* mutant embryos were further characterized by histological analysis. The pronounced disorganization of the dorsal telencephalon of *cbs/cbs* mutant embryos was at first investigated and anatomically described on the basis of hematoxylin-stained coronal sections. A detailed analysis by *in situ* hybridization (ISH) was followed, using different markers, which are specific for various areas of the developing telencephalon such as *Ttr1* for the choroid plexus, *Wnt2b* for the cortical hem, as well as *EphB1* and *Lhx2* for the hippocampal anlage. Furthermore both the dorsal-ventral and rostral-caudal compartmental boundaries of the forebrain were investigated by ISH.

Towards the identification of *Ift88* as the candidate gene, a detailed analysis of mRNA levels of Ift88 in the *cbs/cbs* mutant was undertaken by Northen Blot analysis as well as quantitative real-time RT-PCR. At the same time the Ift88 protein levels were also investigated by Western blot analysis. A complementation analysis by crossing *cbs* heterozygotes to mice heterozygous for a targeted deletion of the *Ift88* gene ($Ift88^{tm1.1Bky}$) (Haycraft *et al*., 2007) was done to ascertain, if the genetic defect in the *cbs/cbs* mutant is located in the *Ift88* gene.

Primary cilia, microtubule-based organelles that protrude from the surface of most cells of the vertebrate body, are dependent on Ift88 for their formation and maintenance. Because of this the ultrastructure of primary cilia was simultaneously investigated by transmission and scanning electron microscopy.

It is well established that cilia are important for the proper function of the Hedgehog (Hh) signalling pathway and are also supposed to be involved in the Wingless/Integrated (Wnt) signalling pathway. An examination of the Wnt signalling pathway in cbs/cbs mutant embryos was performed through a histological as well as a quantitative real time RT-PCR analysis of its target genes. A similar approach was undertaken for the Hh signalling pathway. Additionally,mRNA and protein levels of Gli3, the main mediator of the Hh pathway, were also determined. In a final step it was tested whether cells in the cbs/cbs mutant embryos loose their competence to respond to Hh signalling by a Luciferase assay.

Summary

… In the represented study I could ascertain that cbs is a hypomorphic allele of the gene Ift88, in which both Ift88 mRNA and protein levels are reduced by 70% to 80%, respectively. cbs/cbs mutants display defects in the formation of dorsomedial telencephalic structures, such as the choroid plexus, cortical hem and hippocampus. Furthermore mutants exhibit a relaxation of both dorsal-ventral and rostral-caudal compartmental boundaries of the forebrain, resulting in the intermixture of otherwise separated cell populations. I further demonstrate in that the proteolytic processing of Gli3 is reduced in the cbs/cbs mutant, leading to an accumulation of the full-length activator isoform. In addition the cbs/cbs mutant exhibits an upregulation of canonical Wnt signalling in the neocortex and in the caudal forebrain. The ultrastructure and morphology of cilia of the ventricle of the cbs/cbs mutants are still intact

Taken together, these results indicate a fundamental role for primary cilia in the development of the forebrain.

Zusammenfassung

In der vorliegenden Studie wurde dieMausmutante *cobblestone* (*cbs*) von mir in ihrer Wirkung auf die Entwicklung des Vorderhirns analysiert. Die *cbs* Mutation ist im Rahmen eines Ethyl-Nitroso-Urea (ENU) Screens entdeckt worden. Für den Screen wurde eine Mauslinie namens *tauGFP* verwendet, welche das grün fluoreszierende Protein (GFP) unter dem Promotor des Mikrotubuli bindenden Proteins Tau exprimiert. Da das Tau Protein für Nervenzellen spezifisch ist, kann somit das gesamte sich entwickelnde Nervensystem unter ultraviolettem (UV) Licht sichtbar gemacht werden.

Als ich mit meiner Analyse der *cbs* Mutation begann, war der Phenotyp der *cbs/cbs* Mutante zwar schon bekannt, aber auf Grund der mutagenen Eigenschaften von ENU, das zufällige Mutationen verursacht, war das betroffene Gen noch unbekannt. Mittels Positional Cloning war ich in der Lage, *Intraflagellär Transport 88* (*Ift88*) als Kandidatengen zu identifizieren.

Gleichzeitig wurde der beobachtete Phenotyp, der im Vorderhirn von *cbs/cbs* mutanten Embryonen zu erkennen ist, mittels histologischer Analyse weiter charakterisiert. Die auffällige Desorganisation des dorsalen Telencephalons der *cbs/cbs* mutanten Embryonen wurde zuerst an Hand von Hämotoxylin-gefärbten coronalen Schnitten untersucht und dann anatomisch beschrieben. Eine detailierte Analyse mittels *in situ* Hybridisierung (ISH) folgte, wobei verschiedene Marker, die spezifisch für die unterschiedlichen Areale des sich entwickelnden Telencephalons sind, verwendet, wie *Ttr1* für den Choroid Plexus, *Wnt2b* für den corticalen Saum, und *EphB1* und *Lhx2* für die hippocampale Anlage. Außerdem wurden sowohl die dorsal-ventralen als auch die rostral-caudalen Grenzen innerhalb des Vorderhirns mittels ISH untersucht.

Nach der Identifizierung von *Ift88* als Kandidatengen wurde eine detailierte Analyse der mRNA-Level von Ift88 in der *cbs/cbs* Mutante mittels Northen Blot Analyse und quantitative real-time RT-PCR unternommen. Zur gleichen Zeit wurden auch die Protein-Level von Ift88 mit Hilfe einer Western Blot Analyse untersucht. Außerdem wurde eine Komplementationsanalyse durchgeführt, indem heterozygote *cbs*-Mäuse mit Mäusen, die heterozygot für eine gezielte Deletion des *Ift88* Gens (*Ift88*$^{tm1.1Bky}$) (Haycraft *et al*., 2007) sind, gekreuzt wurden. Ziel war es, festzustellen, ob der genetische Defekt der *cbs/cbs* Mutante im *Ift88* Gen lokalisiert ist.

Primäre Zilien sind Mikrotubuli enthaltende Zellfortsätze, die an der Oberfläche der meisten Zelltypen bei Vertebraten vorkommen. Die Ausbildung und Aufrechterhaltung von Zilien ist von Ift88 abhängig. Aus diesem Grund wurde auch die Ultrastruktur von primären Zilien in der *cbs/cbs* Mutante mittels Transmissions- und Rasterelektronenmikroskopie untersucht.

Es ist bekannt, dass Zilien wichtig sind für das einwandfreie Funktionieren des Hedgehog (Hh) Signalweges, und es wird angenommen, dass sie auch am Wingless/Integrated (Wnt)- Signalweg beteiligt sind. Eine Untersuchung des Wnt- Signalweges in Embryos mutant für *cbs/cbs* wurde durchgeführt, indem eine histologische als auch eine quantitative real-time RT-PCR Analyse von Zielgenen des Wnt- Signalweges ausgeführt wurde. Mittels einer ähnlichen Herangehensweise wurde

auch der Hh- Signalweg analysiert. Zusätzlich wurden sowohl die mRNA- als auch die Proteinlevel von Gli3, der Hauptmediator des Hh- Signalweges, bestimmt. Abschließend wurde getestet durch einen Lciferase- Assay getestet, ob Zellen in der *cbs/cbs* Mutante ihre Kompetenz verlieren, auf Hh-Signal zu antworten.

… In dieser Studie ist es mir möglich gewesen festzustellen, dass cbs ein hypomorphes Allel des Gens *Ift88* ist, und dass sowohl die mRNA- als auch die Proteinlevel von Ift88 in der *cbs/cbs* Mutante um 70 bis 80% reduziert sind. *cbs/cbs* Mutanten weisen Defekte in der Ausbildung der dorsomedialen Strukturen des Telencephalons auf, darunter der Choroid Plexus, der corticale Saum und der zukünftige Hippocampus. Außerdem sind die Grenzen des dorso-ventralen als auch des rostro-caudalen Kompartements des Vorderhirns in der *cbs/cbs* Mutante aufgelockert, so dass dort eine Vermischung von ansonsten getrennten Zellpopulationen stattfindet. Ich zeige ebenfalls auf, dass die proteolytische Prozessierung von Gli3 in der *cbs/cbs* Mutante reduziert ist, was zu einer Anhäufung der unprozessierten Aktivator-Isoform von Gli3 zur Folge hat. Die *cbs/cbs* Mutante weist ebenfalls eine Hochregulierung des kanonischen Wnt- Signalweges im Neocortex und im caudalen Vorderhirn auf. Die Ultrastruktur und Morphologie der Zilien im Ventrikel der *cbs/cbs* Mutante sind noch intakt.

Zusammengefasst weisen die Resultate auf eine kritische Rolle der primären Zilien in der Entwicklung des Vorderhirns hin

Table of contents

1 Introduction

The nervous system is a network of specialized cells that control the actions and reactions of the body. Almost all animals have at least a rudimentary nervous system, but the vertebrates exhibit the most complex developed one. The nervous system of the vertebrates consists of the central (CNS) - and the peripheral (PNS) nervous system, and the central nervous system is subdivided into the brain and the spinal cord. A range of ganglia and nerves, which are part of the peripheral nervous system, are connected with the spinal cord. The functional components of the nervous system are neurons, glial cells and oligodendrocytes (Campell, 1997).

1.1 Induction of the nervous system

The nervous system becomes first visible during gastrulation when the ectoderm at the dorsal side of the embryo thickens and starts to unfold itself at the edges. This structure is called the neural plate (Smith and Schoenwolf, 1989; Keller et al., 1992). The vertebrate CNS originates from the neural plate (Saxen, 1989; Wilson and Edlund, 2001). The forebrain arises from the expanded anterior end of the neural plate during gastrulation (Rubenstein et al., 1998; Varga et al, 1999; Inoue et al, 2000; Whitlock and Westerfield, 2000).

The precursors of the telencephalon are located rostral and lateral to the future eye tissue, which itself is positioned rostral to the diencephalic anlage. This locates the anlage of the telencephalon at the margin of the anterior neural plate. This position it under the influence of signalling pathways that both are involved in the anterior-posterior (A-P) and dorsal-ventral (D-V) patterning of neural tissue. A two-signal model for neural induction proposed by Nieuwkoop (Nieuwkoop et al., 1954; reviewed and updated in Foley et al., 2000) suggests that neural tissue acquires an anterior identity by default (the induced neural tissue has already anterior (forebrain) character) , and that a “transforming” (posteriorizing) signal specifies more posterior neural fates (Fig. 1).

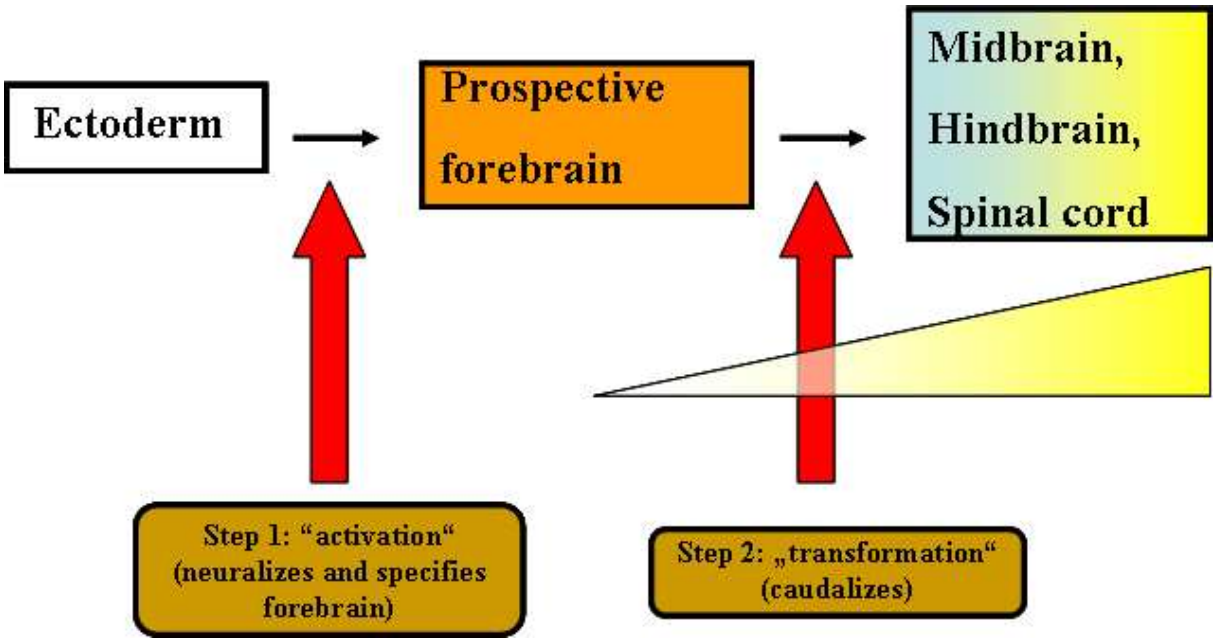

Fig. 1. Model defining the initial head-tail patterning of the embryo The "activation-transformation" model of Nieuwkoop. (Adapted from Stern et al., 2006).

1.1.1 Bmp antagonists and Fgfs assist neural development

Bone morphogenetic protein (Bmp) and fibroblast growth factor (Fgf) signalling are thought to be involved in the process of neural induction. High levels of Bmp activity in fish and frogs inhibits the anterior neural development and the abrogation of Bmp signalling assists neural specification (Munoz-Sanjuan and Brivanlou, 2002). Thus, Bmp signalling is an important negative regulator for neural induction (Reversade *et al*., 2005; Reversade and De Robertis, 2005) and a potent epidermalizing factor (Fig. 2). The organizer (Spemann´s organizer in frog, the shield in fish, and node in chick and mouse) and its early derivates (such as the prechordal mesoderm) is thought to be the origin of the Bmp signalling antagonists (Fig. 3). They include in *Xenopus noggin* (Zimmermann *et al*., 1996), *chordin* (Piccolo *et al*., 1996), *follistatin* (Fainsod *et al*., 1997) and *cerberus* (Bouwmeester *et al*., 1996). They can bind to the Bmp ligands in the extracellular space and prevent activation of the receptors. When they are applied to embryonic ectoderm, neural tissue forms instead of epidermis (Meinhardt, 2001; Vonica and Gumbiner, 2007), thus acting as neural inducers. Mouse mutants, in which the Bmp antagonists *chordin* (Bachiller *et al*., 2000), *noggin* (McMahon *et al*., 1998), or *cerberus* (Belo *et al*., 2000) are missing, are expressing only posterior neural genes, and double mutants for *noggin* and *chordin* don´t develop forebrain structures (Bachiller *et al*., 2000). This results indicate that a conserved and necessary role for Bmp inhibition for the induction of anterior neural tissue across vertebrates existes (Fig. 2).

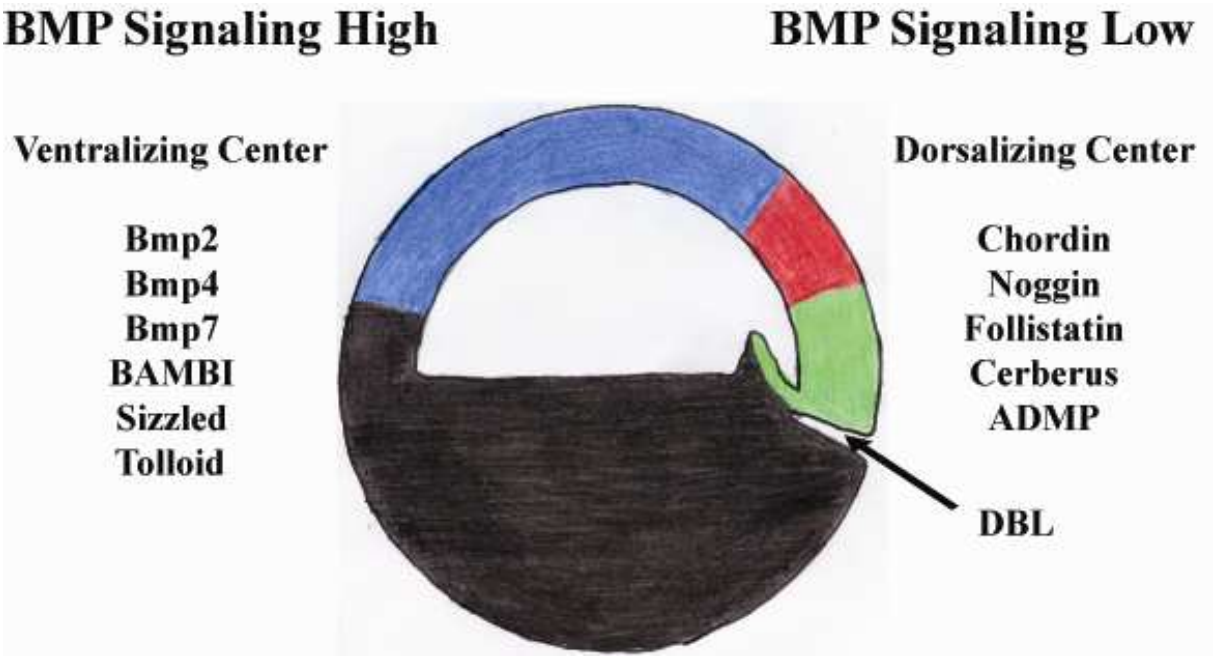

Fig. 2. Bmp signalling and its influence on the dorsal-ventral patterning of the ectoderm. Embryos exhibit a ventralizing center at the blastula stage, that maintains Bmp signalling, and a dorsalizing center, that initiates the formation of neural tissue by suppressing Bmp signalling. (Adapted from Squire *et al*., 2008).

The results from other studies imply that suppression of Bmp signalling alone is not sufficient to induce neural identity and that other signals such as Fgfs are also necessary (Linker and Stern, 2004; Delaune *et al*., 2005; Wawersik *et al*., 2005). The results lead to the idea that an initial Fgf signal is needed for neural induction before the inhibition of Bmp signalling can function as a neural stabilising event. Fgf signalling seems also to act as an inducer of posterior neural tissue (Hongo *et al*., 1999; Ishimura *et al*., 2000; Wilson *et al*., 2000; Wilson *et al*., 2001; Sheng *et al.*, 2003; Rentzsch *et al*., 2004) besides its role as a "priming" signal by suppressing Bmp signalling through the phosphorylation and inactivation of Smad1 (Schier, 2001; Pera *et al*., 2003) and thus reinforcing the antagonism of the Bmp pathway. The inhibition of the Wingless/Integrated (Wnt) signalling seems also to be important for neural induction (Heeg-Truesdell and Labonne, 2006; Wilson *et al*., 2001).

1.1.2 Protection of the anterior neural tissue from posteriorizing factors

To maintain the induced anterior neural character, the rostral located neural tissue must be insulated from posteriorizing factors, which is achieved by three mechanisms: 1) restricted expression of the posteriorizing factors; 2) restricted expression of antagonists of the posteriorizing factors; 3) morphogenetic movements that avoid that the anterior neural plate comes in contact with the posteriorizing factors.The anterior visceral endoderm (AVE) in mouse seems to be an important source of antiposteriorizing signals (Kimura *et al*., 2000; Perea-Gomez *et al*., 2001). The AVE is an extra-embryonic tissue, that moves rostrally from the distal tip of the blastula and underlies afterwards the anterior (prechordal) neural plate (Thomas *et al*.) (Fig. 3). Mutations in genes important for the

development of the AVE results in defects of the anterior neural plate including the telencephalon (Knoetgen *et al*., 1999; Perea-Gomez *et al*., 2000). The formation of the AVE is dependent upon the expression of *Nodal* in the epiblast (Brennan *et al*., 2001) (future neural plate), the outer layer of the blastula, which gives rise to the ectoderm after gastrulation. Further on during gastrulation the AVE is moved proximally (Thomas and Beddington, 1996). The ongoing patterning of the neuroectoderm is then transferred to the anterior streak derivates.

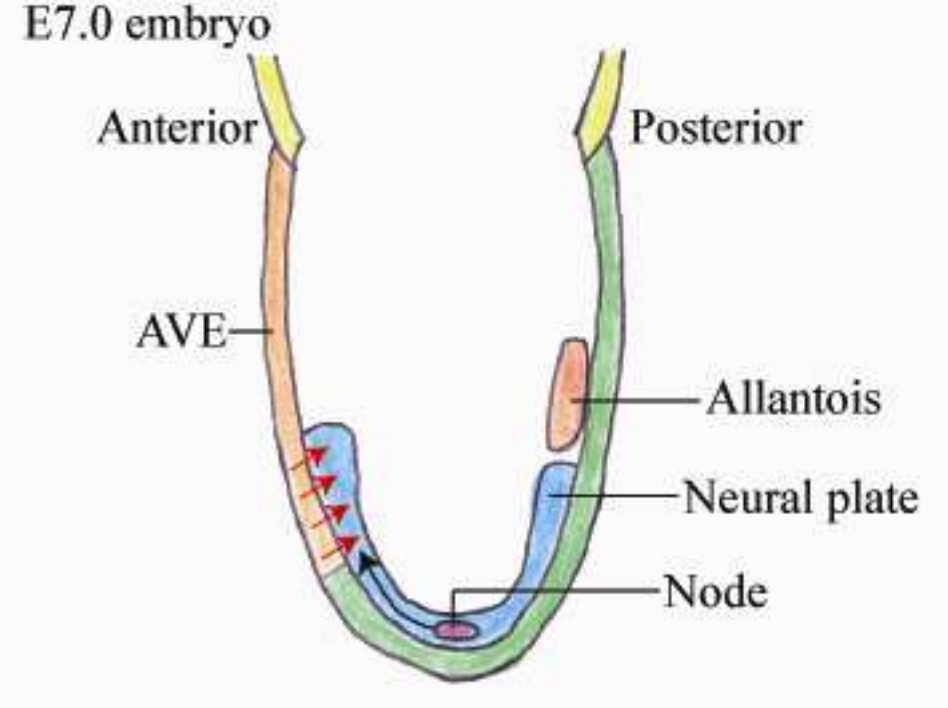

Fig. 3. The anterior visceral endoderm (AVE). Schematic drawing of a early head stage mouse embryo. The node is the source of signals that create an anterior pattern (black arrow). The anterior visceral endoderm and the node act together to initiate and/or maintain anterior character in the neural plate. The anterior visceral endoderm lies beneath the prospective neural plate and generates molecules such as Cerberus and dickkopf (red arrows), that suppress the function of posteriorizing factors and thus prevents the anterior neural plate to become posteriorized. The figure displays the end stage at which this signals are acting. (Adapted from Rallu *et al*., 2002).

Furthermore inhibition of Wnt signalling at the anterior end of the neural plate is necessary for normal formation of the prechordal plate (Niehrs, 1999; Kazanskaya *et al*., 2000) (Fig. 4). Dickkopf (Dkk1), a secreted antagonist of Wnt signalling, is necessary for the formation of the prechordal plate during gastrulation, and is later expressed in the anterior mesendoderm where it is required for the induction of telencephalic markers such as *Hesx1* (*homeobox gene expressed in ES cells*) and *Six3* (*sine oculis-related homeobox 3 homolog*) and is also required for dorosoventral patterning (Kazanskaya *et al*., 2000; Hashimoto *et al*., 2000; Mukhopadhyay *et al*., 2001). Mice mutant for *Dkk1* have no telencephalon and lack anterior cranial skeletal elements (Mukhopadhyay *et al*., 2001). It

seems to be that signals that promote forebrain development anatgonize or otherwise negatively regulate factors that would normally posteriorize the anterior neural plate.

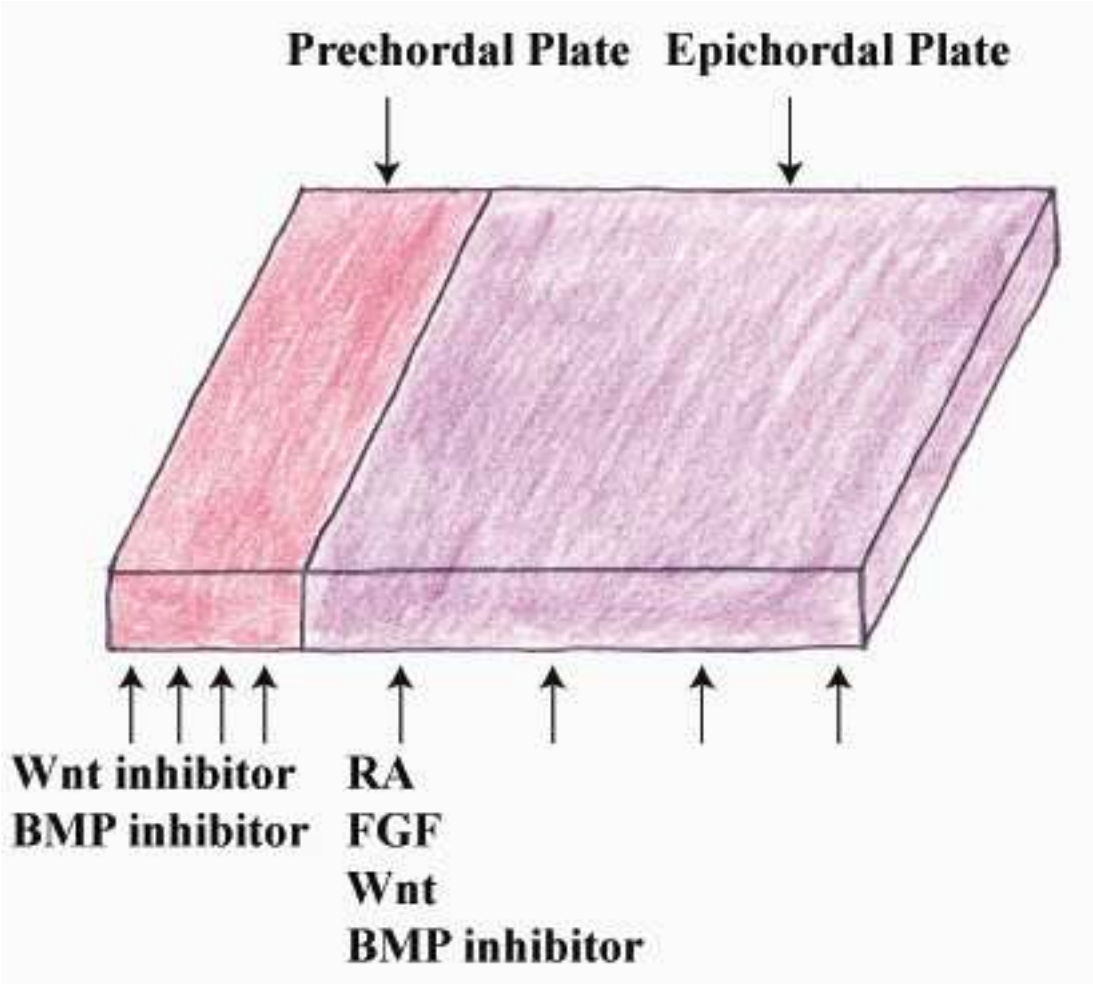

Fig. 4. Early A-P patterning in the vertebrate nervous system. Schematic drawing showing the signals that are presumed to divide the developing nervous system into a prechordal (anterior) and epichordal (posterior) neural plate. (Adapted from Squire *et al*., 2008).

Wnt, Fgf , Bmps, retinoic acid (RA) and Nodal family transforming growth factor β (TGFβ) proteins are proposed to be posteriorizing factors, and it is most likely the case that the combined activity of several signalling pathways is needed to create an early A-P pattern (Fig. 5A) (Kudoh et al., 2002; Haremaki et al., 2003). Taken together, the A-P pattern begins to develop within the embryo, and within the context of the developing A-P pattern, neural induction proceeds, and the anterior neural tissue protected from the effect of posteriorizing factors forms the future forebrain (Fig. 5B).

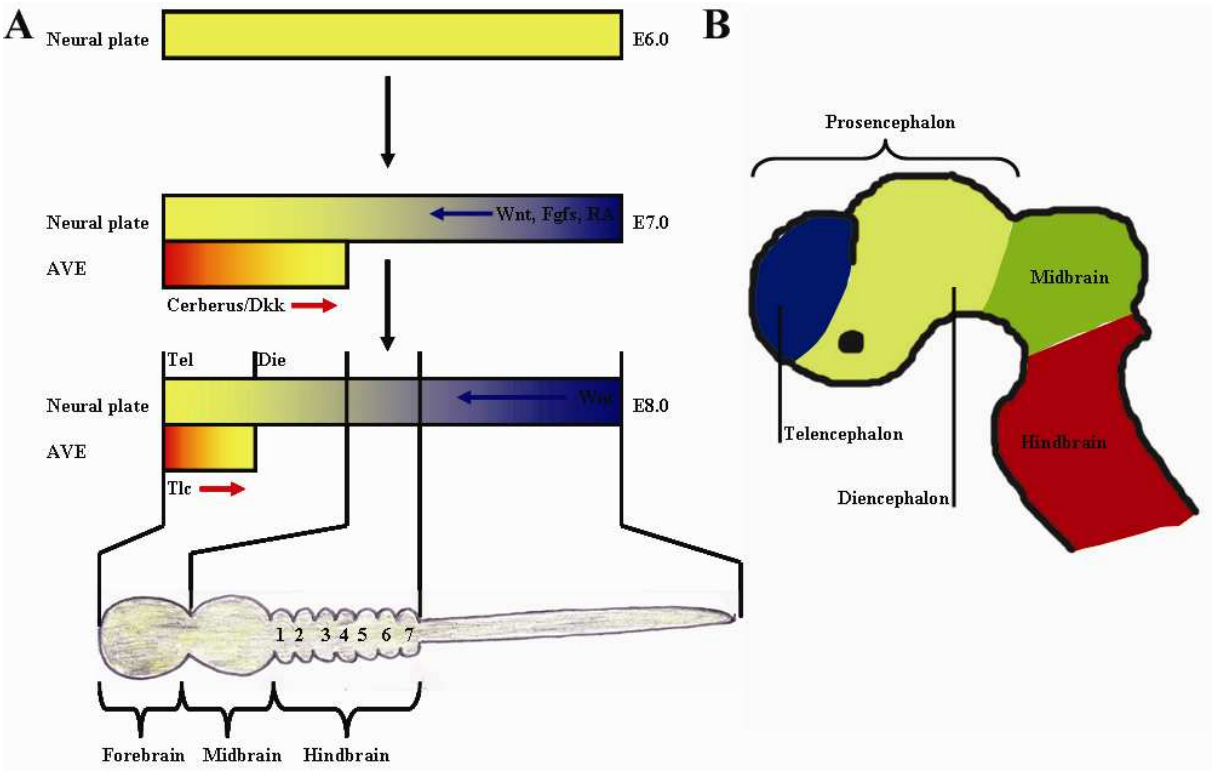

Fig. 5. Proceeding specification of the mammalian forebrain. A. Because of neural induction the neural plate is generated. Markers that are first expressed in the whole early neural plate will be in the end confined to specific anterior domains of the CNS. Wnts, FGFs and RA can act at this stage of development as signals that posteriorize the neural plate. Antagonists of this signals, such as cerberus and dickkopf, are expressed in the AVE (and node). They are crucial to prevent that the anterior neural plate adopts a posterior character. The anterior neural plate is afterwards divided into specific domains by graded Wnt signalling. **B.** Side view of the brain of a E10.0 old mouse embryo, showing the main subdivisions. (Adapted from Rallu *et al*., 2002).

1.2 Induction of the forebrain

1.2.1 The anterior neural ridge

The anterior neural ridge (ANR) resides at the rostral edge of the neural plate between the neural and non-neural ectoderm. The ANR starts to express *Fgf8* shortly after the initiation of the neural induction (Fig. 6). The expression of *Fgf8* in the ANR is under the control of signals from the axial mesendoderm. The axial mesendoderm gives rise to the anterior definitive endoderm, the prechordal plate mesoderm, the progenitors of the node and its derivates, the notochord and floor plate (Camus and Tam, 1999). The formation of the axial mesendoderm is dependent on the expression of *Nodal* (Wall *et al.*, 2000; Andersson *et al*., 2006).

Fgf8 expression in the ANR needs protection from the posteriorizing effect of Wnt signals. The Wnt signals originate from the lateral-ventral mesoderm and posterior ectoderm (Chang *et al*., 1998; Smith *et al*., 1991; Wolda *et al*., 1993; Kazanskaya *et al*., 2000; Mukhopadhyay *et al*., 2000; Hashimoto *et al*., 2000). *Fgf8* expression is thus limited to the ANR, where it is responsible for the induction of

markers for the prosencephalic identity in the anterior neuroectoderm (Shimamura *et al*., 1997; Shanmugalingam *et al*., 2000; Fukuchi-Shimogori *et al*., 2001).

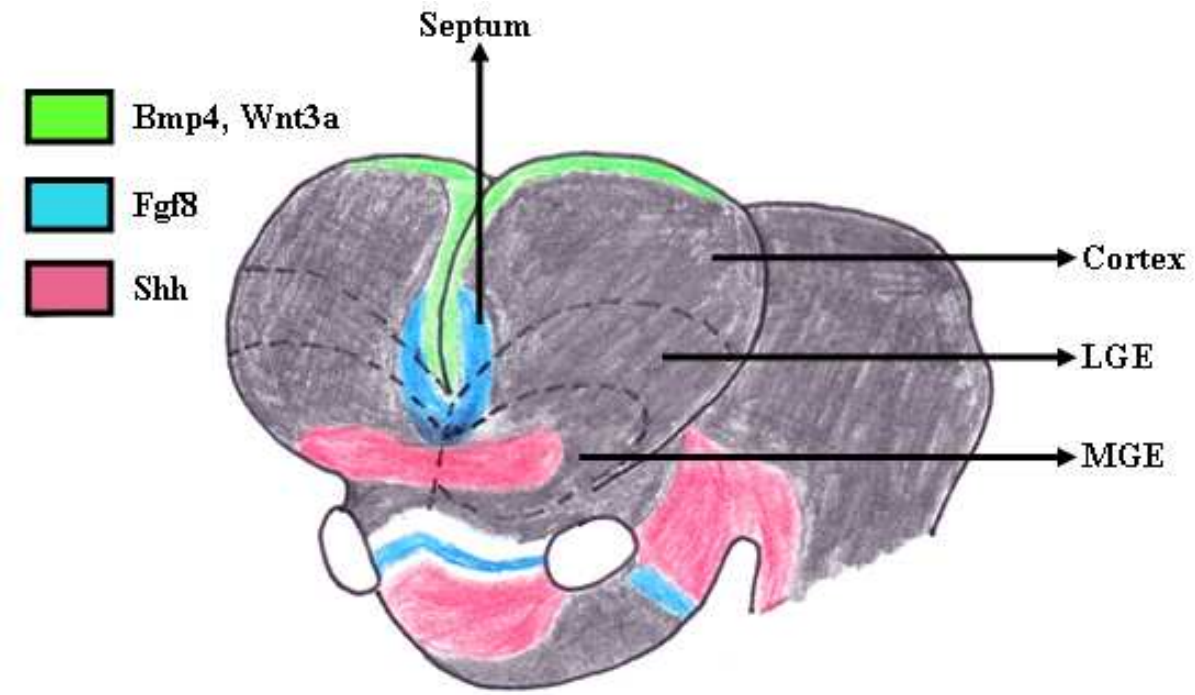

Fig. 6. Signalling centers in the developing telencephalon. For the patterning of the developing telencephalon four signalling centers are neede. 1) The anterior neural ridge (ANR) (blue) is loacated in the anlage of the septum (S) and emits Fgfs. 2) The cortical hem (green) functions as a caudodorsal signalling center by emitting Wnts and Bmps. 3) A center necessary for the ventral patterning of the telencephalon emits Shh. 4) A lateral center at the pallial-subpallial boundary (not shown), also called the anti-hem, emits Fgf7, Fgf15, neuregulins, TGFα and the Wnt antagonist secreted frizzled-related protein 2 (Sfrp2). Abbreviations: Cx, Cortex; LGE, lateral ganglionic eminence; MGE, medial ganglionic eminence; S, septum. (Adapted from Hoch *et al*., 2009)

Fgf8 is necessary and sufficient to regulate the expression of the telencephalic marker *forkhead box G1* (*Foxg1*) (Fig. 7A) (Shimamura and Rubenstein, 1997; Ye *et al*., 1998). The onset of *Foxg1* expression at embryonic day 8.5 (E8.5) in mice marks the specification of the telencephalic primordium. The telencephalon becomes subdivided into several distinct areas right after the expression of *Foxg1*. The different areas are first distinguished by the expression of specific molecular markers, but after a short time they can be kept apart by local differences in their levels of proliferation.

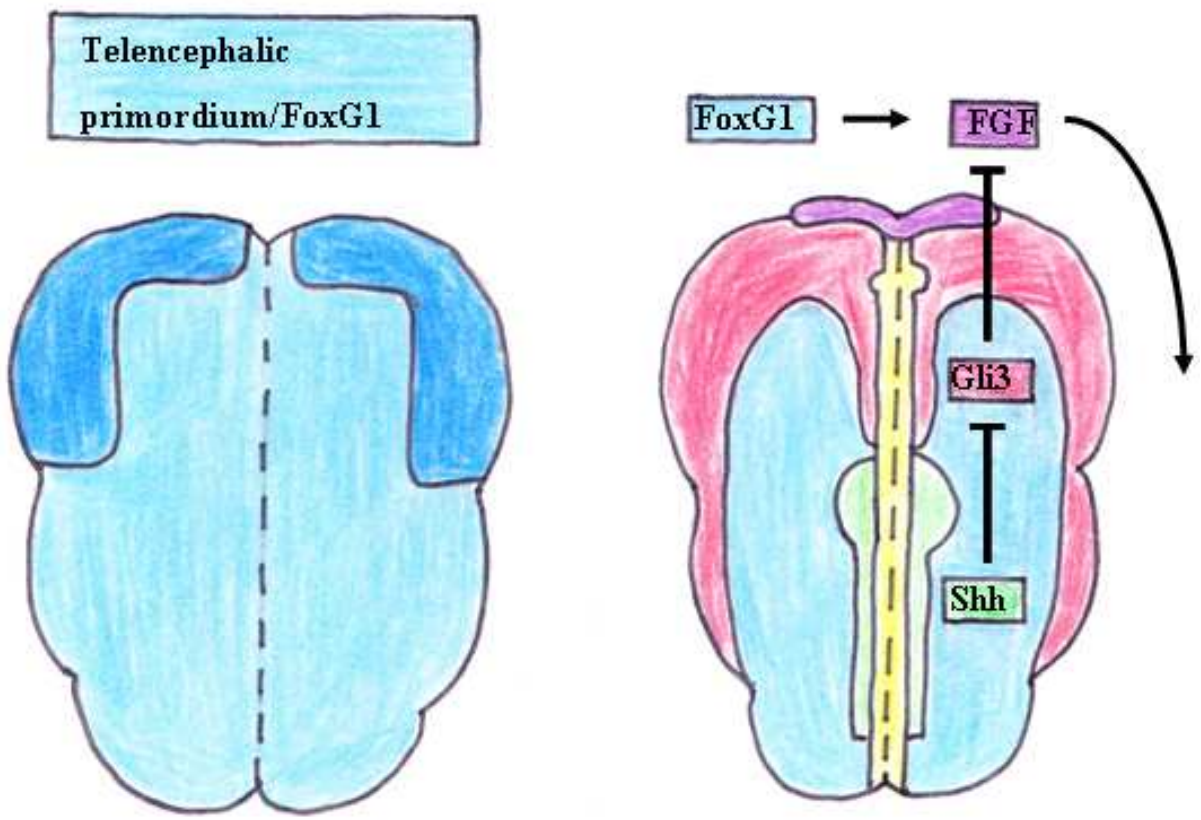

Fig. 7. Definition of the dorsal and ventral subdivisions in the developing telencephalon. Schematic drawing of the anterior neural plate at five somite stage (dorsal view, anterior is up). **A.** The developing telencephalon is marked by the expression of *FoxG1* (blue). **B.** FoxG1 and Shh (green) promote both the expression of *Fgf* (purple) in the ANR, which patterns the developing telencephalon (indicated by the curved arrow). Shh promotes the expression of *Fgf* by suppressing the repressor activity of Gli3. *Gli3* expression is depicted in red. Thus the development of a ventral telencephalic subdivision is promoted by Shh through the inhibition of the dorsalizing effect of Gli3. (**A,B**) Dorsal view, anterior is up. (Adapted from Hebert and Fishell, 2008).

Several transcriptional factors, including *GLI-Kruppel familiy member Gli3*(*Gli3*), *paired box gene 6* (*Pax6*) and *FoxG1*, are expressed in a region of the developing anterior neural plate (Fig. 7B) that will form the telencephalon. These genes play an important role in dividing the telencephalon into its dorsal and ventral sections. The embryonic dorsal telencephalon, which mainly produces glutamatergic neurons, can be divided into an anterior and lateral area that gives rise to the neocortex, and into a posterior and medial area that gives rise to the hippocampus, cortical hem and the choroid plexus. The embryonic ventral telencephalon can be divided into a medial area named the medial ganglionic eminences (MGE) and two posterior and lateral domains known as the lateral ganglionic eminences (LGE) and the caudal ganglionic eminences (CGE). All three domains of the ventral telencephalon contributes neurons to the basal ganglia and to corresponding limbic structures such as the amygdala and the nucleus accumbens.

1.2.2 Dorsal and ventral domains of the telencephalon are defined by Shh and Gli3

The subdivision of the telencephalon into a dorsal and a ventral domain is controlled by the dorsalizing effect of *Gli3* expression and the ventralizing effect of *sonic hedgehog* (*Shh*) expression. At the beginning, *Gli3* is expressed in the whole telencephalon (Fig. 7B) and is then gradually downregulated in the ventral part of the telencephalon (Aoto *et al*., 2002; Corbin *et al*., 2003). The depletion of *Gli3* expression results in a lack of the choroid plexus, cortical hem, the hippocampus and the neocortex (Grove *et al*., 1998; Theil *et al*., 1999; Tole *et al*., 2000; Kuschel *et al*., 2003).
Shh is expressed in the midline of the developing neural plate (Fig. 7B) and its expression is maintained along the ventral midline of the CNS during development (Echelard *et al.*, 1993). In the absence of *Shh* expression the size of the telencephalon is diminished and ventral cell types fail to form (Ericson *et al*., 1995; Chaing *et al*., 1996; Ohkubo *et al*., 2002; Corbin *et al*., 2003). The ventral patterning can mainly rescued in double mutants for *Gli3* and *Shh* (Aoto *et al.*, 2002; Rallu *et al*., 2002; Rash *et al*., 2007), which indicates that *Shh* restricts the dorsalizing effect of *Gli3* and also controls the positioning of the dorsoventral boundary.

1.2.3 The telencephalon is supported by the expression of *Gli3* and *Foxg1*

Early anterior neural plate cells destined to form the telencephalon express *Foxg1* (Fig. 7A) (Shimamura *et al*., 1995; Shimamura *et al*., 1997; Hebert *et al*., 2000), which is independent of the *Shh* expression (Rash *et al*., 2007). The result of the impairment of *Foxg1* expression is a loss of ventral cell types (Xuan *et al*., 1995; Dou *et al*., 1999; Martynoga *et al*., 2005;) and the complete telencephalon is lost in double mouse mutants for *Foxg1* and *Gli3* (Hanashima *et al.*, 2007), leading to the suggestion that both genes are necessary for creating and maintaining the dorsal and ventral subdivisions of the telencephalon (Fig. 8A).

Foxg1 is also needed for the expression of *Fgf8* (Martynoga et al., 2005) and Fgf signalling is, together with Shh signalling, essential for the formation of the ventral telencephalon (Shanmugalingam *et al*., 2000; Shinya *et al*., 2001; Walske and Mason, 2003; Gutin *et al*., 2006; Storm *et al*., 2006).

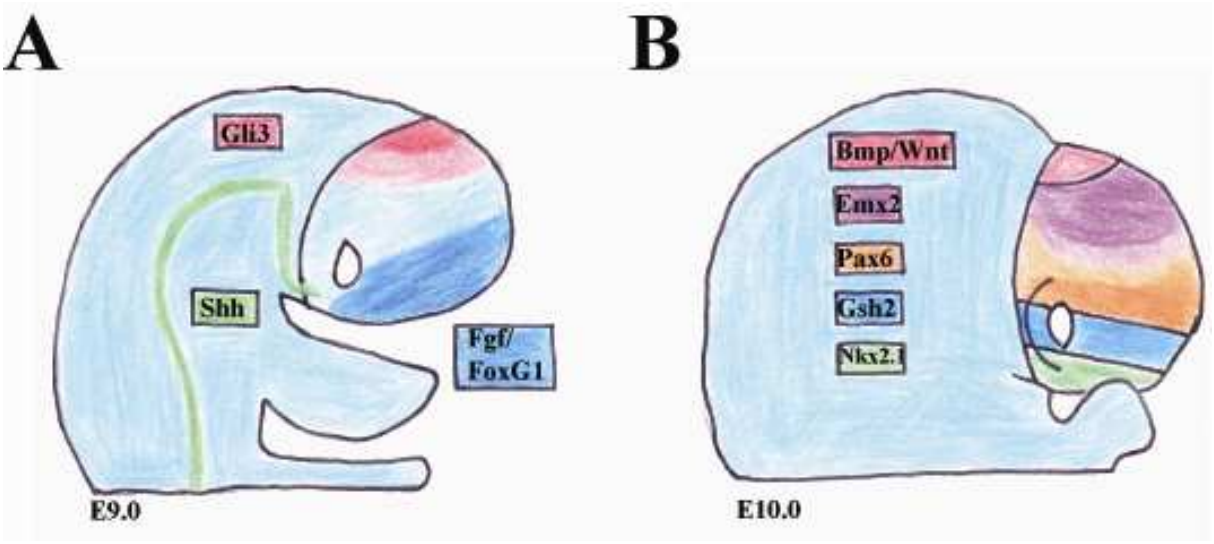

Fig. 8. The dorsal and ventral areas of the telencephalon are subdivided into four main regions. Drawing shows the dorsal and ventral subdivisions of the embryonic mouse telencephalon at E9.0 **(A)** and at E10.0 (**B)**. **A.** The Gli3-expressing dorsal area at E10.0 is divided at E10.0 into a Bmp- and Wnt-expressing medial area and and a more lateral located cortical area that expresses reverse gradients of Emx2 and Pax6. Between E9.0 and E10.0 the ventral region is divided into medial Nkx2.1-expressiong domains and Gsh2-expressing domains. At E10.0 the expression area of Gsh2 overlaps with that of Nkx2.1 (not shown). The expression of Shh, Fgf and FoxG1 is skipped. (**A,B**) Dorsal is up, ventral is down. (Adapted from Hebert and Fishell, 2008).

1.2.4 Fgfs specify ventral telencephalic identity downstram of *Shh*

Shh maintains indirectly the expression of several Fgf genes in the anterior medial telencephalon (Aoto *et al*., 2002; Ohkubo *et al*., 2002; Gutin *et al*., 2006; Rash *et al*., 2007) by its ability to negatively regulate the repressor function of Gli3 (Fig. 7B), and Fgf receptors are required for the ventralizing effect of *Shh*. Fgf expression is lost in $Shh^{-/-}$ mutants, and ventral cell types fail to form due to the uncontrolled repressive influence of *Gli3*. The expression of *Fgf* is no longer impaired in $Shh^{-/-};Gli3^{-/-}$ double mutants, and ventral development is rescued (Theil *et al*., 1999; Aoto *et al*, 2002; Kuschel *et al*., 2003; Rash *et al*., 2007). The influence of the Fgf signalling concerning the patterning of the telencephalon is not confined to the ventral regions, but also expands to the dorsal regions. In *Fgf8* mutants not only are ventral precursors lost, but also the neocortex is reduced in size and anterior-lateral markers are lost (Storm *et al*., 2006). This and other results indicate that Fgf signalling plays an important role as an organizer of the telencephalon.

1.2.5 Establishment of cortical regions by *Pax6*

Pax6 is absolutely necessary for the establishment of the sharp border, called the anti-hem, that separates the ventral telencephalon from the dorsal telencephalon. *Pax6* is expressed in the whole forebrain primordium during neural plate stage (Inoue *et al*., 2000) and at the neural tube stage its

expression is limited to the dorsal region of the developing telencephalon, simultaneous with the upregulation of *Nk 2 homeobox 1* (*Nkx2.1*) in the ventral telencephalon (Corbin *et al*., 2003) (Fig. 8B). The pallial-subpallial boundary is defined by the intersection of *Pax6* and *GS homeobox 2* (*Gsh2*) expression (Fig. 8B). In *Pax6*$^{-/-}$ mutants the most ventral portion of the telencephalon becomes the dorsal LGE, and in *Gsh2*$^{-/-}$ mutants the dorsal LGE adopts a ventral cortex fate (Corbin *et al*., 2000; Stoykova *et al*., 2000; Toresson *et al*., 2000; Yun *et al*., 2001). *Pax6* seems to interact with *Gli3* to promote dorsal telencephalic development (Fuccillo *et al*., 2006), whereupon *Gli3* is required for maintaining *Pax6* expression (Theil *et al*, 1999; Aoto *et al*., 2002; Kuschel *et al*., 2003).

1.2.6 Division of the dorsal telencephalon into different domains

The dorsal telencephalon is divided into two areas: the cerebral cortex, which develops to the neocortex and the hippocampus, and the dorsal midline, which forms the cortical hem and the choroid plexus (Fig. 9). The transcription factor *Lim homeobox protein 2* (*Lhx2*) is essential for specifying cells to become cortical instead to adopt a dorsal midline character, by inhibiting a hem or antihem fate (Fig. 9) (Mangale *et al.*, 2008). In *Lhx2* null mutants the cortex is lost and the cortical hem and choroid plexus are expanded (Monuki *et al*., 2001). The expression of *Foxg1* also restricts the dorsal midline development (Dou *et al*., 1999; Martynoga *et al*., 2005).

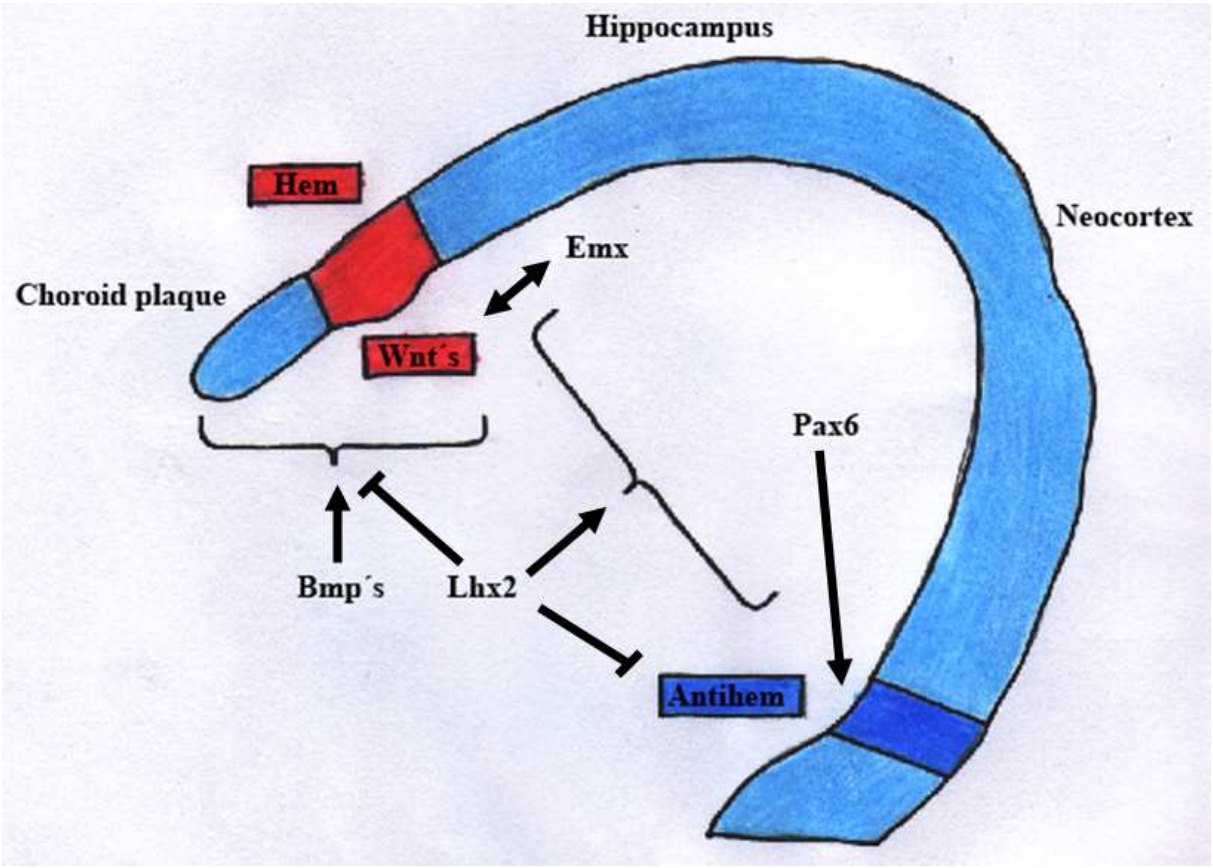

Fig. 9. The dorsal telencephalic midline emits signals necessary to subdivide the dorsal telencephalon.

Bmps expressed by midline cells are needed for the development of the choroid plaque and the cortical hem (red), which is the organizer required for the formation of the hippocampus. The cortical hem is defined by the expression of several Wnts. The formation of the neocortex needs the expression of *Pax6* and *Emx1/2*. *Pax6* expression is necessary for the formation of the anti-hem (blue), which represents the pallial-subpallial border. The expression of *Lhx2* inhibits the expansion of the cortical hem and anti-hem. (Adapted from Hebert and Fishell, 2008).

The dorsal midline itself is defined by the expression of *Bmp*s and *Wnt*s, and Bmp signalling can induce dorsal midline character (Fig. 9) (Furuta *et al*., 1997; Panchision *et al*., 2001). The depletion of Bmp signalling results in a loss of the cortical hem and choroid plexus (Fernandes *et al*., 2007). The development of the hippocampus depends upon the activity of the cortical hem. Wnts are likely candidates to administrate this organizer activity of the cortical hem (Fig. 9). Depletion of *wingless-related MMTV integration site 3a* (*Wnt3a*) from the cortical hem results in a lack of a recognizable hippocampus (Lee *et al.*, 2000). The normal development of the hippocampus also requires *empty spiracles homolog 1* (*Emx1*) and *empty spiracles homolog 2* (*Emx2*) (Fig. 9) (Shinozaki *et al*., 2004). The expression of *Emx2* can be regulated by binding of Bmp and Wnt signalling effectors to specific enhancer elements of *Emx2*. Thus *Wnt3a* can maybe act together with Bmps to aid hippocampal formation by directly influencing the expression on *Emx* genes (Theil *et al*., 2002; Shinozaki *et al*., 2004).

1.3 Primary cilia

The formation of the telencephalon starts as a single layer of neuroepithelial cells and requires the proliferation, differentiation and migration of neural precursor cells. The study of the primary cilium, a small protrusion of the cell surface into the extracellular matrix, gives insight to the mechanisms that are responsible for the development of the telencephalon. The primary cilium arises from the basal body, which originates from the mother centriole. The mother centriole, which belongs to the centrosomes that are responsible for the organization of the mitotic spindle during cell divisions, functions as a microtubule-organizing center underneath the cell membrane (Davenport and Yoder, 2005). Because the primary cilium is associated with the centrosome, it is absorbed just before the cell enters mitosis. Thus, this connection between cell cycle and ciliogenesis indicates that the primary cilium may be involved in cell proliferation and differentiation during development (Pan and Snell, 2007; Pugacheva *et al*., 2007; Spektor *et al*., 2007). Results from recent studies also demonstrated that the primary cilium senses extracellular signals that control brain development (Eggenschwiler and Anderson, 2007; Gerdes *et al*., 2009). Almost every cell in the brain exhibits a primary cilium (Doetsch et al., Banizs *et al*., 2005; Bishop *et al*., 2007; Cohen and Meininger, 2007; 1999; Dubreuil *et al*., 2007).

1.3.1 Ciliary structure

The cilium is an appendage-like, microtubule-based organelle that is found on almost every eukaryotic cell (Pazour and Witman, 2003). The membrane of the cilium is connected with the cell membrane, covering a microtubule core structure called the axoneme. The basal body fixes the cilium at the proximal end of the axoneme (Fig. 10). The ciliary axoneme consists of nine outer microtubule doublets grouped in a concentric circular pattern. These doublets surround either a central pair of microtubles (this ultrastructure is known as "9+2") (Fig. 10), or the axoneme has no central pair (this structure is referred to as "9+0") (Fig. 10). Inner and outer dynein arms attached to the outer microtubule doublets are responsible for ciliary motility (Fig. 11). Historically the "9+2" structure was linked with a motile function for cilia, whereas the "9+0" structure was implicated with immotile sensory (primary) cilia. However, this historical classification is not correct. Flagella in many protists function in motility as well as sensory reception (Fliegauf *et al*., 2006). Vertebrates exhibit motile "9+0" cilia on the embryonic node that generate fluid movement, which is critical for left-right asymmetry (Essner *et al*., 2002; McGrath *et al*., 2003; Essner *et al*., 2005), as well as motile ependymal cilia in the central canal of the zebrafish spinal cord possess a "9+0" structure (Kramer-Zucker *et al*., 2005). Cilia of olfactory sensory neurons in frog olfactory epithelium have a "9+2" configuration and are immotile (Reese, 1965). At the distal end of the basal body is the transition area (Fig. 11). It has been suggested that the basal body and the corresponding transition-fiber proteins have a regulating function concerning the entry and exit of proteins from the cilia compartment (Marshall, 2008; Pazour and Bloodgood, 2008).

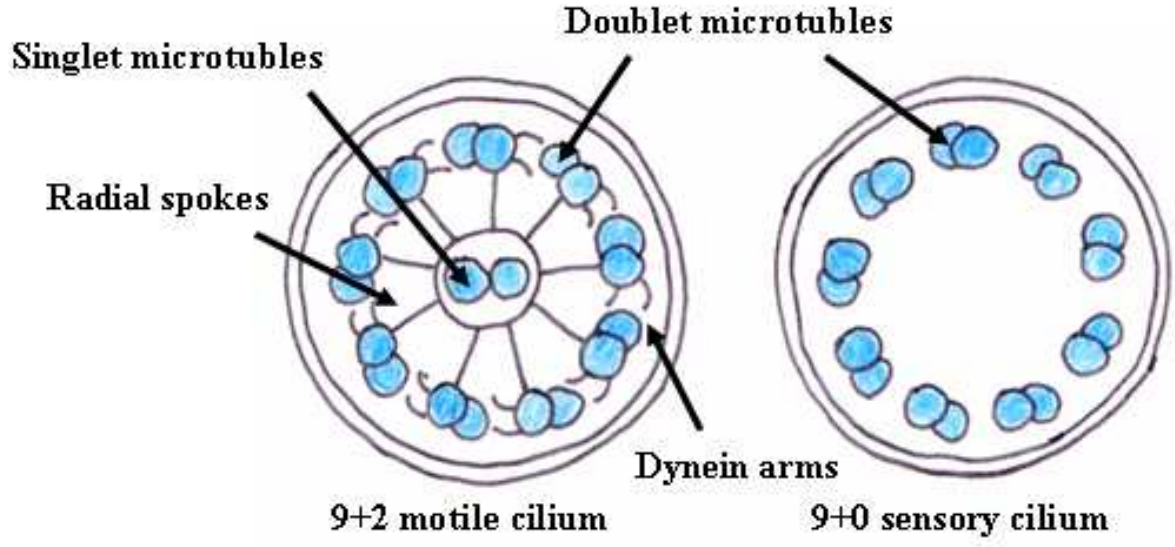

Fig. 10. A cross-section through a "9+2" and "9+0" cilium. (Adopted from Bisgrove and Yost, 2006)

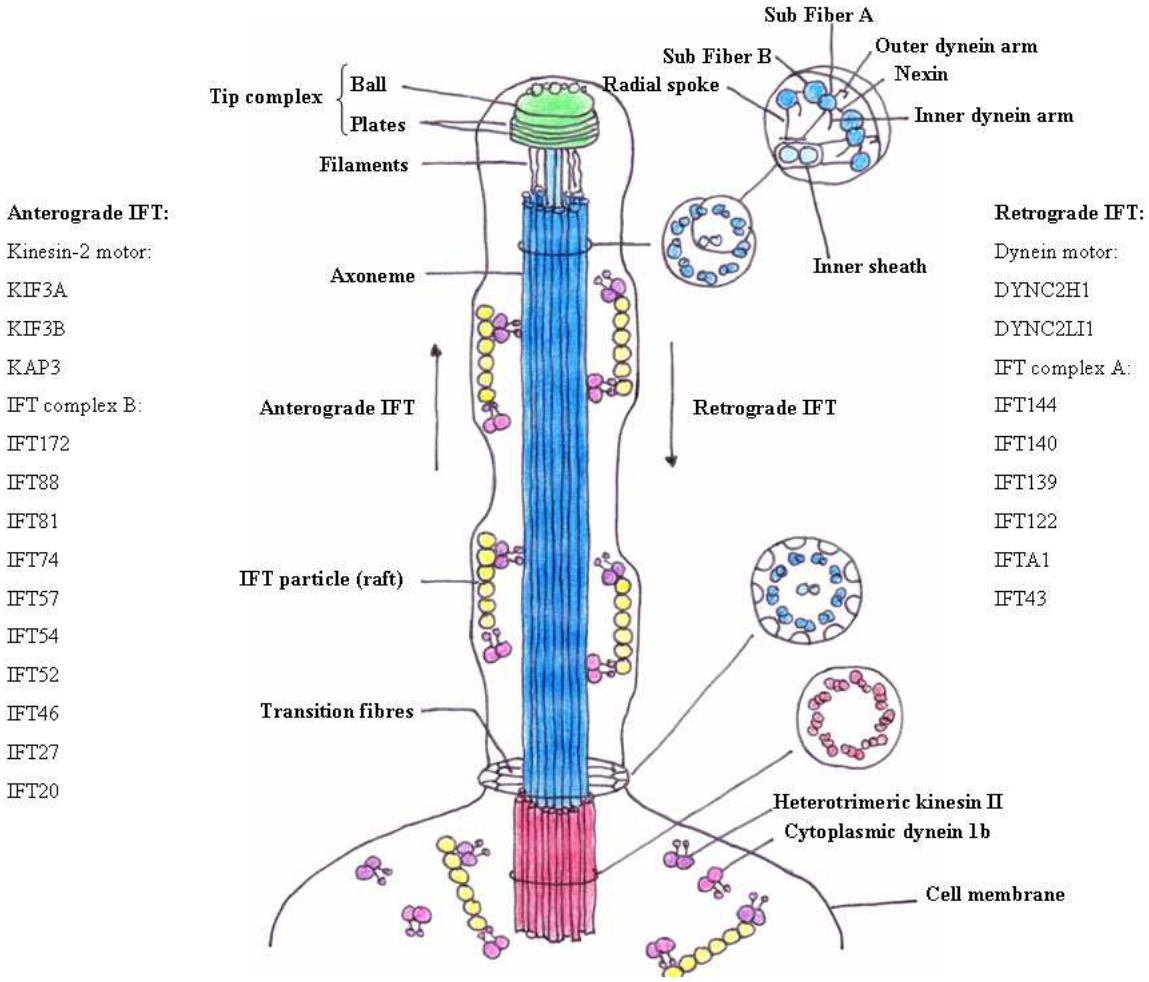

Fig. 11. Ciliary structure and intraflagellar transport (IFT). The figure shows the structure of a "9+2" primary cilium and the components of its IFT, which is necessary for the assembly and maintenance of cilia. **+** = microtubule plus end; **-** = microtubule minus end. (Adapted from Eley *et al*., 2005).

1.3.2 Intraflagellar transport

Proteins necessary for the assembly and maintenance of the cilium have to be synthesized in the cell body and transported into the cilium, because the cilium itself lacks the machinery needed for protein synthesis. The transport occurs by a microtubule-based process known as intraflagellar transport (IFT) (Pazour *et al*., 2002; Scholey, 2003; Pedersen and Rosenbaum, 2008) (Fig. 11). Ciliary components are moved from the cell body into the cilium (anterograde transport) by kinsein-II motors (Fig. 12), whereas cytoplasmic dyneins are responsible for their transport from the cilium to the cell body (retrograde transport) (Fig. 12).

IFT particles are composed of two distinct subcomplexes (complexes A and B). Complex B is involved in anterograde transport (Kozminski *et al*., 1993; Cole *et al*., 1998) and complex A is responsible for the retrograde transport (Pazour *et al*., 1998; Piperno *et al*., 1998).

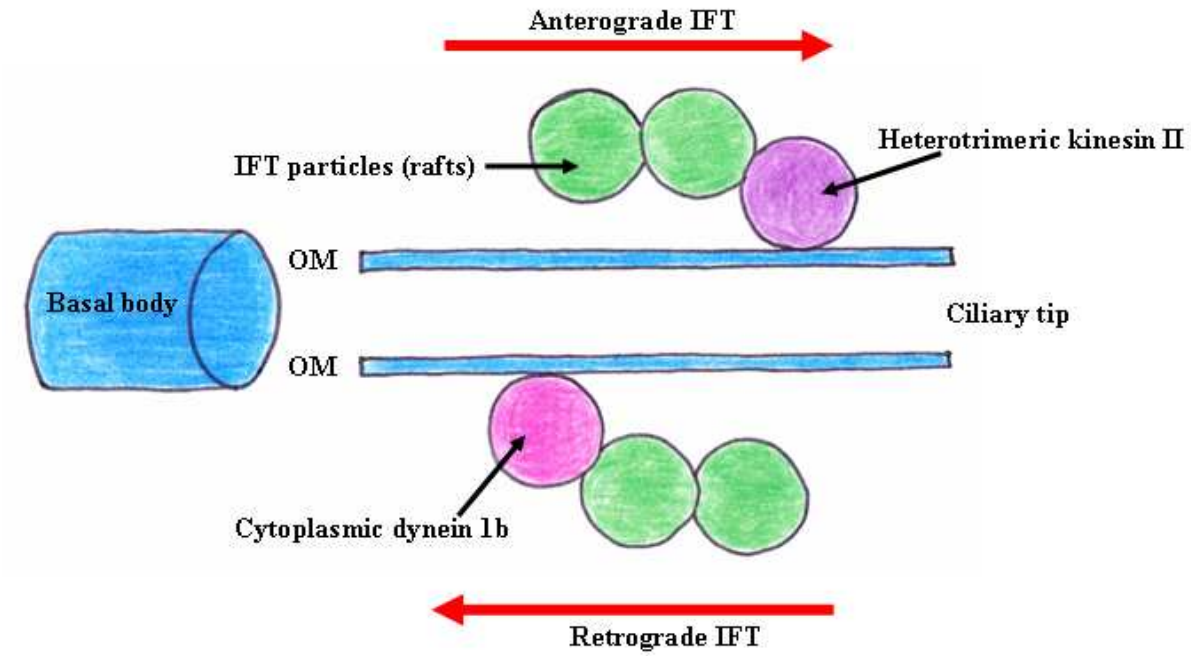

Fig. 12. Intraflagellar transport. So called IFT particles are transported to the ciliary tip of the cilium (anterograde IFT) by kinesin along the outer microtubule doublets (OM) and under the ciliary membrane. They are transported back to the basal body and the cell (retrograde IFT) by the molecular motor cytoplasmic dynein. (Adapted from Badano *et al*., 2006).

1.3.3 Ciliary function

The function of motile cilia is for example to recognize and remove foreign substances out of the trachea (Shah *et al*, 2009). Motile cilia are in the adult brain located on ependymal cells along the ventricle and some choroid plexus cells, generating the cerebrospinal fluid flow, which is crucial for the migration of young neurons from the adult subventricular zone (Sawamoto *et al*., 2006). Primary cilia function as a sensory organelle and mediate chemo-, photo-, and mechanotransduction. Olfactory cilia located on olfactory sensory neurons mediate chemotransduction (McEwen *et al*., 2008; Jenkins *et al*., 2009); the outer segment of photoreceptors is a highly modified cilium and mediates phototransduction (Ramamurthy *et al*., 2009), and primary cilia of renal epithelial cells mediate mechanotransduction (Praetorius *et al*., 2001; Praetorius *et al*., 2003). Primary cilia on embryonic nodal cells have a machanosensory function that controls left-right asymmetry in the early embryo (McGrath *et al*., 2003). Primary cilia are also crucial for the proper function of mammalian signal transduction pathways such as the Hegehog- (Hh) and Wingless/Integrated- (Wnt) signalling (Eggenschwiler and Anderson, 2007; Gerdes *et al*., 2009).

1.3.4 Primary cilia and Hedgehog signalling

Hedgehog (Hh) proteins are secreted lipoproteins that are involved in the regulation of developmetal processes in invertebrates as well as in vertebrates ((Nusslein-Volhard and Wieschaus, 1980; Jiang and Hui, 2008). Mammals have three Hh genes, Sonic hedgehog (Shh), that is important for the regulation of embryonic development as well as post-natal homeostasis (Echelard *et al*., 1993; Chiang *et al*., 1996), Indian hedgehog, that is involved in bone development, and Desert hedgehog, that participate in spermatogenesis (Bitgood *et al*., 1996; Vortkamp *et al*., 1996; St-Jacques *et al*., 1999) and is involved in the development of peripheral nerves (Paramtier *et al*, 1999).

Components of the Hh pathway are localized in cilia (Corbit *et al*., 2005), and cells without cilia are not able to initiate the pathway in response to Shh ligand (Ocbina and Anderson, 2008; Haycraft *et al*., 2005). The Hh pathway is triggered by binding of Hh protein to the transmembrane receptor Patched1 (Ptch1) in the membrane of the cilium (Fig. 13A) (Rohtagi *et al*., 2007). The activity of the seven transmembrane protein Smoothened (Smo) is inhibited by Ptch1 in the absence of Hh signal. Binding of Hh signal to Ptch1 results in the internalization of Ptch1 from the membrane of the cilium and Smo enters the cilium (Fig. 13B) (Corbit et al., 2005; Rohatgi et al., 2007). This cancels the repression of Smo and triggers a conformational change in Smo, thus resulting in the activation of the pathway (Zhao *et al.*, 2007). The connection between Smo and the Gli transcription factors, which mediate in the nucleus the expression of the Hh pathway targeted genes (Kalderon, 2000; I Altaba et al., 2007), is still unclear. Besides Ptch1 and Smo, other regulators of the Hh signalling pathway, such as Suppressor of Fused (SuFu) and the Gli transcription factors Gli1, Gli2 and Gli3 (Ruppert *et al*, 1990) localize to the cilium (Haycraft *et al*., 2005; Kiprilov *et al*., 2008; Nielsen *et al*., 2008; Chen *et al*., 2009). Gli2 functions basically as a strong transcriptional activator with a weak repressor function. Gli3, on the other hand, has mainly a strong repressor function and a weak activator activity (Hui and Joyner, 1993; Ding *et al*., 1998; Matise *et al*., 1995; Buttitta *et al*., 2003; McDermott *et al*., 2003; Wang *et al*., 2007; Pan *et al*., 2008; Pan *et al*., 2009). Both regulate the expression of the *Gli1* gene (Bai *et al.*, 2004), a direct target of Hh signalling (Hynes *et al*., 1997; Dai *et al.*, 1999; Bai and Joyner, 2001). Gli1 has no N-terminal repressor domain and it undergoes no proteolytic processing (Dai *et al*., 1999; Sasaki *et al*., 1999; Kaesler *et al*., 2000). Gli1 is expendable in mice (Park *et al*., 2000; Bai *et al*., 2002), but not in the zebrafish (Karlstrom *et al*., 2003). Thus, it is probable that Gli1 is in mice not really necessary for initiation of the Hh signal transduction, but to enhance the expression of Hh target genes after activation.In the absence of Hh signalling, the main part of the full-length Gli3 isoform and only a small fraction of the full-length Gli2 isoform are proteolytically processed by cleaving the C-terminal activator domains to become N-terminal repressors (Wang *et al*., 2000; Pan *et al*., 2006) and Gli1 is not expressed (Hynes *et al*., 1997; Lee *et al*., 1997; Dai *et al*., 1999; Bai and Joyner, 2001; Karlstrom *et al*., 2003). For the processing of full-length Gli2 and Gli3 the phosphorylation of several serine and threonine residues at their C-terminus is necessary.This is conducted by protein kinase A

(PKA) and thereafter by casein kinase 1 (CK1) and glycogen synthase kinase 3 (GSK3) (Pan *et al*., 2006; Tempe *et al*., 2006; Wang and Li, 2006). After phosphorylation has taken place, they are bound and ubiquitinated by the Skp1-Cul1-F-box protein-E3-ubiquitin ligase complex and then processed by the proteasome in a site-specific manner to their N-terminal repressor isoforms (Tempe *et al*., 2006; Wang and Li, 2006). Binding of a Hh signalling molecule to Ptch1 leads to a reduction of the processing of Gli2 and Gli3 into their short repressor form and to an increased activity of Gli1 and Gli2 (Fig. 13B) (Wang *et al.*, 2000; Litingtung *et al*., 2002; Huangfu and Anderson, 2005). The normal functioning cilium seems to be crucial for the processing of Gli2 and Gli3 to their repressor form and the activation of Gli2 and Gli3 in response to induced Hh signalling (Huangfu *et al*, 2003; Haycraft *et al*., 2005; Liu *et al.*, 2005).

Normal limb development, for example, is dependent on a specific ratio between Gli3 activator and Gli3 repressor (te Welscher *et al*., 2002; Wang *et al*,. 2007). Mutations that remove IFT in mice alter the Gli3 activator-to-repressor ratio by misregulation of the production of the Gli3 repressor form, resulting in severe polydactyly (Haycraft *et al*., 2005; Liu *et al*., 2005; Tran *et al*., 2008). These results indicate an important role for primary cilia for the regulation of the Hh signalling pathway.

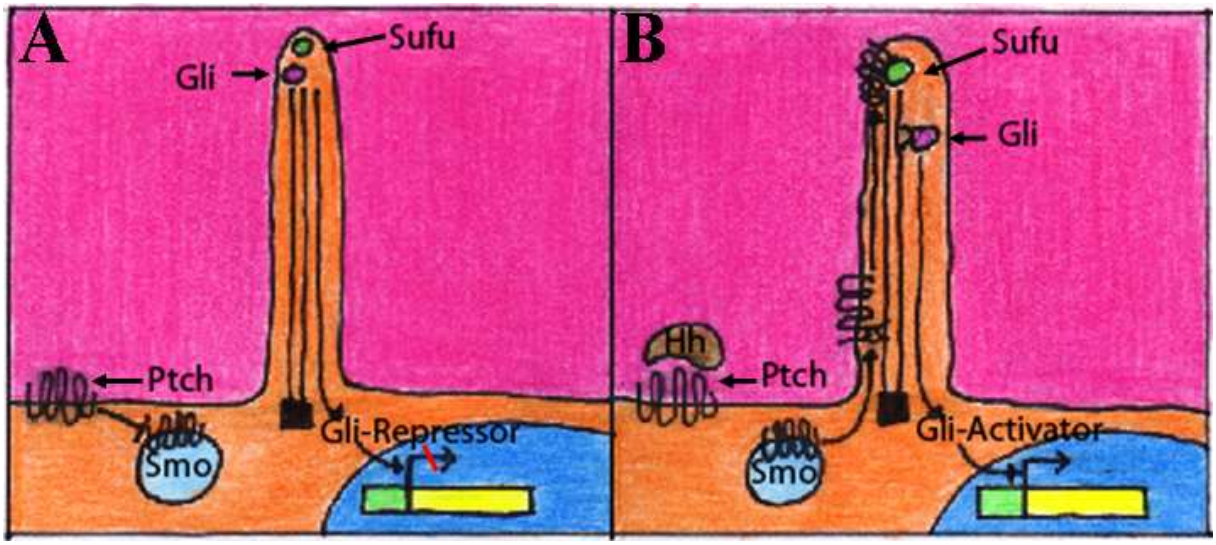

Fig. 13. The primary cilium and Hh signalling. A. In the absence of Hh, Smo is repressed by Ptch. Gli3 is proteolytically processed to a transcriptional repressor, which inhibits the transcription of Hh signalling target genes. **B.** The binding of a Hh signal results results in the internalization of Ptch1 from the membrane of the cilium and Smo enters the cilium. In the cilium Smo interacts with Sufu, which results in inhibition of the proteolytic procession of Gli3, activating Gli transcriptional activators. (Adapted from Scholey and Anderson, 2006).

1.3.5 Sufu and proteolytic processing of Gli2 and Gli3 in relation to primary cilia

It has been recently shown that the formation of the two different isoforms of Gli3 are dependent of the interaction between Gli3 and Sufu (Humke *et al*., 2010), and that this interaction seems partly to be

independent of primary cilia (Chen *et al*., 2009). Sufu is an important negative regulator of the mammalian Hh signalling pathway and its removal results in a constitutive activation of Hh target genes in mice (Cooper *et al.,* 2005; Svard *et al*., 2006). Sufu can directly bind to both the N-and C-terminal regions of the three different Gli proteins in mammals (Pearse *et al*., 1999; Stone *et al.,* 1999; Dunaeva *et al*., 2003; Merchant *et al*., 2004), and the interaction between Sufu and Gli3 controls the generation of the Gli3 repressor as well as activator isoform (Humke *et al*., 2010). The loss of Sufu leads to the destabilization of Gli2 and Gli3 full-length activators, but their C-terminal processed repressors are unaffected (Wang *et al*., 2010). The knockdown of Spop (a substrate-binding adaptor for the cullin3-based ebiquitin E3 ligase) in Sufu mutant mouse embryonic fibroblasts (MEFs) is able to recover the levels of Gli2 and Gli3 full-length proteins (Wang *et al*., 2010), and overexpression of Spop assists Gli2 and Gli3 degradation and Gli3 processing (Wang *et al.*, 2010). Sufu antagonizes Spop in the process of regulating the protein levels of Gli2 and Gli3 (Chen et al., 2009) by protecting the full-length isoforms of Gli2 and Gli3 from Spop-mediated ubiquitination and complete degradation by the proteasome (Chen *et al*., 2009, Wang *et al*., 2010).

Without the activation of the Hh signalling, full-length Gli3 is held back by Sufu in the cytoplasm, which favours the processing of Gli3 into a transcriptional repressor (Humke *et al.*, 2010). The association of full-length Gli3 with Sufu seems to be independent of primary cilia, because in cells without IFT components Sufu has still the competence to inhibit Hh signalling (Chen *et al*., 2009; Jia *et al*., 2009). The subsequent processing of the full-length Gli3 into its transcriptional repressor form depends on intact primary cilia (Huangfu and Anderson, 2005), but the activity of the Gli3 repressor form does not need Sufu or primary cilia (Humke *et al.*, 2010; Wang *et al.*, 2010). Sufu dissociates from Gli3 after the activation of Hh signalling (Humke *et al.*, 2010) and the full-length Gli3 is able to enter the nucleus (Humke *et al.,* 2010). Once the full-length Gli3 isoform has entered the nucleus, it is turned into an instable, differentially phosphorylated transcriptional activator .The protein Kif3a is necessary for the dissociation of Sufu from Gli3, and it may also be PKA dependent. Activation of the Hh signalling pathway leads to an accumulation of inactive PKA at the base of the primary cilium, and its inactivation triggers the activation of PKA at the same location (Barzi *et al*., 2010). The activation of PKA can inhibit the dissociation of the full-length Gli3/Sufu complex (Humke *et al.,* 2010), and full-length Gli3 bound by Sufu is not able to enter the nucleus to activate target genes of the Hh signalling.

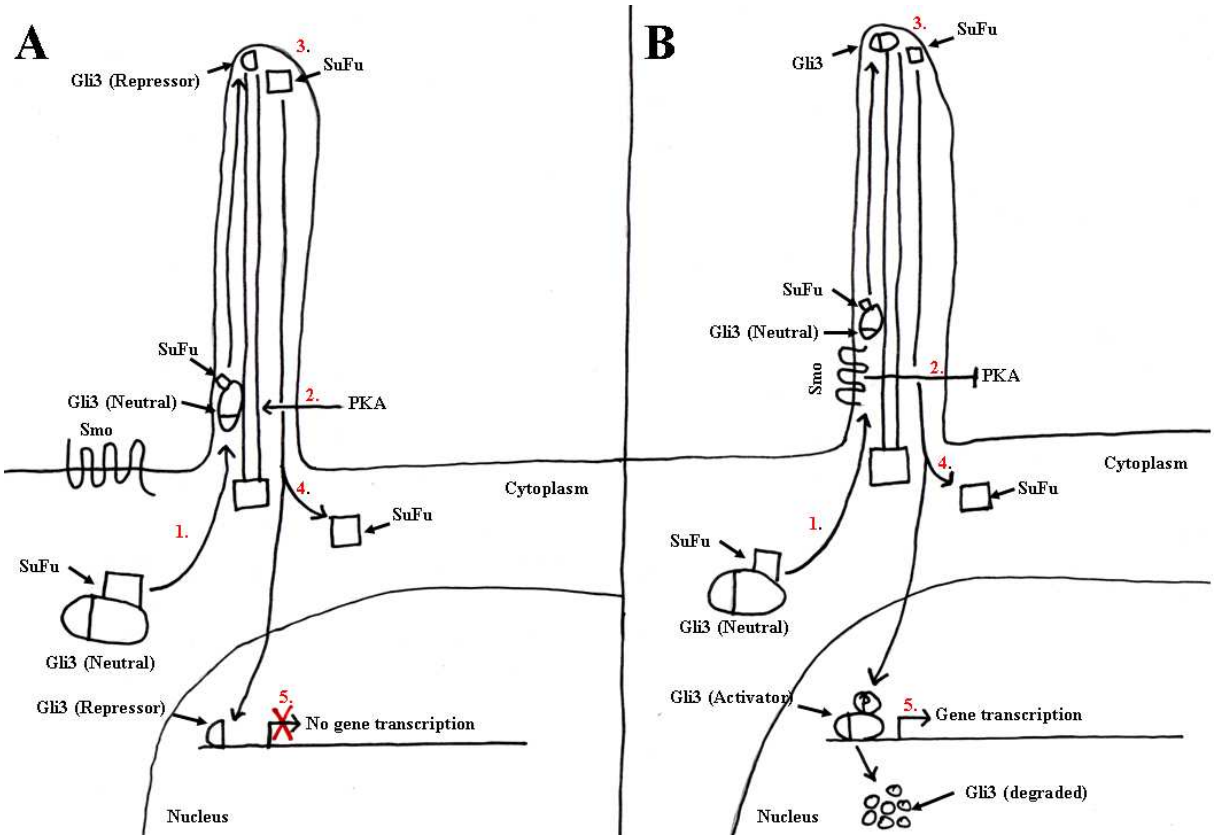

Fig. 14. SuFu controls Gli3 processing. A. The full-length form of Gli3 is in association with SuFu in the cytoplasm and is kept in this way in a neutral state. Without the activation of the Hh signalling pathway, the SuFu-Gli3 complex is recruited to the primary cilium (1), leading to the processing of the full-length Gli3 to the cleaved Gli3 isoform (2), which leads to its dissociation from SuFu (3). The cleaved Gli3 isoform is now able to enter the nucleus (4), where it acts as a transcriptional repressor of Hh target genes (5). **B.** Activation of the Hh signalling pathway results in the dissociation of SuFu from the Gli3 full-length isoform (3) and the formation of the cleaved Gli3 isoform is stopped (2). Free full-length Gli3 can now enter the nucleus (4), where it is phosphorylated, destabilized, and converted into a transcriptional activator (5). The level of PKA activity in the primary cilium may be able to control the rate of flow between pathways leading to the formation of Gli3 repressor and activator generation (Adopted from Humke *et al*., 2010)

1.3.6 Primary cilia and Wingless/Integrated signalling

The Wingless/Integrated (Wnt) signal pathway plays during development a crucial role in cell proliferation and differentiation. (Logan and Nusse, 2004; Clevers, 2006). Wnt proteins are secreted growth factors interacting with the complex of the Frizzled (Fz) receptor and the low-density lipoprotein receptors LRP5 or LRP6, thereby activating the canonical Wnt/β-catenin pathway, or interacting with the Fz receptor alone, which results in triggering the non-canonical Wnt/planar cell polarity (PCP) pathway (Veeman *et al*., 2003; He *et al*., 2004). The Wnt/β-catenin pathway controls the stability of the transcription coactivator β-catenin, and thus the expression level of target genes of the Wnt/β-catenin pathway (Fig. 14, upper two panels). The non-canonical Wnt/PCP pathway is

important for the architecture of the cytoskeleton in the context of cell polarity and movement (Fig. 14, lower panel).

1.3.6.1 Primary cilia and canonical Wnt/β-catenin pathway

The main mediator for the downstream effects of the canonical Wnt/β-catenin pathway is β-catenin. In the absence of a canonical Wnt signal a complex consisting of the proteins Axin, Glycogen synthase kinase 3β (GSK3β) and Adenomatous polyposis coli (APC) promotes the proteolytic degradation of cytosoliy β-catenin (Fig. 15, upper left panel). Binding of Wnt signals to the receptor complex of Fz and LRP5/6 activates cytosolic Dishevelled (Dvl), which inhibits the Axin/GSK3β/APC complex (Fig. 15, upper right panel). This leads to a stabilization and increase of cytosolic β-catenin levels.

In the absence of β-catenin in the nucleus the transcription factors T cell factor (TCF) and lymphocyte enhancer factor (Lef) are in a complex with the transcriptional suppressors Groucho and transducin-like Enhancer of split (TLE). This results in an inhibition of the downstream target genes of the canonical Wnt/β-catenin pathway (Fig. 15, upper left panel). Because the binding of Wnt signals stabilizes the pool of β-catenin in the cytoplasma, some β-catenin is able to enter the nucleus where it interacts with TCF and Lef as a transcriptional coactivator (Fig. 15, upper right panel), inducing cell cycle progression, proliferation, differentiation and growth in addition to migration and regulation of embryonic development (Vlad *et al*., 2008).

Primary cilia are thought to be involved in canonical Wnt/β-catenin signalling, but the research results are inconsistent and controversial. Inversin (Inv), encoded by the gene *Nephrocytin 2*, is located in primary cilia and interacts with Dvl (Otto *et al*., 2003; Watanabe *et al*., 2003; Simons *et al*., 2005). Inv can cooperate with Dvl and is thus able to inhibit the ability of Dvl to activate Wnt/β-catenin signalling (Simons *et al*., 2005). This led to the hypothesis that Wnt/β-catenin signalling is repressed by primary cilia. Gene knockdown experiments of the genes *Biedl-Bardet Syndrome 1*and *4* (*BBS1/4*) and *Kif3a* showed an stabilization of β-catenin and resulted in an upregulation of the Wnt/β-catenin pathway in cultured cells (Gerdes *et al.,* 2007).Mice mutant for the genes *Kif3a, Ift88* or *outer dense fiber of sperm tails 1 (odf1)* show an upregulation of canonical Wnt/ β-catenin signalling in mouse embryos (Corbit *et al*., 2008).

On the other hand other data implicates that primary cilia do not play an important role in canonical Wnt/β-catenin signalling. Zebrafish embryos mutant for the maternal-zygotic *ift88* exhibit a normal expression pattern of the canonical Wnt/β-catenin target genes *axin2, trans-acting transcription factor 5* (*sp5)* and *sp5 transcription factor-like* (*sp5l)* (Huang and Schier, 2009). In mice mutant for *Ift88, Ift72* or *Kif3a* no real Wnt-specific phenotypes were detected (Ocbina *et al*., 2009).

1.3.6.2 Primary cilia and non-canonical Wnt/PCP pathway

Non-canonical Wnt/PCP signalling is independent of the Axin/GSK3β/APC degredation complex and β-catenin. It is induced by binding of Wnt ligands to Fz and transmission of the non-canonical Wnt signalling needs Dvl which is localized to the plasma membrane (Fig. 15, lower panel) (Axelrod et al., 1998; Rothbacher et al., 2000; Seto and Bellen, 2004). Dvl acts through intercellular Ca^{2+} levels and by regulating RhoA, Rock, and Jnk kinase, all with crucial impact on the cytoskeleton and the regulation of planar cell polarity (PCP) (Fig. 15, lower panel) (Kikuchi *et al*., 2008).

As with the canonical Wnt/β-catenin signalling, the results for the role of primary cilia in non-canonical Wnt/PCP signalling is contradictary. Non-canonical Wnt/PCP signalling is important for convergent extension (CE), a process during development whereby the embryonic tissue is reorganized with the help of cell movements to narrow along one axis and to expandalong an upright axis (Sokol, 1996; Heisenberg *et al*., 2000; Tada and Smith, 2000; Wallingford *et al*., 2000). Defective CE results in incomplete neural tube closure in *Xenopus* as well as in mice (Wallingford and Harland, 2002; J. Wang *et al*., 2006; Y. Wang *et al*., 2006; Ybot-Gonzalez *et al*., 2007). Inv interacts with Dvl, which is involved in Wnt/β-catenin as well as in Wnt/PCP signalling (Simons *et al*., 2005), and the loss of Inv leads to defective CE (Simons *et al*., 2005). These findings led to the hypothesis that Inv, located at the primary cilium, acts as a switch between canonical Wnt/β-catenin and non-canonical Wnt/PCP signalling. In zebrafish the outcome of the mutation of the basal body proteins Bbs1, Bbs4 and Bbs6 are defects in convergent extension (Gerdes *et al*., 2007). The *Bbs* genes can interact with the PCP gene *van gogh-like 2* (*Vangl2*). *Vangl2* itself is localized to the axoneme and basal body of primary cilia (Ross *et al*., 2005). Mice mutant for the genes *Ift88* and *Ift20* exhibit non-canonical Wnt/PCP specific defects in the cochlear and kidney ducts (Jonassen *et al*., 2008; Jones *et al*., 2009). However, in Zebrafish embryos mutant for the maternal-zygotic *ift88* display normal convergent extension (Huang and Schier, 2009). Taken together, the role of primary cilia in both Wnt pathways is still disputed, and it may be that their function in the Wnt pathways is either specific for certain tissues and developmental stages or not as simple as thought at the beginning.

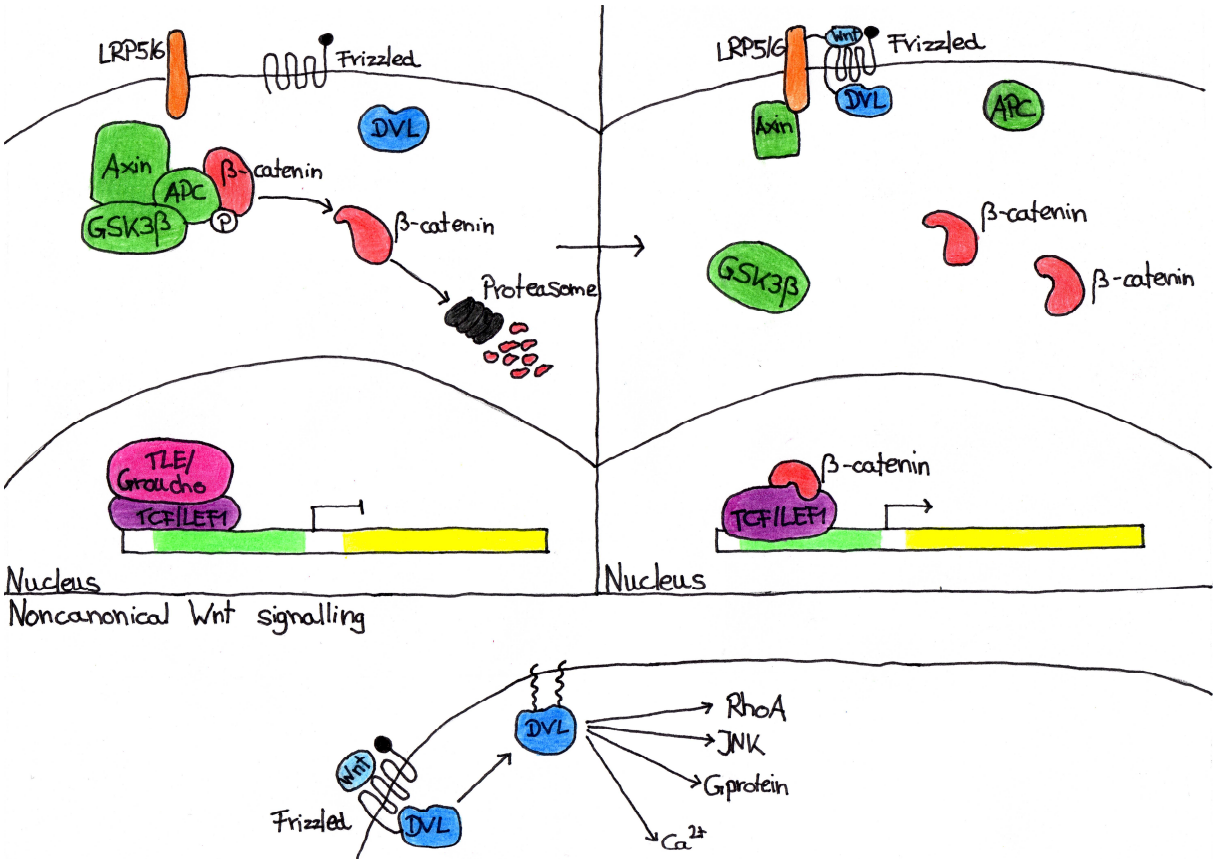

Fig. 15. The primary cilium and Wnt signalling. Upper left panel. β-catenin is phosphorylated in the absence of a Wnt signal by the β-catenin destruction complex, which is composed of Axin, APC and GSK3β. Phosphorylated β-catenin is the target for degradation. The transcription of Wnt target genes is suppressed by a complex of TCF/Lef1 and TLE. **Upper right panel.** The canonical Wnt signal binds to a receptor comples of Frz receptor and LRP5/6 coreceptor, which in turn binds to Axin and Dvl. This leads to a stabilization of β-catenin in the cytoplasm. β-catenin migrates then into the nucleaus, replaces TLE, which leads to an activation of TCF/Lef1/ β-catenin-responsive genes. **Lower panel.** The activated Dvl is targeted to the membrane by binding of a non-canonical Wnt signal to its receptor complex, which results in an activation of downstream target genes. (Adapted from Gerdes *et al*., 2009).

1.3.7 Primary cilia and brain patterning

Two studies have shown lately that primary cilia play a crucial role for the brain to develop normally. Misshaped cilia with a bulge at their distal tip are occur in mice with a null mutation of the gene *alien* (*aln*) in *tetratricopeptide repeat domain 21B* (*Ttc21b*). The gene encodes Ift139, a component of retrograde IFT. The bulges are packed with IFT components and even in the absence of Shh activation the primary cilia permanently produce Gli activators (Tran *et al*., 2008). However, anterograde IFT mutants have no cilia and fail to make Gli activators as well as Gli3 repressor. This indicates that both anterograde and retrograde IFT play different roles in mediating Hh signalling. Anterograde IFT seems to be required for the activation of Gli, whereas retrograde IFT seems to be needed for the restriction of the activity of Gli activators.

Ift139$^{aln/aln}$ mutants exhibit loss of dorsal cortex, dorsal-ventral patterning defects, and loss of a distinct boundary between telencephalon and diencephalon (Stottmann *et al*., 2009). These phenotypes resemble defects seen in *Gli3* mutants (Theil *et a*l., 1999; Tole *et al*., 2000; Fotaki *et al*., 2006), and the ratio of Gli3 full-length to Gli3 repressor is increased by 10-fold in *Ift139*$^{aln/aln}$ mutants compared to wild-type (Tran *et al*., 2008). The *Ift139*$^{aln/aln}$ mutants also exhibit ectopic Shh signalling activity, whereas in *Gli3* mutants this is not the case. The abrogation of one copy of *Shh* can to some extent rescue the *Ift139*$^{aln/aln}$ mutant phenotype (Stottmann *et al*., 2009), but it is not clear, how the loss of Ift139 enhances the expression of *Shh*.

In another study the gene *selective Lim-domain binding Slb* (*Slb*), which encodes the anterograde IFT component IFT172, was removed by gene targeting (Gorivodsky *et al*., 2009). The removal of *Slb* is responsible for the total loss of cilia and early patterning defects (Gorivodsky *et al*., 2009). The *Ift172*$^{slb/slb}$ mutants show as a phenotype the inability to express *Fgf8* in the midbrain-hindbrain boundary and in the commissural plate. They display as further phenotypes holoprosencephaly, exencephaly, truncation of forebrain, and a severe reduction in diencephalic structures. *Ift172*$^{slb/slb}$ mutants also exhibit a decrease in *Nodal* expression in the epiblast and the node between E7.0 and E7.5. The expression of *Nodal* in the epiblast is necessary for the formation of the AVE (Brennan *et al*., 2001), an important source of antiposteriorizing signals in mice (Kimura *et al*., 2000; Perea-Gomez *et al*., 2001). Mutations in genes important for the development of the AVE results in defects of the anterior neural plate including the telencephalon (Knoetgen *et al*., 1999; Perea-Gomez *et al*., 2000). The formation of the axial mesendoderm is also dependent on the expression of *Nodal* (Wall *et al*., 2000; Andersson *et al*., 2006), which is necessary for the *Fgf8* expression in the midbrain-hindbrain boundary and forebrain growth (Camus *et al*., 2000). *Fgf8* expression is responsible for the induction of markers for the prosencephalic identity in the anterior neuroectoderm (Shimamura *et al*., 1997; Shanmugalingam *et al*., 2000; Fukuchi-Shimogori *et al*., 2001), such as *Foxg1* (Fig. 7A) (Shimamura and Rubenstein, 1997; Ye *et al*., 1998). The onset of *Foxg1* expression at embryonic day 8.5 (E8.5) in mice marks the specification of the telencephalic primordium. The diminished *Nodal* expression further on explains the randomization of left-right asymmetry and failure to form anterior mesendoderm. The reported early phenotypes in *Ift172*$^{slb/slb}$ mutants lead to the hypothesis that Ift172 and primary cilia are active in tissues before neural tissue is established and thus influence the development of the brain.

1.3.8 Primary cilia and other brain structures

1.3.8.1 Primary cilia and hippocampal development

The granule neurons of the hippocampal dentate gyrus (DG) are mostly generated during early postnatal life. Besides the postmitotic neurons, also intermediate progenitors or granule neuron

precursors (GNPs) migrate away from the primary germinal zone in the ventricular zone (VZ) into the inner layer of the developing DG. There they will become postnatal neural stem cells that continue to produce new neurons during the whole life (Altman *et al*., 1990). The constant generation of new neurons in the DG is believed to be important for circuit plasticity, learning and memory. It has recently been shown that primary cilia play a crucial role for the expansion of embryonic neural progenitors and conversion into a population of radial astrocytes. They are thought to be the origin of primary progenitors in the postnatal DG (Breunig *et al*., 2008; Han *et al*., 2008). In the first study the gene *Kif3a* was conditional deleted by using a *hGFAP::Cre* mouse line (Han *et al*., 2008), and the second study used *nestin::Cre* mouse line to conditionally delete the gene *stumpy* (Breunig *et al*., 2008). The gene *stumpy* encodes a protein related to the basal body and cilia (Ponsard *et al*., 2007; Town *et al*., 2008). The number of proliferating GNPs was by both approaches severely diminished. A potential explanation for this phenotype is the increase in cell cycle exit (Breunig *et al*., 2008). A hypomorphic allele of *Ift88*, $Ift88^{orpk/orpk}$, as well as the homozygous mutation of $fantom^{-/-}$, which encodes a basal body protein, also exhibited a diminished proliferation of GNPs (Han *et al.*, 2008). This results further indicates that the phenotypes in the DG are connected with the loss of cilia.

1.3.8.2 Primary cilia and cerebellar development

The so called cerebellar GNPs (CGNPs) that have migrated away from the VZ are responsible for the postnatally generation of most of the cerebellar granule neurons. Shh, produced by the underlying Purkinje neurons, acts as a mitogen for CGNPs (Wallace *et al*., 1999; Wechsler-Reya *et al*., 1999; Dahmane *et al*., 2007). Primary cilia are necessary for the proliferation of the CGNPs. This is in agreement with the crucial role of primary cilia in Shh signalling. The conditional abrogation of *Kif3a*, *Ift88* or *stumpy* in CGNPs lead to severe hypoplasia and defective foliation of the cerebellum (Chizhikov *et al*., 2007; Breunig *et al*, 2008; Spassky *et al*., 2008). In the cerebellum of ciliary mutants the proliferation of the GNPs and also the expression of target genes of the Shh pathway are profoundly reduced. CGNPs devoid of primary cilia can not respond to Shh signalling *in vitro* (Spassky *et al*., 2008). Cerebellar development is also perturbed by mutations in the two basal bodies proteins Fantom and Oral-facial-digital syndrome 1 gene homolog Odf1 (Odf1) (Ferrante *et al*., 2006; Delous *et al*., 2007; Vierkotten *et al*., 2007).

2 Materials and Methods

2.1 Materials

2.1.1 General

2.1.1.1 Equipment

ABI PRISM 7000 Sequence Detection System	Applied Biosystems
Amaxa nucleofection device	Amaxa Biosystems
Autoclave Fedegari FVA3	Integra Biosciences GmbH, Fernwald, Germany
Avanti J-25 centrifuge	Beckman Coulter, USA
Biostatin IM	Nikon, Japan
Centrifuge MIKRO 20	Hettich, Tuttlingen
Confocal microscope C1si with spectral analysis	Nikon GmbH
CO_2 incubator, HERA cell 150	Kendro laborytory products GmbH, Thermo scientific
Compact shaker KS 15 control	Edmund Bühler GmbH, Germany
CPD 030 Critical Point Dryer	BAL-TEC, Wetzlar
Cryostat CM3050 S	Leica Microsystems, Nussloch
Curix60 table top processor	Agfa
Digital CCD camera F-View II	Soft Imaging Systems GmbH, Münster
Digital Camera COOLPIX 5000	Nikon, Japan
Digital Camera Leica DFC 320	Leica Microsystems Ltd, Heerbrug
E.A.S.Y 440 K CCD Camera	Herolab
Electrophorese chamber	Feinmechanikwerkstatt, University of Heidelberg
EM 906 Electron Microscope	Zeiss
Fastblot B33	Biometra
Fiber Optic Illuminator KL 1500 LCD	Leica
Fluorescence microscope BX61W1	Olympus Germany GmbH, Hamburg
Fluorescent confocal laser scanning microscope C1si	Nikon Instrument Europe B.v.
Fujinon Lens VRF 43LMD	Fujifilm
GS-800 USB Calibrated Densitometer	Bio-Rad Laboratories
Hybridisation Incubator 7601	GFL Gesellschaft für Labortechnik mbH, Germany
Incucell incubator	MS Laborgerätehandel, Wiesloch

Inverse fluorescent microscope CKX41	Olympus Germany GmbH, Hamburg
Kodak BioMax Cassette with BioMax MS Intensifying Screen	Kodak
Leica DMLB Microscope	Leica Mikroskopie und Systeme GmbH, Wetzlar
LEO 1530 Gemini	Zeiss, Oberkochen
Luminescent Image Analyzer LAS-3000	Fujifilm
Mastercycler Gradient	Eppendorf
MED 020 Coating Systems	BAL-TEC, Wetzlar
Microslicer DTK-1000	Dosaka EM Co., LTD
Mini-PROTEAN Tetra Cell	Bio-Rad Laboratories
Olympus U-RLF-T	Olympus
Oven Heraeus	Kendro, Thermo scientific
Owl B2 EasyCast Mini Gel System	Thermo Scientific
PCR cycler T*personal*	Whatmann Biometra, Göttingen
Plan Apo 1x WD70	Nikon
Potter S Homogenizer	Sartorius Stedim Biotech
Qualifreeze Cryo-Einfriergerät	Qualilab
Radiographic cassette	Dr. Goos-Suprema GmbH, Heidelberg
Rotary Microtome Leica RM 2235	Leica Microsystems
Seven easy pH meter	Mettler, Toledo
Short plates	Bio-Rad Laboratories
Spacer plates (0.75 mm / 1.0 mm)	Bio-Rad Laboratories
Spectrophotometer Ultrascope 3100 pro	Amersham, Biosciences
SIGMA laboratory centrifuge 2-5	Sigma Laborzentrifugen GmbH, Osterode, Germany
Stereomicroscope SMZ800	Nikon
Sterile hood, LaminAir model 1.2	Holten, Denmark
Ultramicrotome Ultracut UCT	Leica
Ultra Pure Water Purification System	membraPure GmbH, Germany
Ultra Turrax T8 Homogenizer	IKA Werke GmbH&Co.KG
UV Transilluminator UVT-20 S/L	Herolab
Veritas Microplate luminometer	Turner BioSystems
Water bath	Memmert, Schwabach

2.1.1.2 Special Software

AIDA Image Analyzer	raytest
AnalySIS	Soft Imaging Systems GmbH, Münster
Adobe Photoshop 7.0 and CS4	Adobe Systems
EndNote X3	Thomson Reuters
EZ-C1 Free Viewer 3.30	Nikon
ImageJ	Wayne Rasband NIH
Leica FireCam 3.1	Leica Microsystems
Quantity One	Bio-Rad Laboratories
4D Client	4D

2.1.1.3 Dissection tools

Fine forceps	Fine Science tools, Germany
Scissors	Fine Science tools, Germany

2.1.1.4 Consumables

96F Nunclon Delta White Microwell SI	Nunc
96 Well Optical Bottom Plate PolymerBase	Nunc
Amersham Hyperfilm ECL	GE Healthcare
Cellstar culture dishes and plates	Greiner Bio-One GmbH
Conical test tubes, RNase free, 15 ml/ 50 ml	nb nerpe plus
Coverslips (24x60 mm)	Roth, Karlsruhe
CryoS, cryo vials, PP, with screw cap	Greiner Bio-One GmbH
Hybond-N+ membrane	Amersham, Biosciences
Immobilon-P Transfer Membrane (VDF)	Millipore corporation
Leica 819 Low Profile Microtome Blades	Leica Microsystems
Micro Amp Optical 96-well Reaction Plate	Applied Biosystems
Microscope Slides Super Frost	Roth, Karlsruhe
Microscope Slides Superfrost Ultra Plus	Roth, Karlsruhe
Micro tubes (1.5 ml/ 2.0 ml)	Sarstedt, Germany
Novex Tris-Acetate SDS running buffer (20x)	Invitrogen
NuPage 3-8% Tris-Acetate gel (1.5 mm, 10 well)	Invitrogen
Optical Adhesive Film Kit	Applied Biosystems
Pasteur Capillary Pipetts (150 mm/ 230 mm)	WU Mainz

PCR cup (G002 / G003)	G. Kisker GbR
Probe Quant G-50 Micro Columns	Amersham, Biosciences
Ready-to-Go DNA Labelling beads (-dCTP)	GE Healthcare
Safe-Lock tubes (1.5 ml/ 2.0 ml)	Eppendorf
Stericup Filter Unit 0.22 µm	Millipore corporation
Sterile pipettes	Gibco, Invitrogen
Syringe driven filter unit 0.22 µm/ 0.45 µm	Millipore corporation
Tissue Culture Flasks (25 cm^2, 50 cm^2)	Greiner Bio-One GmbH
Tissue freezing medium	Jung, Leica, Nussloch, Germany
Tissue freezing molds	Polysciences Europe, Eppelheim, Germany
Razor blades	Thermo Fisher
3 MM Chromatography paper	Whatmann Int., England

2.1.1.5 Reagents

Aceton	Zentrallager INF 367, Heidelberg, Germany
Agar	Merck, KGaA, Darmstadt
Agarose	Roth, Karlsruhe
Ampicillin	Sigma-Aldrich
Aprotinin	Sigma-Aldrich
Azure II	Merck
B-Mercaptoethanol	Sigma-Aldrich
Benzyl benzoate	Sigma-Aldrich
Benzyl alcohol	Sigma-Aldrich
Boric acid	AppliChem
Bromphenol blue 4F057	Division Chroma, Münster
CHAPS	Fluka
Citric acid	Sigma-Aldrich
Chloroform	Fluka
Coomasie R 250	Serva
DAB	Sigma-Aldrich
DMSO	Acros Organics
Ethanol absolut puriss	Sigma-Aldrich
Ethidium bromide	Fluka
Formaldehyde (40%, m/v)	Carlo Erba Reagents
Glacial acetic acid	Sigma-Aldrich
Glutaraldehyde (25% solution)	Merck

Glycerol	Sigma-Aldrich
Glycine	Sigma-Aldrich
Hydrogen peroxide	Merck
Isopropanol	AppliChem
Kanamycin	Sigma-Aldrich
Lead(II) nitrate	Sigma-Aldrich
Leupeptin	Sigma-Aldrich
Maleic acid	Fluka
Methylene blue	Merck
MOPS	Sigma-Aldrich
Natriumchloride	Sigma-Aldrich
Nitric acid	Mallinckrodt Baker B.V.
Orange G	Sigma-Aldrich
Osmium tetraoxide (2% solution)	Polysciences, Inc.
PIPES	AppliChem
PMSF	Sigma-Aldrich
Polyvidon 25	Merk
Potassium ferrocyanide	Sigma-Aldrich
Roti-Phenol	Roth, Karlsruhe
Sodium cacodylate	Merck
Sodium citrate dihydrate	Sigma-Aldrich
Sodium tetraborate decahydrate	Sigma-Aldrich
Sucrose	Sigma-Aldrich
TEMED	Sigma-Aldrich
Tris	Roth, Karlsruhe
Uranyl acetate	Serva
Xylene cyanol	Sigma-Aldrich
Xylol	AppliChem

2.1.1.6 Reagents for Cell Culture

DMEM (41966)	Gibco, Invitrogen
FBS	Gibco, Invitrogen
FCS	Gibco, Invitrogen
L-Glutamine 200 mM (25030)	Gibco, Invitrogen
Pen Strep (14140)	Gibco, Invitrogen
Trypsin	Gibco, Invitrogen

2.1.1.7 Enzymes and Molecular Weight Markers

Taq-polymerase	Frementas
Proteinas K	Roth, Karlsruhe
25 bp ladder	Promega
50 bp ladder	Promega
100 bp ladder	Fermentas
1 kb bp ladder	Invitrogen
λ/Hind III ladder	Fermentas
2-Log DNA ladder (0.1-10.0 kb)	New England Biolabs
PageRuler Prestained Protein	Fermentas
peqGOLD Prestained Protein-Marker III	peqLab

2.1.1.8 Restriction Enzymes and Buffers

Apa I	New England Biolabs
BamH I	New England Biolabs
BspE I	New England Biolabs
Bstx I	New England Biolabs
BSA (100x)	New England Biolabs
Buffer P1 (10x)	New England Biolabs
Buffer P2 (10x)	New England Biolabs
Buffer P3 (10x)	New England Biolabs
Buffer P4 (10x)	New England Biolabs
Dra I	New England Biolabs
EcoR I	New England Biolabs
Hind III	New England Biolabs
Kpn I	New England Biolabs
Msc I	New England Biolabs
Nco I	New England Biolabs
Not I	New England Biolabs
Pst I	New England Biolabs
Pvu I	New England Biolabs
Pvu II	New England Biolabs
Sac I	New England Biolabs
Sal I	New England Biolabs
Sca I	New England Biolabs

Xba I	New England Biolabs
Xho I	New England Biolabs
Xmn I	New England Biolabs

2.1.1.9 Kits

BCA Protein Assay Kit	Thermo Scientific
Dual Luciferase assay system	Promega
ECL Plust Western Blotting Detection System	GE Healthcare
Gel Drying Frames	Roth, Karlsruhe
GenElute HP Plasmid Midiprep Kit	Sigma-Aldrich
GenElute HP Plasmid Miniprep Kit	Sigma-Aldrich
Nucleospin Extract II	Macherey and Nagel
QIAEX II Agarose Gel Extraction Kit	Quiagen
Rat Neuron Nucleofactor Kit	Amaxa Biosystems
RNeasy MiniKit	Quiagen
TOPO TA Cloning Kit for subcloning	Invitrogen
Zero Blunt TOPO PCR cloning Kit	Invitrogen

2.1.1.10 Vectors

pCMV-SPORT6	RZPD
pCRII-TOPO	Invitrogen
pCR2.1-TOPO	Invitrogen
pCR-BluntII-TOPO	Invitrogen
pSPORT-1	RZPD

2.1.1.11 Primers

2.1.1.11.1 Primers for Genotyping

The primers were ordered from the company Thermo Fisher Scientific GmbH for genotyping:

cbs	
D14Mit62 F	5´-AGG ACT CAA TGA GCA GGG AA-3´
D14Mit62 R	5´-ACT CTC CTG CCA CCC CTC-3´
D14Mit121 F	5´-TTG ACA TCT GGA TAT GAC AAT GC-3´
D14Mit121 R	5´-TGT GCA TGT TTG TGT ACA TAT GTG-3´
D14Mit141 F	5´-CCA GCA TTC CGA AGT CAT TT-3´
D14Mit141 R	5´-AGG GAA AGA AGA CAG CAC GA-3´
D14Mit259 F	5´-TGG TGT CTC CTT CGG AAT TT -3´
D14Mit259 R	5´-TAA ATG TAA AAG GTA AAG GCA ATG G-3´
Gli3^{XtJ}	
XtJ580 F	5´-TAC CCC AGC AGG AGA CTC AGA TTA G-3´
XtJ580 R	5´-AAA CCC GTG GCT CAG GAC AAG-3´
C3 F	5´-GGC CCA AAC ATC TAC CAA CAC ATA G-3´
C3 R	5´-GTT GGC TGC TGC ATG AAG ACT GAC-3´
Ift88$^{tm1.1Bky}$	
BY598 (common 5´ primer)	5´-GCC TCC TGT TTC TTG ACA ACA GTG-3´
BY919 (3´ flox and WT allele primer)	5´-GGT CCT AAC AAG TAA GCC CAG TGT T-3´
BY956(3´ delta allele primer)	5´-CTG CAC CAG CCA TTT CCT CTA AGT CAT GTA-3´
tauGFP	
WT-F	5´-CTC AGC ATC CCA CCT GTA AC-3´
WT-R	5´-CCA GTT GTG TAT GTC CAC CC-3´
KO-F	5´-CAG GTC TTG AAC CAG TAT GG-3´
KO-R	5´-TGA ACT TGT GGC CGT TTA CG-3´

2.1.1.11.2 Primers for Sequencing

The primers were ordered from the company Thermo Fisher Scientific GmbH for sequencing the open reading frame of the gene *Ift88*:

IFT88pp1 F	5´-GGC CTG CCT AGG ATC AGG-3´
IFT88pp1 R	5´-CTT GCT CTC GTT GTC TCA CC-3´
IFT88pp2 F	5´-ACA GGG ACA ATT CAG GAT GG-3´
IFT88pp2 R	5´-AAA GAC GCT TCG ATC ACA GG-3´
IFT88pp3 F	5´-TCG GGA GAA AAT GAA GAA GG-3´
IFT88pp3 R	5´-GGG AAT CAG TTG GAA CAA CG-3´
IFT88pp4 F	5´-CTG AAC CGT CTG GAT GAA GC-3´
IFT88pp4 R	5´-TGG CAC TCA GTC GTT CAC TC-3´
IFT88pp5 F	5´-AAG TGG CAG CTG ATG GTA GC-3´
IFT88pp5 R	5´-TGG AGG ACC TGA GTT CAA GC-3´
IFT88pp6 F	5´-TGA ATG TTT GCG TTT CTT GG-3´
IFT88pp6 R	5´-GAC AGC ACA AAC CCA TCC TC-3´
IFT88pp7 F	5´-CAC CTT AGG CAA ATG GAA CG-3´
IFT88pp7 R	5´-CGC AAA CAT TCA ACA TTC TCC-3´

2.1.1.11.3 Primers for testing of the cDNA-Quality

The primers were ordered from the company Thermo Fisher Scientific GmbH and used for testing the quality of the cDNA after the *in vitro* translation:

G3PDH F	5´-AAC ACA GTC CAT GCC ATC AC-3´
G3PDH R	5´-TCC ACC ACC CTG TTG CTG TA-3´

2.1.1.11.4 Primers for real time RT-PCR

The following TaqMan Gene Expression Assays were ordered from Applied Biosystems and used for qPCR:

Number	Gene	Species	Amplicon Length
Mm_01265783_m1	*Axin2*	mouse	114
Mm_00494654_m1	*Gli1*	mouse	83
Mm_00493675_m1	*Ift88*	mouse	79
Mm_00436031_m1	*Ptch1*	mouse	135
Mm_00437357_m1	*Wnt7b*	mouse	62
Mm_00442108_m1	*Wnt8b*	mouse	72

Table 1: TaqMan Gene Expression Assays

2.1.2 Histology

2.1.2.1 General Reagents

Aqua-Poly/Mount	Polysciences Europe, Eppelheim, Germany
Aquatex	Merck
Entellan	Merck
Immune Edge Pen	Vector Laboratories Inc, Burlingame
Paraplast-Plus	Roth, Karlsruhe
Roti-Liquid Barrier Marker	Roth, Karlsruhe
Triton X-100	Roth, Karlsruhe
Tween-20	Roth, Karlsruhe

2.1.2.2 Alcian Blue Staining

Alcian Blue 8 GX	Sigma-Aldrich

2.1.2.3 Hemotoxylin-Eosin staining

Eosin	Division Chroma, Münster, Germany
Hemotoxylin	Sigma-Aldrich

2.1.2.4 Fluorescent Immunohistochemistry

2.1.2.4.1 Sera

Bovine serum albumine	Roth, Karlsruhe
Native goat serum	Sigma-Aldrich

2.1.2.4.2 Dyes

DAPI	Sigma-Aldrich

2.1.2.4.3 Primary Antibodies

Epitope	Species		Dilution	Source
β-Galactosidase (Clone 55976)	rabbit	polyclonal	1:2000	ICN/Cappel
β-Tubulin III (TuJ1 clone)	mouse	monoclonal	1:1500	Covance
Nestin (Rat 401 clone)	mouse	monoclonal	1:500	BD PharMingen
Pax6 (AB5409)	rabbit	monoclonal	1:3000	Millipore
Phospho-histone H3 (Ser10, rabbit 06-750)	rabbit	polyclonal	1:200	Upstate
RC2	mouse	monoclonal	1:10	DSHB
2H3 (anti-165 kDA neurofilament)	mouse	monoclonal	1:100	DSHB

Table 2: Primary antibodies

2.1.2.4.4 Secondary Antibodies

Name	Dilution	Source
Goat anti-mouse Alexa Fluor 488	1:1000	Invitrogen
Goat anti-mouse Alexa Fluor 546	1:1000	Invitrogen
Goat anti-rabbit Alexa Fluor 488	1:1000	Invitrogen
Goat anti-rabbit Alexa Fluor 546	1:1000	Invitrogen

Table 3: Secondary antibodies

2.1.2.5 *In situ* Hybridization

2.1.2.5.1 Reagents

Blocking Reagent (Boehringer Block)	Roche
CHAPS	Fluka
DEPC	AppliChem
DIG RNA Labeling Mix, 10x. Conc.	Roche
Formamide	Sigma-Aldrich
Glutaraldehyde (25% solution)	Merck
Glycine	Sigma-Aldrich
Heparin	Sigma-Aldrich
NBT/BCIP stock solution	Roche
Ribolock RNase Inhibitor	Fermentas
RNaseZAP	Sigma-Aldrich
5x Transcriptionbuffer	Fermentas
Yeast tRNA	Roche

2.1.2.5.2 Antibodies

Anti-Digoxigenin-AP, Fab fragments	Roche

2.1.2.5.3 Enzymes

RNA Polymerase (T3, T7, Sp6)	Fermentas

2.1.3 Plasmids

2.1.3.1 *In situ* hybridization

mRNA probe	**Reference/ Origin**
Axin2	Theil, 2005
Dbx1	Yun *et al*, 2001
Dlx2	Theil, 2005
Emx1	Kuschel *et al*, 2003
Emx2	Kuschel *et al*, 2003
EphB1	Kind gift from D. Wilkinson, National Institute for Medical Research, London

Foxd1	Hatini *et al*, 1996
FoxG1	Tao and Lai, 1992
Gli3	Kind gift from A. Joyner, Skirball Institute, New York, NY
Lhx2	Porter *et al*, 1997
Ngn2	Kuschel *et al*, 2003
Pax6	Kuschel *et al*, 2003
Ptch1	Goodrich *et al*, 1996
Reelin	Theil, 2005
Shh	Kind gift from M. Treier, EMBL, Heidelberg, Germany
Ttr1	Duan *et al*, 1989
Wnt2b	Kuschel *et al*, 2003
Wnt7b	Theil, 2005
Wnt8b	Kind gift from J. Mason, University of Edinburgh, Edinburgh, UK

Table 4: mRNA probes

2.1.3.2 Northern blot analyis

Ift88 cDNA	RZPD
Gli3 cDNA	RZPD
α-tubulin cDNA	Lemischka *et al*., 1981

Table 5: Northern blot probes

2.1.4 Antibodies for Western blot analysis

2.1.4.1 Primary antibodies

Epitope	**Species**	**Dilution**	**Source**
Ift88	goat	1:1000	Pazour *et al*., 2002
Gli3 (s.c.-20688)	rabbit	1:1000	Santa Cruz Biotechnology
β-actin (clone AC-15)	mouse	1:5000	Sigma

Table 6: Primary antibodies for WB analysis

2.1.4.2 Secondary antibodies

Name	Dilution	Source
HRP-conjugated mouse anti-goat IgG (cs-2354)	1:10.000	Santa Cruz Biotechnology
HRP-conjugated goat anti-rabbit IgG	1:10.000	KPL
HRP-conjugated goat anti-mouse IgG	1:10.000	KPL

Table 7: Secondary antibodies for WB analysis

2.1.5 Animals

Mouse embryos (*Mus musculus domesticus*) of the following mouse lines were used for experiments:

tauGFP	ENU mutagenesis screen	AG Tucker, IBF Heidelberg
cbs	Positional cloning, Northern blot, Western blot, Cryosections, Paraffinsections, Cell culture, Scanning and Transmission electron microscopy, Complementation analysis	AG Tucker, IBF Heidelberg
$Gli3^{XtJ}$	Northern blot, Western blot	Lab of Prof. Ulrich Rüther, University of Düsseldorf, Germany; AG Tucker, IBF Heidelberg (Hui and Joyner, 1993)
$Ift88^{tm1.1Bky}$	Complementation analysis	Lab of Bradley K. Yoder, Birmingham, USA (Haycraft *et al*., 2007); AG Tucker, IBF Heidelberg
$Ift88^{\lambda 2\text{-}3\beta gal}$	Cryosections	Lab of Richard P. Woychik, Alameda, USA (Murcia *et al*, 2000)
C57BL/6J	Maintaining the colonies in general	Charles River
CBA/J	Maintaining the *cbs* colony	Janvier

Table 8: Mouse colonies

2.1.6 Solutions and buffers

2.1.6.1 General

1x PBS (pH 7.4)	140 mM NaCl 2.7 mM KCl 10 mM KH_2PO_4

2.1.6.2 Gel electrophoresis

50x TAE	2 M TRIS 0.05 M EDTA pH 8.0 57.1 ml glacial acetic acid (96%)
5x TBE	0.45 M TRIS 0.01 M EDTA pH 8.0 0.04 M Boric Acid
10x Orange G	0.006 % (w/v) Orange G 50% Glycerol 50% MP-Water
10x Xylene cyanol	0.006% (w/v) Xylene cyanol 50% Glycerol 50% MP-Water
Ethidium bromide	0.5 µg/ml 100 ml 1x TAE
Lysis buffer (Tail buffer)	0.1 M Tris-Cl (pH 8.5) 5 mM EDTA (pH 8.0) 0.2% (w/v) SDS 0.2 M NaCl 100 µg/ml Proteinase K

2.1.6.3 Microbiology

LB-Medium	1% (w/v) NaCl 1% (w/v) Trypton 0.5% (w/v) Yeast extract
Agar plates	1.2% (w/v) Bacto-Agar 0.8% (w/v) Bacto-Tryptone 0.8% (w/v) Bacto Yeast-Extract 0.8% (w/v) NaCl

2.1.6.3.1 Antibiotics

Antibiotic	Stock concentration	Final concentration
Ampicillin	50 mg/ml	0.1 mg/ml
Kanamycin	10 mg/ml	0.05 mg/ml

Table 9: Antibiotics

2.1.6.4 Northern Blot

20x SSC, pH 7.0	3 M NaCl 3.3 M $Ca_6H_5Na_3O_7*2H_2O$
Church buffer	1% (w/v) BSA 1mM EDTA (pH 8.0) 7% (w/v) SDS 0.5 M Phosphate buffer
Phosphate buffer	1 M Na_2HPO_4 1 M NaH_2PO_4
5x Formaldehyde running buffer	0.1 M MOPS 40 mM NaAcetat 5mM EDTA (pH 8.0)

RNA Gel loading buffer	95% (w/v) deionized Formamide 0.025% (w/v) Bromphenol blue 0.025% (w/v) Xylene cyanol 5mM EDTA (pH 8.0) 0.025 % (w/v) SDS
TE buffer (pH 8.0)	10 mM Tris-HCl (pH 8.0) 1 mM EDTA (pH 8.0)
Washing solutions	1x – 0.1x SSC/ 1% - 0.1% SDS

2.1.6.5 Western Blot

10x TBS	1.4 M NaCl 0.03 M KCl 0.25 M Tris-HCl (pH 7.5)
TBST	1x TBS 0.1% - 0.25% (v/v) Tween-20
SDS-Running buffer	25 mM TRIS 1.92 M Glycine 1% (w/v) SDS
Transfer buffers	
Anode I	0.3 M TRIS (pH 10.4) 20% (v/v) MeOH
Anode II	25 mM TRIS (pH 10.4) 20% (v/v) MeOH
Cathode	25 mM TRIS (pH 9.4) 40 mM 6-amino-n-caproic acid 20% (v/v) MeOH
Blocking buffers	1x TBS 0.1% (v/v) Tween-20 5% (w/v) Milk

	1x TBS 0.1% (v/v) Tween-20 5% (w/v) BSA
	1x PBS 10% (v/v) Goat serum 0.25% (v/v) Tween-20
5x Laemmli-SDS buffer	0.125 M TRIS-HCl (pH 6.8) 5% (w/v) SDS 5% (v/v) β-MercaptoEtOH
Buffer H	20 mM TRIS-HCl (pH 7.4)
5x Gel Loading buffer	312.5 mM TRIS-HCl (pH 6.8) 50% (v/v) Glycerol 0.05% (v/v) Bromphenol blue

2.1.6.5.1 Proteinase inhibitors

Inhibitor	Stock concentration	Final concentration
Leupeptin	1 mg/ml	1 µg/µl
Aproptin	10 mg/ml	1 µg/µl
PMSF	17 mg/ml	17 µg/µl

Table 10: Proteinase Inhibitors

2.1.6.5.2 Coomassie staining

Coomassie	0.25% (w/v) Coomassie 40% (v/v) MeOH 10% (v/v) Glacial acetic acid
Destaining solution	50% (v/v) MeOH 10% (v/v) Glacial acetic acid

2.1.6.6 Immunohistochemistry

Antigen retrieval buffer (pH 6.0)	10 mM Tris-Sodium-Citrate (dihydrate)
Blocking buffer	1% (v/v) BSA 5% (v/v) NGS 0.25% (v/v) TritonX-100
Washing solutions	1x PBS

2.1.6.7 *In situ* Hybridization

10x PBS	1.37 M NaCl 0.027 M KCl 0.015 M KH_2PO_4 0.065 M Na_2HPO_4*$2H_2O$
Proteinase K	20 µg/ml in 1x PBS
PBST	1x PBS 0.1% (v/v) Tween-20
Hybmix	50% (v/v) Formamide 5x SSC (pH 4.5) 10 mg/ml Boehringer Block 0.005 M EDTA (pH 8.0) 0.1% (v/v) Tween-20 0.1% (v/v) CHAPS 0.02 mg/ml Heparin 1mg/ml tRNA
B-Block	2% (w/v) Boehringer Block 0.1 (v/v) Tween-20 10% (v/v) NGS
NTM	0.1 M Tris-HCl (pH 9.5) 0.1 M NaCl

	0.05 M $MgCl_2$
20x SSC	3 M NaCl 3.3 M $Ca_6H_5Na_3O_7*2H_2O$
Solution I	50% (v/v) Formamide 2x SSC

2.1.6.8 Electron microscopy

2.1.6.8.1 Scanning electron microscopy

Fixation buffers	2.5% (v/v) Glutaraldehyde 0.1 M PIPES (pH 7.4)
	1% (v/v) OsO_4
Washing buffer	0.15 M PIPES (pH 7.4)

2.1.6.8.2 Transmission electron microscopy

Fixation buffers	2.5% (v/v) Glutaraldehyde 2% (v/v) PVP (MW 25000) 0.1 M PIPES buffer (pH 7.6)
	1.5% (v/v) OsO_4 1.5% (w/v) $C_6N_6FeK_4$
Na-cacodylate buffer (0.1 M)	0.1 M $Na(CH_3)_2AsO_2*3H_2O$ (pH 7.6)
Teorell-Stenhagen buffer (0.05 M, pH 10.0)	0.05 M H_3PO_4 0.05 M H_3BO_3 0.03 M $C_6H_8O_7$ 0.345 M NaOH

DAB	0.01 M Teorell-Stenhagen buffer (pH 10.0) 0.15 % (v/v) H_2O_2 0.01 M DAB
Osmification buffer	1.5% (v/v) OsO_4 0.1 M Na-cacodylate buffer (pH 7.6)
Maleat buffer	0.2 M $C_4H_4O_4$ 1 N NaOH
Uranyl acetate staining solution	1% (w/v) $UO_2(CH_3COO)_2*2H_20$ 0.05 M Maleatbuffer (pH 5.2)
Epon	1.5 M Epoxy embedding medium 1 M Epoxy embedding medium hardener DDSA 1.8 M Epoxy embedding medium hardener MNA 1.5 % (v/v) Epoxy embedding medium accelerator
Azure II solution	1% (w/v) $C_{16}H_{18}N_8S*C_{15}H_{16}N_3S*2Cl$
Methylene blue solution	1% (w/v) $C_{16}H_{18}ClN_3S*3H_2O$ 1% (w/v) $Na_2B_4O_7*10H_2O$
Richardsons staining solution	0.5% (v/v) Azure II 0.5% (v/v) Methylene blue 0.5 M $C_{12}H_{22}O_{11}$
Lead citrate staining solution (pH 12.0)	0.08 M $Pb(NO_3)_2$ 0.12 M $Na_3(C_6H_5O_7)*2H_2O$

2.1.6.9 Tissue culture

CRYO/Freezing medium	20% (v/v) DMSO (tissue culture grade) 30% (v/v) FBS 50% (v/v) DMEM

MEF medium	DMEM 10% (v/v) FCS 100 U/ml penicillin/streptomycin 2 mM L-Glutamine
2x Trypsin	1x PBS 0.1% (v/v) Trypsin 1.1 mM EDTA

2.1.6.10 Fixatives

4% PFA (pH 7.4)	4% (w/v) PFA 2 N NaOH 1x PBS
2% Glutaraldehyde	2% (v/v) Glutaraldehyde 1x PBS
Bouin´s solution	75% saturated aqueous picric acid solution 25% formaldehyde (40%) 5% glacial acetic acid

2.1.6.11 Bacteria

DH5α Competent *E. coli*	Invitrogen
One Shot TOP10 Competent *E. coli*	Invitrogen

2.2 Methods

2.2.1 Animal handling

The mouse experiments were carried out according to the guidelines of the University of Heidelberg and the State of Baden-Württemberg.

2.2.1.1 Tansgenic lines

The mice were kept in the animal facility of the University of Heidelberg (IBF). They were exposed to light from 6.00 am to 6.00 pm. The programme 4D Client (TierBase) was used to set up matings on

Monday and female animals were controlled for vaginal plug from Tuesday to Friday by the animal care taker. Embryonic day (E) 0.5 was assessed at noon of the day when the vaginal plug was detected.

2.2.1.1.1 tauGFP mice

The tauGFP mouse line was generated as described in Tucker *et al*, 2001. The mouse line was backcrossed to wild-type C57BL/6J mice for over ten generations to maintain it as a homozygous mutation. It was already at the IBF Heidelberg and only had to be maintained there.

2.2.1.1.2 cbs mice

The *cbs* mouse line was generated as described in Willaredt *et al*, 2008. The mouse line was outcrossed to wild-type mice of the inbred strain CBA/J for positional cloning. It was further on backcrossed to wild-type CBA/J and C57BL/6J mice for over ten generations to maintain the heterozygous strain background. It was already at the IBF Heidelberg and only had to be maintained there. Mutant embryos resulting from matings between adult animals heterozygous for *cbs* are termed *cbs/cbs* in this study.

2.2.1.1.3 Gli3^{XtJ} mice

The *Gli3*^{XtJ} mouse line (Hui and Joyner, 1993) was imported from the lab of Prof. Dr. Rüther at the Heinrich Heine University of Düsseldorf, Germany. After a rederivation at the IBF of the University of Heidelberg, we received several litters to set up a new colony.
Genotyping by PCR identified animals heterozygous for *Gli3*^{XtJ}, which were mated to obtain homozygous Gli3^{XtJ} mutant mouse embryos. Male mice heterozygous for *Gli3*^{XtJ} were also mated with wild-type C57BL/6J female mice to maintain the colony. Mutant embryos resulting from matings between adult animals heterozygous for *Gli3*^{XtJ} are termed *Xt*^{J} in this study.

2.2.1.1.4 Ift88$^{tm1.1Bky}$ mice

The *Ift88*$^{tm1.1Bky}$ mouse line (Haycraft *et al*., 2007) was imported from the lab of Prof. Bradley K. Yoder at the University of Alabama, Birmingham, USA. After a rederivation at the IBF of the University of Heidelberg, we received several litters to set up a new colony.
Genotyping by PCR identified animals with the following genotypes: wt/wt, flox/wt or Δ/wt. For maintaining of the colony male *Ift88*$^{flox/wt}$ and *Ift88*$^{\Delta/wt}$ mice were mated with wild-type C57BL/6J female mice. Male *Ift88*$^{\Delta/wt}$ were mated with female *cbs*/+ mice for a complementation analysis.

Resulting compound heterozygous embryos for both alleles are termed *Ift88^{ko}/cbs* in this study, whereas embryos heterozygous for only one of the alleles are termed either *Ift88^{ko}*/+ or *cbs*/+.

2.2.1.1.5 Ift88$^{\Delta 2\text{-}3\beta gal}$ mice

Embryos carrying the *Ift88$^{\Delta 2\text{-}3\beta gal}$* allele (Murcia *et al*, 2000) were received from the lab of Prof. Richard A. Woychik at the Parke-Davis Laboratory of Molecular Genetics, Alameda, California, USA. The embryos were sent to Germany in 1x PBS. Tail samples were taken for genotyping by PCR and embryos were embedded for cryosections. Embryos used in this study are termed *Ift88$^{\Delta 2\text{-}3\beta gal}$*.

2.2.2 Molecular biology

2.2.2.1 Isolation of genomic DNA from embryonic and adult tissue

For the isolation of genomic DNA from embryonic and adult tissue a modification of the protocol of Laird *et al*., 1991 was used.

500 µl of lysis buffer containing 100 µg/ml Proteinase K was added to each sample of adult tissue (tail biopsy) or embryonic tissue. Digestion took place o/N at 55°C under agitation. 500 µl of isopropanol was added to each sample, mixed thoroughly and put to -80°C for one hour, followed afterwards by a centrifugation step for thirty min at 4°C at 13.000 rpm. The supernatant of each sample was discarded and the pellets washed with 300 µl of 70% ethanol in another centrifugation step at RT at 13.000 rpm for ten minutes. The 70% ethanol was removed carefully by aspiration and the DNA pellets were air dried. Afterwards the DNA pellets were dissolved in 60-100 µl of water or 10 mM Tris-HCl, pH 8.5, o/N at 55°C under agitation.

2.2.2.2 Polymerase chain reaction (PCR)

DNA fragments were amplified using taq-Polymerase which was applied in optimized concentrations. For genotyping the different adult mice and embryos used for the experiments, specific primers were utilized (2.1.1.6.1 Primers for genotyping).
A standard PCR mix was as follows:

16.2 µl	H2O
02.0 µl	10x PCR reaction buffer
00.4 µl	10 µM Primer F
00.4 µl	10 µM Primer R
00.4 µl	10 mM dNTPs

00.1 µl Taq-Polymerase
00.5 µl DNA (50-300 ng)

2.2.2.3 Gel electrophoresis

Gel electrophoresis was performed to identify the correct DNA size of PCR products, to verify the results of digestion reactions of plasmid DNA and for separation of RNA for Northen blot (NB) analysis and proteins for Western blot (WB) analysis.

For the separation of DNA fragments of PCR products and digestions 0.75%-2% agarose gels were normally used, prepared with 1x TAE buffer and 0.5 µg/ml ethidiumbromide and run at 100-130 V at RT. In the case of the genotyping of *cbs*, the DNA fragments were separated using 12% acrylamide gels, prepared with 1x TBE buffer run at 120-140 V at RT. The acrylamidegels were stained with 0.5 µg/ml ethidiumbromide diluted in MP-H_2O.

Proteins were separated by using either 10% acrylamidegels or NuPage 3-8% Tris-Acetate gel (1.5 mm, 10 well).

Total RNA was separated by using 1.2% denaturating agarose/ formaldehyde gel with 0.5 µg/ml ethidiumbromide and 1x Formaldehyde running buffer.

2.2.2.4 Positional cloning

A panel to detect single polymorphisms (SNPs) was constructed from primer triplets, spread evenly across the mouse genome, that specifically amplify SNPs between the C57BL/6 and DBA/2 inbred strains. The two SNP-hybridizing primers in each triplet were recognized by fluorescently labelled primers (Amplifluor SNPs HT Genotyping System for FAM-JOE, Millipore) for use in a Stratagene MX3000P real-time PCR device. Segregating *cbs* embryos were examined using hundred markers covering the twenty murine chromosomes, looking for SNPs in which homozygous *cbs* mutants were enriched for a homozygous C57BL/6 result. SNP analysis identified one marker on chromosome 14 that closely cosegregated with the *cbs* mutants (see Fig. 5). Fine mapping was performed with chromosome 14 SSLP markers (see Fig. 5) (Dietrich *et al*., 1994), which were resolved on 12% acrylamide gels (2.2.2.3 Gelelectophoresis). For *Ift88* sequencing, total mRNA was isolated from E12.5 embryonic brain using the RNeasy Mini Kit according to the manufacturer´s instructions. Total mRNA was reversed transcribed with oligo$(dT)_{12\text{-}18}$ and SuperScript reverse transcriptase according to the manufacturer´s instructions. PCRs were done with *Ift88* specific primers (see 2.1.1.6.2 Primers for sequencing), followed by agarose gel purification of the PCR products and subcloning them into the pCRII-TOPO vector. Sequencing was undertaken by the company MWG with appropriate primers.

2.2.2.5 Quantitative real time RT-PCR

Whole RNA was extracted from embryonic tissue using RNeasy Mini Kit according to the manufacturer´s instructions. 1-5 µg of total RNA was transcribed into cDNA using oligo$(dT)_{12-18}$ (0.5 µg/µl) or random hexamers (50 mM) and SuperScript Ⅱ RNase H^- reverse transcriptase. The quality of the cDNA was assessed by PCR with specific primers for *GAPDH* (2.1.1.6.3 Primers for testing of the cDNA-Quality). Quantitative real time PCRs were performed using TaqMan Gene Expression Assays (2.1.1.6.4 Primers for real time RT-PCR) with 1 µl of cDNA (20 µl of RTase reaction using 1-5 µg of whole RNA input). The standard quantification protocol was applied with the following cycles: 2 min at 50°C, 10 min at 95°C, followed by 45 cycles: 43 seconds at 95°C and 1 min at 60°C. Each individual reaction was performed in triplicate. Primers specific for *GAPDH* (Mm99999915_g1) were used to normalize results.

Statistical analysis was performed as follows: Relative expression (RE) levels were calculated with the function ($RE = 2^{-\Delta\Delta Ct}$), where ΔΔCt is the normalized difference in threshold cycle (Ct) number between wt and *cbs/cbs* samples, calculated from the mean Ct value of triplicate replicates of any given condition. The mean of the RE was calculated from the individual values from four to six independent experiments, and the SEM was calculated from the standard deviation of the four to six values. Statistical significance was evaluated by applying the Student´s *t* test to the four to six values, comparing wt to *cbs/cbs* samples. Application of Student´s *t* test to the original ΔΔCt values produced comparable p values.

2.2.3 Microbiology

2.2.3.1 Agar plates

Bacto-agar, bacto-tryptone, bacto-yeast and NaCl were weighed according to the recipe and put into 1 L bottle. 800 ml of MP-H_2O were added, shaked and let stand for ten min at RT. After autoclaving and cooling down to approximately 60°C, desired antibiotic was added and poured into 10 cm bacterial plates. After further cooling down and hardening of the agar, the plates were stored upside down at 4°C.

2.2.3.2 Transformation

An aliquot of 100 µl of DH5α competent *E. coli* cells was thawed on ice, followed by adding 1-5 µl of plasmids and incubation for 20-30 min on ice. Bacteria were then heat shocked for 1 min at 42°C and put directly afterwards on ice for 1 min. 900 µl of LB medium were added and cells were incubated for one hour at 37°C at 230 rpm. During incubation of the bacteria on the shaker, bacterial

agar plates from 4°C were put into the incubator at 37°C with slightly opened lids. Different volumes (50-200 µl) of the bacteria were plates on the pre-warmed bacterial agar plates and incubated o/N at 37°C.

2.2.3.3 Liquid cultures of *E. coli*

For medium-scale preparations of plasmid DNA 100 ml of LB-medium that contained the desired antibiotic were inoculated with a single colony of transformed bacteria. The liquid cultures of *E. coli* were incubated o/N at 37°C at 230 rpm. The bacterial cultures were centrifuged for 10 min at 5000 rpm at 4°C the next day and the bacterial pellets were frozen away for at least one hour or o/N at -80°C. Cell lysis and Mini/Midiprep were undertaken according to the manufacturer´s instructions. The resulting pellets were dissolved in 10 mM Tris-HCl, pH 8.5, and concentration was measured by spectrophotometry.

2.2.4 Electron microscopy

2.2.4.1 Transmission electron microscopy (TEM)

E12.5 old mouse embryos were collected in cold 1x PBS and fixed for 10 min by transcardial perfusion using a glass micropipette with 2.5% glutaraldehyde in 0.1 M PIPES buffer, pH 7.6, containing 2% polyvinylpyrrolidone. The mouse embryos were additionally fixed for another hour in the same fixative after immersion fixation. After the final fixation 300 µm-thick coronal vibratome sections of the brain were prepared and incubated in the alkaline diaminobenzidine hydrochloride medium as described previously (Gorgas, 1984) for 60 min for enhancement of membrane staining, and postfixed with 1.5% osmium tetraoxide containing 1.5% potassium ferrocyanide for one hour, followed by an additional one hour osmification with 1.5% osmium tetraoxide in 0.1 M sodium cacodylate buffer. The slices were then stained *en bloc* in 1% uranyl acetate for 30 min, dehydrated through a graded ethanol series and embedded in Epon 812. Series of semithin sections were stained with a modified Richardson methylene blue-azure II solution and used for selection of corrospending areas in wild-type and mutant brains. Ultrathin sections were stained with lead citrate and analyzed by electron microscopy using a Zeiss EM 905E.

2.2.4.2 Scanning electron microscopy (SEM)

Heads of E12.5 old embryos were fixed overnight (o/N) at 4°C in 2.5% glutaraldehyde/ 0.1 M PIPES, pH 7.4, and subsequently washed three times in 0.15 M PIPES, pH 7.4, at 4°C. The fixed samples were then embedded in 3% agarose and cut into 300 µm coronal slices in 1x PBS using a

vibratome. The slices were treated for one hour at room temperature (RT) with 1% osmium tetraoxide, washed three times with 0.15 M PIPES, pH 7.4, and subsequently dehydrated through a graded ethanol series. The specimens were dried in a CPC 030 critical point dryer, using CO_2 as a transitional medium, followed by sputter coating of a 20 nm Gold film. For scanning electron microscopy (SEM), a LEO 1530 field emission scanning electron microscope with a Schottky cathode was used (LEO Elektronmikroskopie).

2.2.5 Histology

2.2.5.1 Fixation of embryos

E12.5 old mouse embryos were collected in cold 1x PBS, and embryonic tail samples were collected separately for DNA extraction and genotyping. The embryos were then placed into 4% PFA and fixed o/N at 4°C under agitation. PFA was washed out the next day with 1x PBS before the mounting of the embryos.

2.2.5.2 Embedding of embryos

2.2.5.2.1 Embedding for cryosections

Serial steps of 10%, 20% and 30% Sucrose in 1x PBS were undertaken o/N at 4°C under agitation. The embryos were then placed in small “Peel-Away” mounting moulds that had been before half-way filled with mounting medium (tissue-tek). After 1 hour of incubation in the mounting medium the embryos were orientated as desired and the bottom of the mould was quickly frozen in liquid nitrogen, to fix the embryos in position. The moulds were placed afterwards on dry ice for 10 to 20 min to freeze the mounting medium completely and stored at -80°C.

2.2.5.2.2 Embedding for Paraffinsections

The embryos were dehydrated through a graded ethanol series at 4°C and under agitation as follows: 3x one hour 50% ethanol, 2x one hour 70% ethanol, o/N 70% ethanol, 2x one hour 80%, 2x one hour 90% ethanol, 2x one hour 96% ethanol, 3x one hour ethanol absolute.
After dehydration the embryos were treated with ethanol/acetone (both components in equal parts) for 1 hour at RT under agitation, followed by 3x one hour 100% acetone at RT under agitation. The embryos were then transferred into 100% paraffin, which was already melted before, o/N at 65°C without agitation. The next day the embryos were incubated two times for one hour in 100% paraffin at 65°C without agitation and were then place in reusable mounting moulds that had been before half-

way filled with melted 100% paraffin. The embryos were orientated as desired and the paraffin was allowed to cool down at RT to fix embryos in position. The resulting paraffin blocks were removed out of the reusable mounting blocks and were stored in plastic bags at RT.

2.2.5.3 Sectioning

2.2.5.3.1 Cryosections

The standard conditions used for cutting cryosections are the following: chamber temperature: -21°C, object temperature: -19°C. 10-12 µm thick sections were collected on microscope slides superfrost ultra plus, dried for one to two hours at RT and frozen away at -80°C.

2.2.5.3.2 Paraffin sections

10-12 µm thick paraffin sections were cut and collected at RT to be then transferred immediately to a 50-52°C warm water bath. The sections were allowed to smoothen themselves in the water bath to get rid of wrinkles. The sections were collected on microscope slides superfrost ultra plus, dried o/N at 37°C and stored away at 4°C.

2.2.5.4 Immunofluorescent stainings

2.2.5.4.1 Cryosections

Slides were removed from -80°C and sections were allowed to thaw for 15 min at RT. Roti-Liquid Barriere marker was then used to surround the sections on the slide to contain the liquid on the sections. After the Roti-Liquid Barriere marker was dried the sections were rehydrated by putting the slides into 1x PBS for 15 min at RT. Excessive 1x PBS was carefully removed and 200 µl of blocking buffer with TritonX-100 was added on each slide. The sections were incubated for 1 hour at RT in a wet chamber. After blocking the blocking buffer was removed and 200 µl of blocking buffer without TritonX-100 and with the appropriate primary antibodies was added to the slides. The sections were incubated with the primary antibody in a wet chamber o/N at 4°C. The next day the primary antibody was removed and the sections were washed at least 4x 10 min with 1x PBS at RT. After the washing steps the appropriate secondary antibodies diluted in blocking buffer without TritonX-100 were added to the slides and incubated in a wet chamber covered with aluminium foil for one hour at RT. Afterwards, the secondary antibodies were removed and the sections were washed 1x with DAPI in 1x PBS for 10 min at RT, followed with at least 3x 1xPBS for 10 min at RT and afterwards shortly dunked into water. After removing as much liquid as possible, sections were mounted with coverslips using aqua polymount and stored at 4°C in the dark.

2.2.5.4.2 Paraffin sections

Slides were removed from 4°C and sections were allowed to adjust to RT. Paraffin was removed by treating the sections for 3x seven min in 100% Xylol at RT without agitation, 1x 2 min treatment with ethanol/xylol (both components in equal parts) at RT without agitation, followed by rehydration through a graded ethanol series (100%, 96%, 90%, 70%, 50%, one min each) at RT without agitation. After rehydration an antigen retrieval (2.2.5.4.3 Antigen retrieval) was undertaken, followed by 1x 5 min in 1x PBS at RT without agitation. Excessive 1x PBS was carefully removed and sections on the slide were surrounded with Roti-Liquid Barrier marker to constrain the liquid on the sections. 200 µl of blocking buffer with TritonX-100 was added on each slide and the sections were incubated for 1 hour at RT in a wet chamber. After blocking the blocking buffer was removed and 200 µl of blocking buffer without TritonX-100 and with the appropriate primary antibodies was added to the slides. The sections were incubated with the primary antibody in a wet chamber o/N at 4°C. The next day the primary antibody was removed and the sections were washed at least 4x 10 min with 1x PBS at RT. After the washing steps the appropriate secondary antibodies diluted in blocking buffer without TritonX-100 were added to the slides and incubated in a wet chamber covered with aluminium foil for one hour at RT. Afterwards, the secondary antibodies were removed and the sections were washed 1x with DAPI in 1x PBS for 10 min at RT, followed with at least 3x 1xPBS for 10 min at RT and afterwards shortly dunked into water. After removing as much liquid as possible, sections were mounted with coverslips using aqua polymount and stored at 4°C in the dark.

2.2.5.4.3 Antigen retrieval

To achieve a staining for several antibodies on paraffin sections an antigen retrieval had to be undertaken. Paraffin sections were dewaxed by treating them for 3x seven min in 100% Xylol at RT without agitation, 1x 2 min treatment with ethanol/xylol (both components in equal parts) at RT without agitation, followed by rehydration through a graded ethanol series at RT without agitation. After rehydration the sections were incubated in 1x PBS for 2x 5 min at RT. Slides were put into a metal rack, which was placed into a pressure cooker and covered with the antigen retrieval buffer. The pressure cooker was heated on a heating plate until it reached full pressure. After cooking the sections for 2 min under full pressure, the cooker was removed from the heating plate and cooled down under running water to remove the pressure. The lid was opened and sections were allowed to cool down staying in the antigen retrieval buffer for another 20 min before washing them in 1x PBS and water, each for 1x 5 min at RT.

2.2.5.4.4 Whole mount stainings

Whole-mount stainings were performed using the 2H3 (anti-165 kDa neurofilament) monoclonal antibody (Developmental mental Studies Hybridoma Bank (DSHB), Iowa City, IA).
Dissected embryos were fixed in 4:1 methanol/DMSO o/N at 4°C under agitation. The fixative was removed the next day by washing the embryos 5x 10 min with 100% methanol at RT under agitation, followed by bleaching the embryos with 6% H_2O_2 four at least four hours at 4°C under agitation. The embryos were afterwards rehydrated by serial steps of 75%, 50%, 30% methanol in 1x PBS/0.1% TritonX-100 for 30 min each, followed by a washing step with 1x PBS/0.1% TritonX-100. The embryos were blocked in 80% FCS/20% DMSO for two hours at RT under agitation, followed by an incubation with the 2H3 anti-neurofilament monoclonal mouse antibody at 4°C for 48 hours under gentle agitation. After incubation with the primary antibody embryos were washed at least 10 times with 1x PBS/0.1% TritonX-100 for six hours at RT under gentle agitation, followed with incubation with the secondary antibody for at least 24 hours at 4°C under gentle agitation. After incubation with the secondary antibody embryos were again washed at least 10 times with 1x PBS/0.1% TritonX-100 for six hours at RT under gentle agitation. For the development reaction embryos were at first treated with 0.5 mg/ml DAB in 1x PBS in small glass beakers for 30 min at RT under agitation, until 4 µl of 0.3% H_2O_2 per 5 ml DAB in 1x PBS was added. The colour reaction was allowed to take place in the dark and its progress was checked every 30 min. As soon as the colour reaction seemed completed it was stopped washing the embryos with 1x PBS/ 01.% NaN_3 for several times. The embryos were dehydrated through a graded methanol series in 1x PBS/0.1 % TritonX-100, and then cleared in benzyl alcohol : benzyl benzonate 1:2 in glass beakers.

2.2.5.5 *In situ* hybridization

2.2.5.5.1 Plasmid linearization

Plasmids were linearized using the appropriate restriction enzymes. The digestion reaction of a total volume of 30 µlwas prepared as follows:

DNA	X µl
Restrictionenzyme	1.00 µl
10x Buffer	3.00 µl
100x BSA	0.30 µl
H_2O	X µl

The reaction was incubated in a water bath for two hours at 37°C or at RT, depending on the used restrictionenzyme. Afterwards the digestion was checked by electrophoresis on a 0.75-1% agarose gel (see 2.2.2.3 Gel electrophoresis). If the digestion was not yet complete, another 1 µl of restrictionenzyme was added to the reaction and incubated again at the appropriate temperature for one to two hours, and the efficiency of the digestion was controlled by electrophoresis once more. After completion of the digestion reaction the linearized plasmid was purified using the Nucleospin Extract II Kit according to the manufacturer´s instructions, concentration was measured by spectophotometry and stored at -20°C.

2.2.5.5.2 Probe synthesis

The following components were mixed for probe synthesis (10 µl total volume):

MP-H_2O	X µl
5x transcription buffer	2.00 µl
DIG 10x nucleotide mix	1.00 µl
Linearised plasmid	X µl
RiboLock	0.25 µl
RNA polymerase	1.00 µl

The reaction was incubated in a water bath o/N at 37°C. The next day 5 µl of 10M Ammonium acetate and 40 µl of ethanol were added to the reaction, placed for one hour at -80°C and centrifuged afterwards for 30-45 min at 4°C at 13.000 rpm. The supernatant was carefully removed, 200-300 µl of 70% ethanol was added to the pellet and centrifuged for 10 min at 4°C at 13.000 rpm. The supernatant was carefully removed, pellet was air dried, redissolved in 30 µl of Hybmix and finally stored at -20°C. 2 µl of the redissolved pellet was run on a 2% agarose/TBE gel to estimate the amount of RNA synthesised.

2.2.5.5.3 *In situ* hybridization

Paraffin sections were removed from 4°C and sections were allowed to adjust to RT. Paraffin was removed by treating the sections for 3x seven min in 100% Xylol at RT without agitation, 1x 2 min treatment with ethanol/xylol (both components in equal parts) at RT without agitation, followed by rehydration through a graded ethanol series (100%, 96%, 90%, 70%, 50%, one min each) at RT without agitation, washed 2x with 1xPBS at RT without agitation and incubated for 5 min with 20 µg/ml Proteinase K in 1x PBS. After ProteinaseK treatment the slides were immediately washed 1x with 0.2 Glycine in 1x PBS for 5 min at RT without agitation, followed by 2x washes with 1x PBS at RT without agitation. The sections were then postfixed with 4%PFA and 0.2% Glutaraldehyde in

1xPBS at RT without agitation. During postfixation a wet chamber with 50% formamide/ 2x SSC, pH 4.5, was prepared. The slides were washed again two times with 1x PBS at RT without agitation after postfixation, followed by removing as much liquid as possible. The sections were then encircled using a fat pen (Immune Edge Pen). Hybmix was denatured at 95°C for five min and 7.5 µl of Hybmix per section was added to the slides and prehybridized in the wet chamber for one hour at 70°C. During prehybridization probes were diluted to a final concentration of 1 ng/µl in Hybmix and denatured at 95°C for five min. Slides were taken out of the hybridization oven after one hour, Hybmix was removed, 7.5 µl of Hybmix with probe (1 ng/µl) per section was added and sections were hybridized in the wet chamber o/N at 70°C.

At the next day, probes were removed and slides washed 1x with 2x SSC, pH 4.5, at RT without agitation, followed by two washes with 50% formamide/ 2x SSC, pH 4.5, at 65°C for 15 min each. The slides were then washed 3x 10 min with 1x PBST at RT with gentle agitation. During the wash steps a humid chamber with water was prepared. After washing with 1x PBST, as much liquid as possible was removed from the slides, the sections were covered with B-Block (ca. 100 µl per slide), put into the wet chamber and incubated for one hour at RT. B-Block was removed afterwards, Anti-Digoxigenin-AP antibody diluted 1:1000 in B-Block (ca. 100 µl per slide) was added, incubated for two hours at 37°C, followed by 3x 5 min washing steps with 1x PBST and 1x 10 min with NTM at RT with gentle agitation. NBT/BCIP stock solution was diluted 1:50 in NTM and 300-400 µl per slide were added. Colour reaction was allowed to develop in the dark at RT and its progress was checked every 30 min. As soon as the colour reaction seemed completed it was stopped washing with 1x PBST, followed by a postfixation with 4% PFA for 10-20 min and two further washing steps with 1x PBS for 5 min each at RT. The sections were mounted with aquatex and stored at 4°C.

2.2.5.6 Alcian blue staining

Dissected embryos were fixed in Bouin´s solution for two hours and washed with a solution of 70% ethanol/0.1% NH_4OH for 12-24 hours in five to eight changes. The embryos were afterwards treated with 5% acetic acid for two hours and stained with 0.05% Alcian blue 8GX in 5% acetic acid, followed by several washing steps in 5% acetic acid for two hours and dehydration through a graded methanol series. The embryos were afterwards cleared in benzyl alcohol : benzyl benzonate 1:2 in glass beakers.

2.2.5.7 Hemotoxylin&Eosin staining

Paraffin sections were treated for 2x 5 min with 100% xylol at RT, rehydrated and washed with MP-H_2O at RT. The sections were stained with hemotoxylin for 8-10 min at RT, washed shortly with MP- H_2O, followed by washing the sections for 15 min with tap water for the colour reaction to take

place. The sections were shortly rinsed with MP-H_2O, to be stained afterwards with 0.1% Eosin at RT. After removing the eosin by washing the sections several times with MP- H_2O, they were dehydrated, treated for 2x 5 min with 100% xylol and finally embedded with entellan.

2.2.6 Western blot analysis

2.2.6.1 Preparing of protein lysates

Fresh or frozen tissue was weighted and washed in 20x buffer H with proteinase inhibitors on ice (if the tissue for example is 0.0325 g, the volume will be 650 µl), directly afterwards homogenized using a Potter S homogenizer on ice and mixed with 5x Lämmli-SDS-buffer (5% SDS) to a total volume of 1x Lämmli-SDS-buffer. The homogenates were pulled 10x up and down through a thin needle on ice and then boiled for five min at 95°C. A small aliquot was collected for determination of the protein concentration using the BCA Protein Assay Kit according to the manufacturer´s instructions. After boiling of the homogenates β-Mercaptoethanol was added to a final concentration of 5%, boiled again for five min at 95°C and finally stored at -20°C.

2.2.6.2 Western blot

Acrylamide gels were pre-run for 15-30 min at 60 volt at RT. 5x loading buffer was added to the protein lysates to a final concentration of 1x loading buffer, boiled for 5 min at 100°C and cooled down immediately by putting the samples on ice. The samples were shortly centrifuged before loading on the gel. The gel ran for about two hours at 100-120 volt at RT.
Membrane was treated for 5-10 min in 100% methanol, then washed in cooled transfer buffer. Semi-dry transfer was done for about one to two hours at 16 volt and RT and membrane were blocked o/N at 4°C. The next day the membrane was incubated with the primary antibody for one hour at RT, washed 4x ten min with 1x TBST and again incubated with the secondary antibody for one hour at RT. After 4x ten min washes with 1x TBST, ECL was added to the membrane according to the manufacturer´s instructions, developed using a Luminescent Image Analyzer LAS-3000 and analyzed by using the AIDA Image Analyzer programme.

2.2.7 Northern blot analysis

2.2.7.1 Probe synthesis

Plasmids were digested using the appropriate restriction enzymes. The digestion reaction of a total volume of 30 µl was prepared as follows:

DNA	X µl
Restrictionenzyme	1.00 µl
10x Buffer	3.00 µl
100x BSA	0.30 µl
H_2O	X µl

The reaction was incubated in a water bath for two hours at 37°C or at RT, depending on the used restrictionenzyme. Afterwards the digestion was checked by electrophoresis on a 1% agarose gel (see 2.2.2.3 Gel electrophoresis). If the digestion was not yet complete, another 1 µl of restrictionenzyme was added to the reaction and incubated again at the appropriate temperature for one to two hours, and the efficiency of the digestion was controlled by electrophoresis once more. After completion the whole digestion reaction was put on a 1% agarose gel, the fragment of interest was cut of the gel, put into a 1.5 ml tube of known weight and purified using QIAEX II Agarose Gel Extraction according to the manufacturer´s instructions and dissolved in 25 µl 10 mM Tris-HCl, pH 8.5. Concentration was measured by spectophotometry and stored at -20°C.
For synthesis of the probe DNA was denaturated for two to three min at 95-100°C, put directly afterwards on ice for two min, followed by a short centrifuge step. To the tube containing the Ready-to-Go DNA Labelling beads (-dCTP) the following was added to a total volume of 50 µl:

Denaturated DNA	X µl
[α-^{32}P]dCTP	5.00 µl
H_2O	X µl

Everything was mixed by several times of carefully pipetting up and down, incubated for ten min at 37°C and purified by using the ProbeQuant G-50 Micro Columns according to the manufacturer´s instructions. The finished probe was normally given directly to the membrane or stored at 4°C.

2.2.7.2 Northern blot

Total RNA prepared from the brain and fore- and hindlimb tissue of E12.5 embryos using RNeasy Mini Kit according to the manufacturer´s instructions was put in the following mix before loading on the gel:

4.00 µl 5x Formaldehyde running buffer
7.00 µl Formaldehyde
20.0 µl Formamide

Once in the mix, the total RNA was boiled for 15 min at 65°C, put afterwards directly on ice, shortly centrifuged. After a pre-run of the 1.2% denaturating agarose/ formaldehyde gel with 0.5 µg/ml ethidiumbromide and 1x Formaldehyde running buffer at 5 V/cm (cm referring to the distance between the two poles), the probes were loaded an the gel to separate the RNA. The gel was run o/N 25 V under the hood. At the next day, the gel was washed for one hour in MP-H_2O to remove surplus formaldehyde, checked under UV-light and the 28S- and 18S RNA bands were marked by piercing a hole into the gel with a sterile pipette tip. The membrane was treated for twenty min in 0.005 N NaOH, followed by 45 min in 20x SSC, pH 7.0 at RT under gentle agitation. Afterwards the blotting was performed o/N by the capillary transfer method (Maniatis *et al*.) using 20x SSC, pH 7.0, as transfer buffer onto HbondN+ membrane. After marking the positions of the gel slots and the 28S- and 18S RNA bands on the membrane, it was put into a UV-irridator to crosslink the RNA to the membrane. The membrane was pre-hybridized in 10 ml Church buffer o/N at 65°C with agitation. The following day the α-^{32}P-labelled probe was added directly to the Church buffer and the membrane was hybridized o/N at 65°C under agitation. After hybridization the membrane was washed with 1x – 0.1x SSC/ 1% - 0.1% SDS for 5 to 10 min each at 65°C with agitation, till radioactivity was enough reduced. Membrane was put into a transparent foil and placed together with a Amersham Hyperfilm ECL for 24-72 hours at -80°C. The film was developed using a Curix60 table top processor. The film was scanned in using a GS-800 USB Calibrated Densitometer and analyzed with the Quantity One software.

2.2.7.3 Stripping of the membrane

To completely remove the probes, the membrane was treated with a boiling 0.1% SDS solution. The solution was allowed to cool down, was removed and the membrane was washed with 2x SSC, pH 7.0.

2.2.8 Cell culture

2.2.8.1 Preparation of Mouse Embryonic Fibroblasts (MEFs)

E12.5 old mouse embryos were collected in cold 1x PBS. Individual embryos were dissected and embryonic tail samples were collected separately for DNA extraction and genotyping. After removing the head and soft tissues (liver, heart, and other viscera), the embryonic carcasses were transferred into fresh 1x PBS. The individual carcasses were minced into fine pieces under the sterile hood with a sterile scalpel blade for three min and 600-700 µl of 2x trypsin was added, followed by an incubation for 15 min at 37°C. The trypsin was inactivated afterwards by adding 12 ml MEF medium and the tissues were dissociated by vigorous up and down pipetting till no big pieces were seen anymore and finally transferred into T75 flasks and cultured o/N at 37°C. The medium was removed the following

day and cells were washed once with 1x PBS. After adding 1 ml of 0.75x trypsin to the cells, they were again incubated for 3-5 min at 37°C and 10 ml of MEF medium was added. The cells were resuspended by ten times up and down pipetting and 3 ml of the resuspended cells together with 12 ml fresh MEF medium were put into a T75 flask and further cultured at 37°C. The remaining 7 ml of resuspended cells were centrifuged down for five min at 800 rpm and the MEF medium was carefully removed. Pellet was dissolved by carefully flipping the tube, 2.4 ml of MEF medium was added and pellet was resuspended. 2.4 ml of freezing medium was added and 1.6 ml of resuspended cells was put into cryovials. The cryovials were put into a Qualifreeze Cryo-Einfriergerät and stored at -80°C o/N. The next day the cryovials were finally stored in a liquid nitrogen tank.

2.2.8.2 Luciferase assays

$2x10^6$ MEF cells were electoporated (Amaxa nucleofection device, program with a mixture of 5 µg of a Shh-responsive firefly luciferase-expressing plasmid (Sasaki *et al*., 1997) and 300 ng of a Renilla luciferase reporter plasmid (pRL-TK, Promega) to control for transfection efficiency. Cells were plated into 20 wells of a 24-well plate and allowed to grow 36-48 hours to confluency. Medium was shifted to 0.5% FCS for 36 hours, to allow for the production of cilia, as described (Ocbina and Anderson, 2008). Rcombinant murine sonic hedgehog (1 µg/ml, R&D Biosystems) was then added for 12 hours, and the cells were subsequently lysed for luciferase analysis using the Dual-Luciferase assay system (Promega) with a Veritas Microplate luminometer (Turner BioSystems). All assays were performed at least six times in five-fold replication for each experimental variable; background values were determined with lysates of untransfected cells, and firefly luciferase values were normalized with the Renilla luciferase readouts. Statistical analysis was performed using Student´s *t* tes

3 Results

3.1 The *cobblestone* mutant is a hypomorphic allele of the *Ift88* gene

The *cobblestone* (*cbs*) is a mutation uncovered in ethyl-nitroso-urea (ENU) mutagenesis screen to find defects in the development of the nervous system. ENU is a very potent mutagen, which incorporates into the genome and causes random mutations. A mouse line called *tauGFP* was used for the screen, which expresses ectopically the green fluorescent protein (GFP) under the promoter of the microtubule binding protein Tau (Tucker *et al*, 2001). The Tau protein is specific for the nervous system and thus the whole developing nervous system can be visualized under normal UV light. *tauGFP* male mice were injected with ENU and used to establish separate G1 origins (Fig.1). Each G1 male was treated as a different potential heterozygote carrier and mated to his G2 daughters to uncover reveal recessive mutations. The resulting G3 litters were screened with a fluorescent microscope for defects in neurogenesis and nerve development.

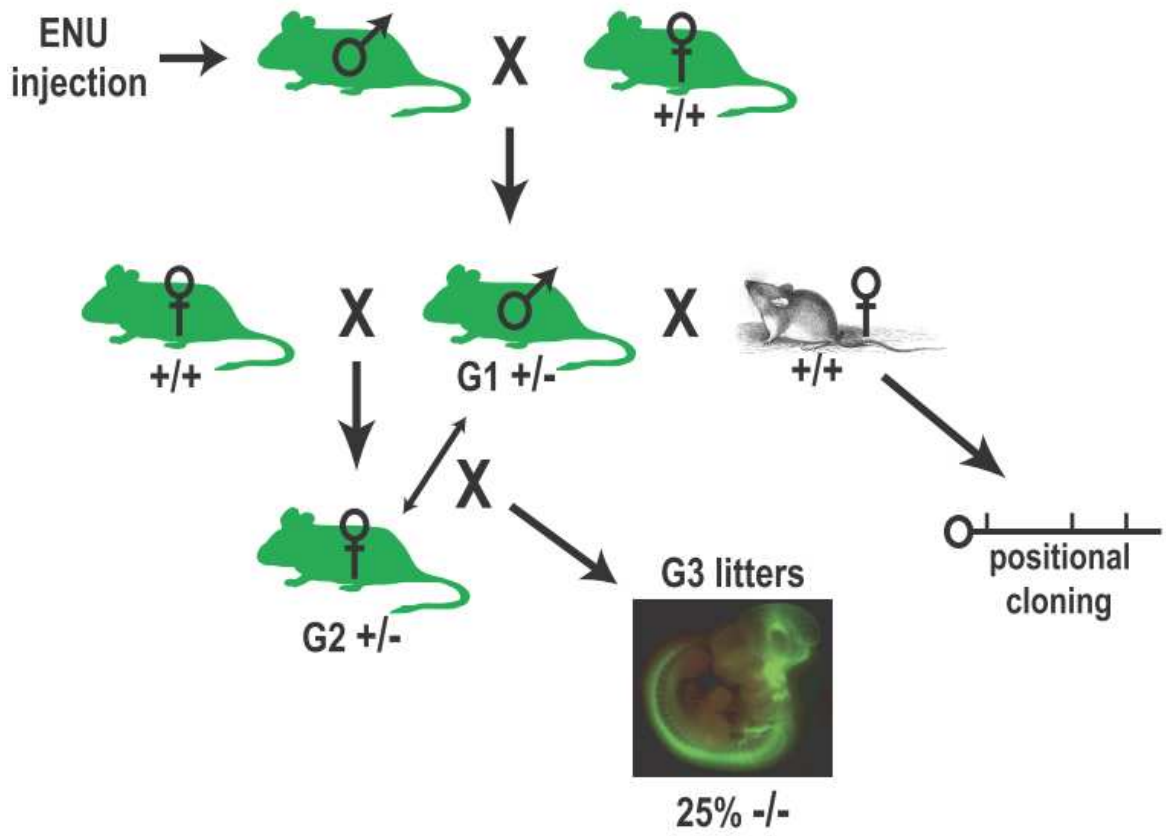

Fig. 1. ENU mutagenesis scheme to uncover recessive mutations. Green mice contain the *tauGFP* reporter transgene and are on a pure C56BL/6J background. Grey mouse is wild-type and on a pure CBA/J background. + and – refer to the ENU-induced mutation of interest.

The *cbs* mutation was identified by the ectopic accumulations of GFP-expresing cells protruding from the pial surface of the E11.0 forebrain (Fig.2A), which gives the brain surface a resemblance of a cobblestone-paved street. The following features were used to classify the heterotopias: in cross-section, these heterotopic structures were (1) 50-150 µm in diameter, (2) "rosette"-shaped, (3) with a central lumen, (4) had an epithelial-like cell layer lining the lumen, whose cells stained positive for the neural precursor marker nestin (Fig. 9A), and (5) an outer layer with GFP-expressing cells (Fig. 2A). The GFP-positive cells were also expressing β-tubulin III (Fig. 2B) and the 165 kDa axonal marker neurofilament (Fig. 2C), reinforcing their character as newborn neurons.

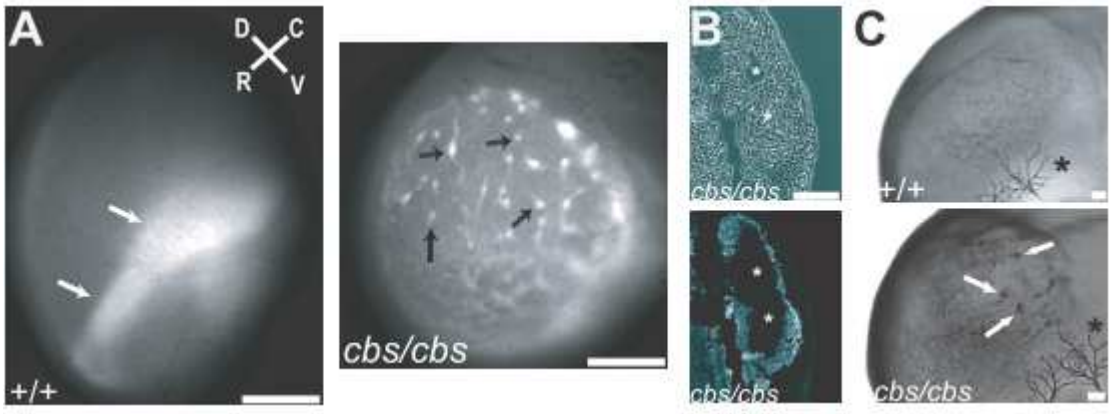

Fig. 2. Heterotopias in the *cbs/cbs* forebrain A. Whole-mount epifluorescence of E12.5 *tauGFP* cortex, looking down upon the pial surface. A wild-type embryo shows GFP-signal where the lateral edge of the cortex folds over, allowing multiple layers of newborn neurons to be seen as a broad stripe of signal (left panel, white arrows). In *cbs/cbs* mutants, heterotopias appear as 40-180 µm wide spheres (right panel, black arrows), often with long trails of green signal corresponding to outgrowing axon bundles. Rostral (R), caudal (C), dorsal (D) and ventral (V) axes are indicated. **B.** Cross section of two subpial heterotopias in E11.5 *cbs/cbs* cortex. Asterik indicates lumen of each heterotopia. Top, phase contrast. Bottom, stained with TuJ1 antibody, indicating newborn neurons in the heterotopia periphery. **C.** Anti-165 kDa neurofilament antibody staining of E11.5 forebrain. White arrows indicate heterotopias in *cbs/cbs* cortex. The smaller number of stained heterotopias, compared with (**A**), is due to reduced antibody penetration. Asterik indicates Nervus opthalmicus. (+/+) = wild-type; Scalebar: 0.5 mm (**A**), 100 µm (**B/C**).

The forebrain of E12.5 *cbs*/*cbs* mutants was shortened along its rostral-caudal axis, while the midbrain was elongated (Fig. 3A, middle embryo). *cbs* segregated as a recessive mutation (255 mutants/1005 embryos, 140 litters), with no heterozygous phenotype. The mutation was not influenced by the presence of the *tauGFP* locus, as seen after the segregation of the *tauGFP* marker. *cbs*/*cbs* mutants showed 8% and 70% mortality by E12.5 and E14.5, respectively. 10% of *cbs*/*cbs* mutants at E12.5 showed exencephaly (Fig. 3A, right embryo, black arrow). The most striking defect in *cbs*/*cbs* mutants outside the developing nervous system is polydactyly on both fore- (Fig. 3C) - and both hind-limbs (Fig. 3B) and bilateral coloboma (Fig. 3A, white arrows). Both of these phenotypes showed 100% penetrance (n = 255).

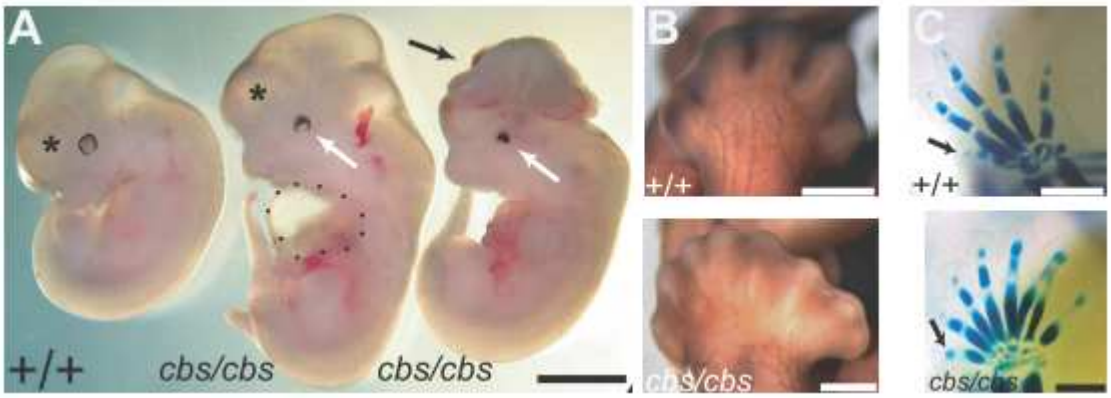

Fig. 3. The live phenotype of the *cbs/cbs* mutant. A. E11.5 *cbs/cbs* display a cortex (asterisk) shortened in the rostral-caudal axis (middle embryo), compared with wild-type littermates (left embryo). 10% of *cbs/cbs* mutants display exencephaly (right embryo, black arrow). *cbs/cbs* embryos display colobomas (white arrows), and an enlarged pericardial sac is often to be seen (black dots). **B/C.** *cbs/cbs* embryos display bilateral polydactyly on hindlimbs (**B**) and forelimbs (**C**). **B.** E13.5 embryos stained with an anti-165 kDa neurofilament antibody, showing hindlimb innervation. **C.** Alcian-blue stained E14.5 embryos, showing skeletal formation. Arrow indicates pollex. (+/+) = wild-type. Scalebar: 1.5 mm (**A**); 0.5 mm (**B**/**C**).

In addition, examination of cardiovascular and pulmonary development between E12.5 and E16.5 revealed a large number of malformations (Fig. 4A-E) that may account for embryonic lethality. Specific malformations in cardiovascular and pulmonary development in E16.5 embryos are the following, with the medical term corresponding to this phenotype in parenthseses:

1. Persistent truncus arteriosus (single outlet of the heart), including absence of the pulmonary arteries (pulmonary atresia-PA) was found. (Fig. 4A) +/+: arrow marks the ascending aorta. Arrowhead points to the pulmonary trunk. *cbs/cbs*: arrow indicates the common truncus arteriosus.
2. Pulmonary arterial perfusion was not provided by antegrade blood flow, but exclusively supplied by one major aortopulmonary artery (MAPCA-main pulmonary collateral artery = bronchial artery), arising as the first branch of the common trunk (type C PA-VSD). (Fig. 4B) *cbs/cbs*: white arrow indicates the single aortopulmonary (bronchial) artery.
3. Dextrotransposition of the common trunk arising from the right ventricle (Fig. 4A) combined with both atrial and ventricular septal defects (Fig. 4B) (ASD-VSD-pars membranacea) was recorded. (Fig. 4A) cbs/cbs: arrow indicates dextrotransposition of the common truncus arteriosus. (Fig. 4B) +/+: arrow marks the interatrial septum, which is missing (black arrow) in cbs/cbs mutants. cbs/cbs: arrowhead points to the ventricular septal defect.
4. Instead of emptying into the right atrium, the coronary sinus emptied into the common atrium. (Fig. 4C) +/+: arrow shows the blood flow from the coronary sinus into the right atrium. *cbs/cbs*: arrow shows the abnormal blood flow from the coronary sinus into the common atrium.

5. Abnormal drainage of the right pulmonary vein into the inferior vena cava was observed. (Fig. 4D) *cbs/cbs*: arrowhead points to the right pulmonary vein emptying into the inferior vena cava.

6. The right lung was present in a caudal location, only two lobes were well defined by fissures, the accessory right lobe that was present was unilobate, and severe hypoplasia of both right lobes with minor arborization of the bronchial tree was observed (Fig. 4D/E). The left lung was absent (Fig. 4D). (Fig. 4D) +/+: arrow indicates the left lung. *cbs/cbs*: arrow marks the empty pleural cavity and absence of the left lung. (Fig. 4E) +/+: arrows indicate the accessory lobe of the right lung lying on the left side. *cbs/cbs*: arrow marks the hypoplastic accessory lobe of the right lung lying on the left side. Note its position in the right pleural cavity. Arrowhead points to hypoplastic right lung.

7. Persistence of the common foregut tube. (Fig. 4A-E) *cbs/cbs*: asterisk indicates common foregut tube. The constellation of cardiovascular abnormalities seen in premortem embryos was extensive, seen in all examined embryos between E14.5 and E16.5 (n = 3), and the cause of death could reasonably be attributed to any of several stochastic cardiac events attendant to such anatomical anomalies, including acute cardiac outflow obstruction, sudden arrythmia, and intrapleural haemorrhage.

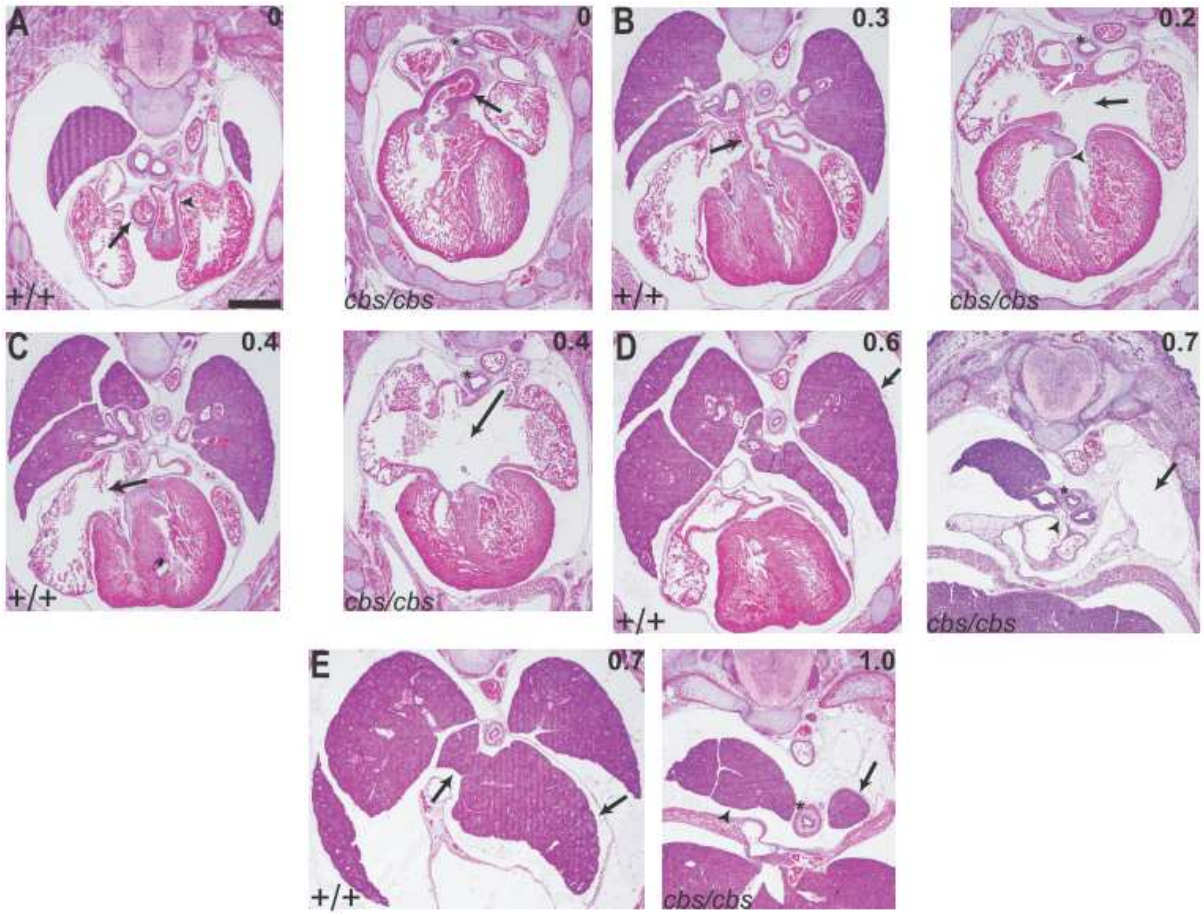

Fig. 4. Cardiovascular and pulmonary development is impaired in cbs/cbs mutants. A-E: Serial 4-µm transverse sections of E16.5 wildtype and cbs/cbs embryos were stained with hematoxylin and eosin. They are presented from cranial to caudal, with distance from the first panels indicated in mm (upper right). The left side of the body is to the right. Scale bar: 0.5 mm. Specific defects in cardiovascular and pulmonary development in E16.5 embryos are described above, with the medical term corresponding to this phenotype indicated in parentheses.

The *cbs* mutation was generated on a pure C57/BL6 background. To perform positional cloning, the *cbs* mutant was crossed to wild-type mice of the CBA/J background, F1 progeny was intercrossed, and genomic DNA from resulting F2 embryos was analyzed with strain-specific markers, which exhibited distinct polymorphisms between the C57/BL6 and CBA/J inbred mouslines. This approach identified one marker on chromosome 14 cosegregating with *cbs*/*cbs* mutants (Fig. 5). Thereon finer mapping of the chromosome 14 for the locus of the *cbs* mutation was done using standard simple sequence length polymorphism (SSLP) markers (Dietrich *et al*, 1994) (Fig. 5). The *cbs* locus was thus positioned 0.5 cM distal to the marker D14Mit259 (Fig. 4).

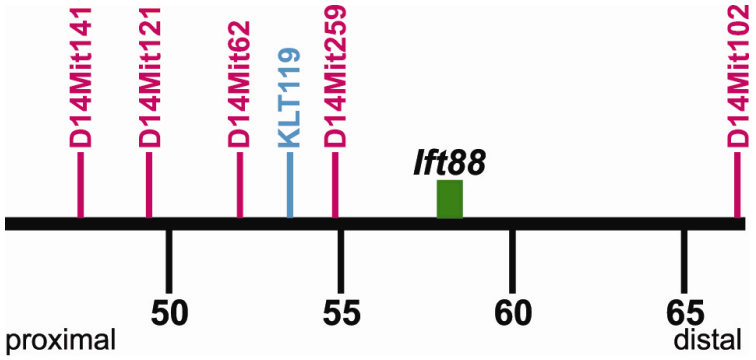

Fig. 5. Positional cloning of *cbs*. Distance from the centromere in million bp (black), the SNP markers used for rough mapping (blue), SSLP markers used for fine mapping (red), and the *Ift88* gene (green box) are indicated.

Examination of candidate genes in this region revealed one gene called *Ift88* (Fig. 4), which had been already reported to exhibit both polydactyly (Zhang *et al*, 2003) and defects in neural tube formation (Murcia *et al.*, 200), when mutated. Northern blot analysis using total RNA isolated from E12.5 brain detected a single transcript both in wild-type and *cbs*/*cbs* embryos (Fig. 6A). Quantitation revealed a 66.7 +/- 2.00% decrease in *Ift88* mRNA levels in *cbs*/*cbs* brains. Western blot analysis of Ift88 protein levels in E12.5 whole brain, using an anti-N-terminal-Ift88 antibody, showed a single band of ~90 kDa in both wild-tybe and *cbs*/*cbs* embryos (Fig. 6C). Quantitation revealed a 75.0 +/- 3.0% decrease in the levels of Ift88 protein in *cbs*/*cbs* brain ($n = 5$, $p < 0.01$, Student´s *t* test). Analysis of mRNA and protein levels in fore- and hind- limbbuds with Northern blots (Fig. 6B), quantative real-time PCR (Fig. 6E), and Western blot using anti-Ift88 antibodies directed against either the N-terminus (Fig. 6C) or the C-terminus (Fig. 6D) showed a similar reduction in mRNA and protein levels, respectively.

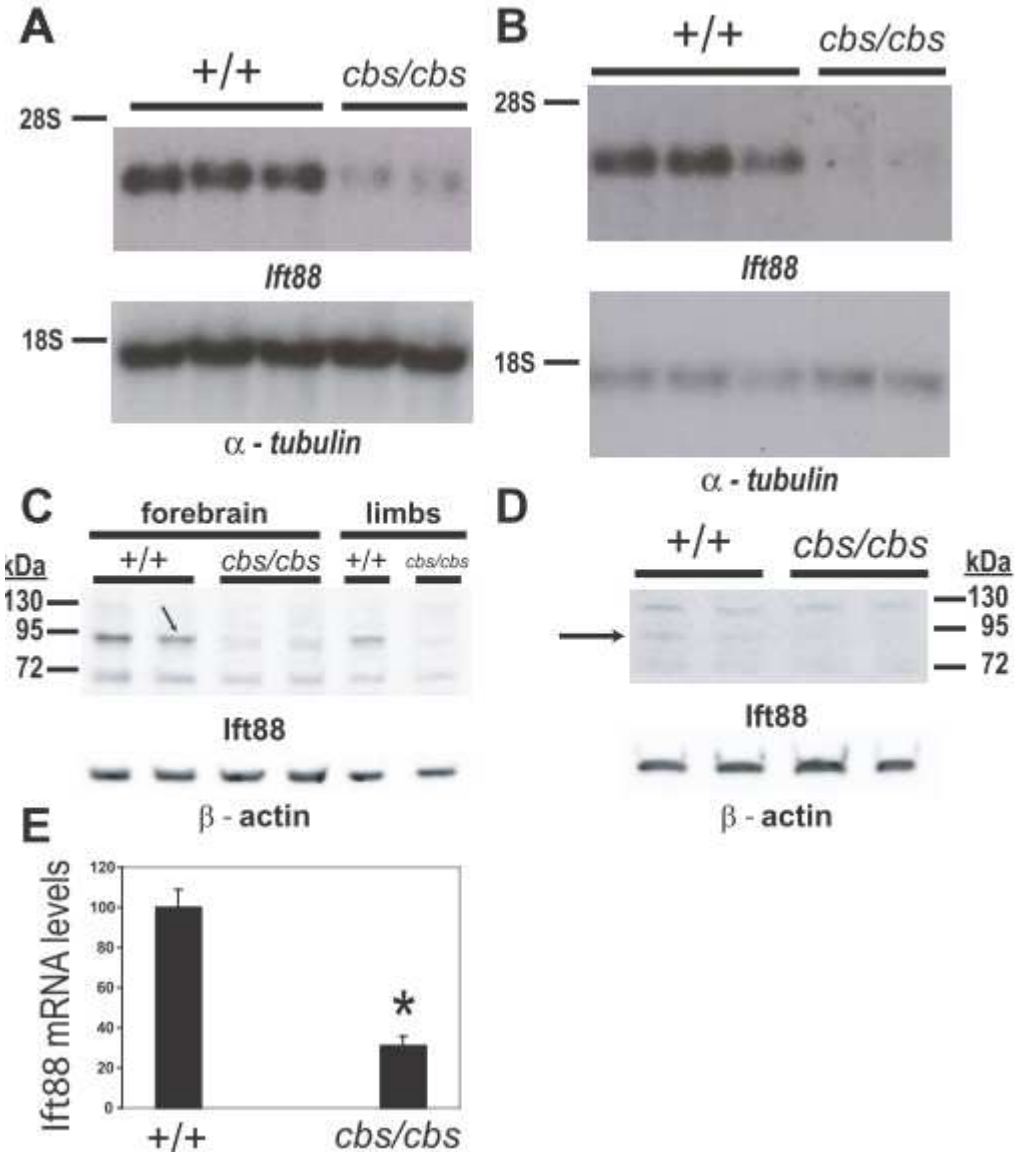

Fig. 6. ***Ift88*** **mRNA and protein expression levels in wild-type (+/+) and** ***cbs/cbs*** **forebrain and limb buds.** **A.** Northern blots of whole mRNA from whole brain from E12.5 wilde-type (+/+) and *cbs/cbs* embryos. Full-length *Ift88* (top) and α-*tubulin* cDNAs (bottom) were used as probes. Ribosomal RNA markers are indicated (left). **B.** Northern blots from whole mRNA from fore- and hindlimbs of E12.5 wild-type (+/+) and *cbs/cbs* embryos. Full-length *Ift88* (upper panel) and α-*tubulin* cDNAs (lower panel) were used as probes. Ribosomal markers are indicated (left). **C.** Western blot of protein from forebrain and fore- and hindlimbs (limbs) of E12.5 wild-type (+/+) and *cbs/cbs* embryos. An anti-N-terminal-Ift88 antibody (top), and an anti-β-actin antibody (bottom) as loading control were used. Arrow indicates the Ift88 band. **D.** Western blot analysis of protein extracted from fore- and hindlimbs of E12.5 wild-type (+/+) and *cbs/cbs* embryos. An anti-carboxal-terminal-Ift88 antibody (upper panel), and an anti-β-actin antibody (lower panel) as a loading control were used. Arrow indicates the Ift88 band. **E.** Quantitative real time RT-PCR performed upon whole mRNA extracted from fore- and hindlimbs of E12.5 wild-type (+/+) and *cbs/cbs* embryos. Relative expression levels of *Ift88* are indicated. Mean values +/- SEM (n = 3). * = $p < 0.05$, Student´s *t* -test.

A complementation analysis by crossing *cbs* heterozygotes to mice heterozygous for a targeted deletion of the *Ift88* gene (*Ift88*$^{tm1.1Bky}$) (Haycraft *et al*., 2007) was done to ascertain, if the genetic defect in the *cbs/cbs* mutant is located in the *Ift88* gene. 7 compound heterozygotes for both alleles were identified by using PCR-genotyping. They showed morphological features of *cbs* homozygotes, including bilateral coloboma, a rostro-caudally shortened telencephalon, and an enlarged midbrain (Fig. 7A). In some cases the compound heterozygotes exhibited a rightward-looping heart tube, an indication of *situs inversus* (3/7 *cbs*/*Ift88*$^{tm1.1Bky}$ embryos) (Fig. 7B, red arrows). *cbs/cbs* mutants by contrast never exhibited *situs inversus* (n = 61). None of 48 littermates genotyped as wild type or heterozygous for either the *Ift88* or *cbs* mutation displayed the phenotypes reported above. The conclusion out of this analysis is, that the two mutations do not complement one another and that *cbs* is a hypomorphic allele of *Ift88*.

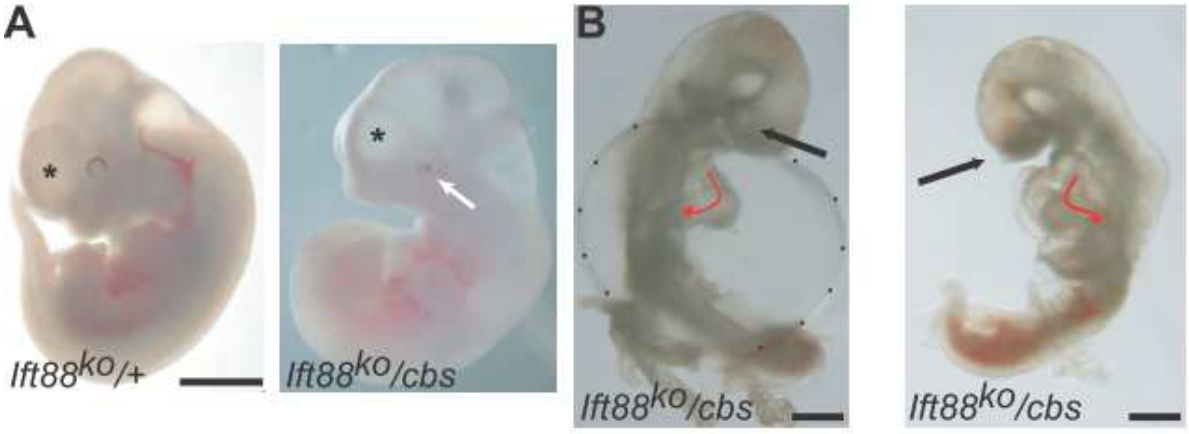

Fig. 7. Complementation analysis. A. E11.5 heterozygous *Ift88* knock-out embryos (*Ift88*^{ko}*/+)* display a wild-type telencephalon (asterisk) with an elongated rostral-caudal profile (cf. Fig. 3A, +/+ embryo). A compound heterozygote of the *Ift88* deletion allel (*Ift88*^{ko}) and the cbs allel (*Ift88*^{ko}*/cbs*) displays coloboma (white arrow) and a rostro-caudally shortened cortex (asterisk). **B.** E11.0 *Ift88*^{ko}*/cbs* compound heterozygous embryos demonstrate situs inversus, as indicated by passage of the bulboventricular loop to the right (left panel, red arrow), and situs solitus, as indicated by passage of the bulboventricular loop to the left (right panel, red arrow). Black dots outline the enlarged pericardial sac (left panel). Black arrows indicate developmentally-delayed forebrain (both panels). Scalebar: 1.5 mm **(A)**; 250 µm (**B**).

As sequencing of the mRNA transcript in the *cbs/cbs* mutant revealed no changes in the ORF or the 5´ and 3´ UTRs, this further is a sign for a mutation in an intron or a regulatory region.

3.2 Cilia are present in the ventricles of *cbs/cbs* mutants

The product of the gene *Ift88*, the intraflegellar transport (IFT) protein Ift88 (Taulman *et al.*, 2001), is involved in the anterograde transport of the IFT particles inside primary and motile cilia (Pazour *at al.*, 2000), organelles that protrude from the surface of most eukaryotic cells. IFT is the mechanism by which protein cargoes are transported in the cilium itself (Kozminski *et al.*, 1993). Primary cilia, protruding into the ventricles, have been reported to be present on neuroepithelial cells of the developing cortex (Nagele and Lee, 1979; Cohen and Meininger, 1987; Mary et *al*, 2005). By transmission electron microscopy (TEM) upon coronal sections of E12.5 brain I was able to confirm this observation. Cilia with varying lengths between 0.5-2 µm were projecting into the ventricle (Fig. 8A). Transverse sections displayed well defined basal bodies (Fig. 8B) and a "9+0" morphology in the proximal cilium (Fig. 8C), verifying them as primary cilia. They showed a proximal-to-distal reduction in the number of microtubule doublets, coming eventually to a "2+0" morphology at the tip (Fig. 8D/E), as reported previously (Cohen and Meininger, 1987).

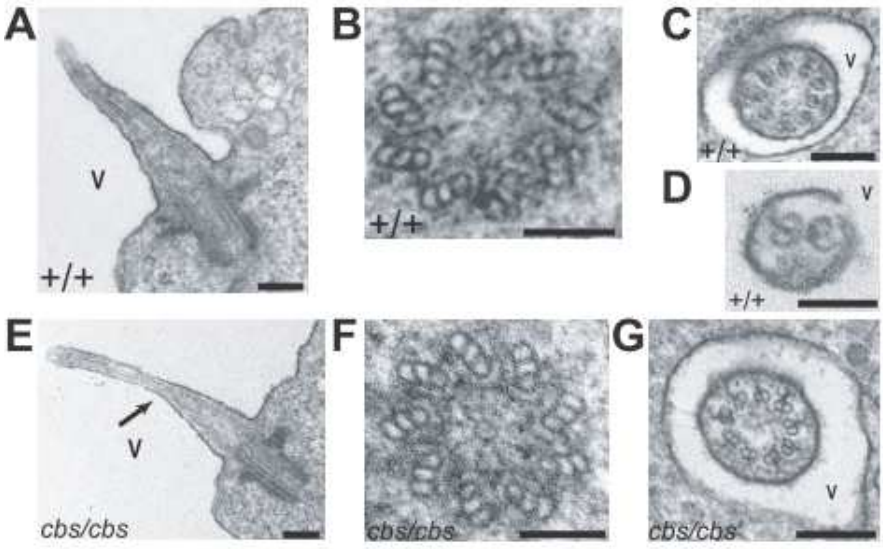

Fig. 8. Transmission electron microscopy reveals primary cilia projecting into the ventricle of wild-type (+/+) and *cbs/cbs* embryonic forebrain. A/E. Cilium cut longitudinally. **B-D, F, G.** Cross sections of ventricular cilia, revealing the basal body (**B**/**F**), characteristic "9+0" ciliary morphology (**C**/**G**), and tapering to a "2+0" structure (**D**). **E.** Proximal-to-distal tapering can be seen (arrow). Scalebar: 200 nm (**A**, **C**, **E**, **G**); 100 nm (**B**, **D**, **F**).

Scanning electron microscopy (SEM) upon forebrain of E12.5 embryos revealed cilia projecting into the ventricle from dorsal and lateral cortex (Fig. 9A), the hippocampal anlage, choroid plexus, and the ganglionic eminences (GEs), with lengths varying between 05-3 µm.

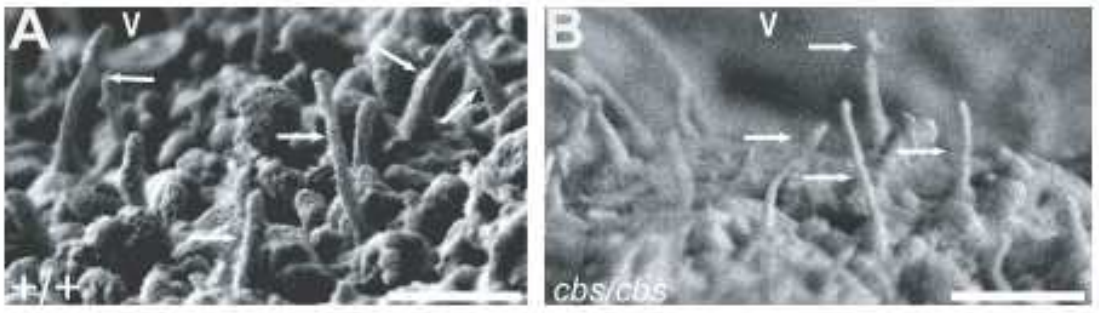

Fig. 9. Scanning electron microscopy reveals cilia projecting into the ventricle of wild-type (+/+) and *cbs/cbs* embryos. A/B. Arrows indicate cilia. Scalebar: 1 µm (**A, B**).

To investigate if neural precursor cells expressed elements of the intraflagellar transport machinery, a mouse line (*Ift88*$^{\Delta 2\text{-}3\beta gal}$) (Murcia *et al*, 2000) was used in which the lacZ cDNA has been inserted into the locus encoding *Ift88*, a component of the B complex particles of the IFT machinery (Rosenbaum and Witman, 2002). Analysis of E11.5 heterozygous *Ift88*$^{\Delta 2\text{-}3\beta gal}$ embryos identified expression of *Ift88::lacZ* by nestin-positive (Fig. 10A) and RC2-positive (Fig. 10B) neural precursor cells. Newly born neurons residing in the subpial mantle zone, labeled by using the TuJ1 antibody (Moody *et al*., 1989), were also revealed to express *Ift88* (Fig. 10C).

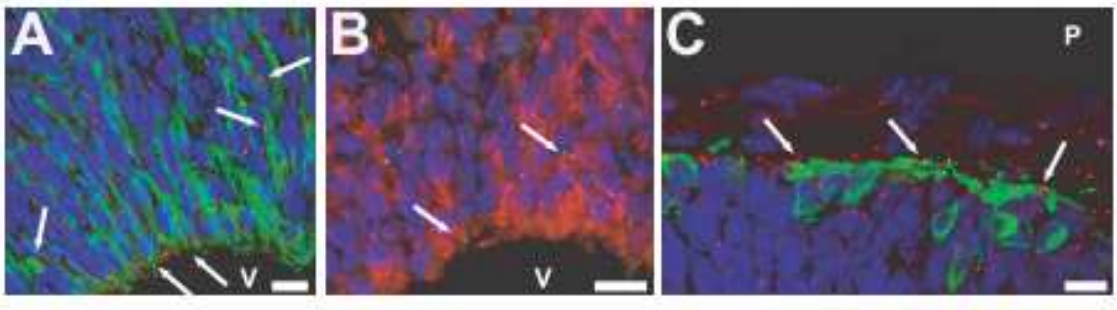

Fig. 10. Immunoflourescence analysis of *Ift88* expression. The expression analysis was undertaken upon the dorsolateral telencephalon of E11.5 *Ift88*$^{\Delta 2\text{-}3\beta gal}$ embryos, using an antibody recognizing β-galactosidase (**A**, **C**, red; **B**, green), which is expressed from the *Ift88* locus. The ventricular (V) and pial (P) surface is at the bottom (**A**, **B**) and top (**C**) of the panels, respectively. Arrow indicates characteristic somatic β-galactosidase deposits in cells colabeled with the following markers: Nestin- (**A**, green) and RC2-positive (**B**, red) VZ cells and newborn neurons (**C**, green, TuJ1-antibody). **A-C**, blue, DAPI-labeled nuclei. Scalebar: 10 µm (**A-C**).

It was shown in preceding reports of *Ift88* mutants (Murcia et al., 2000; Haycraft et al, 2001, 2005, 2007; Kramer-Zucker et al, 2005; Banzis et al, 2005), that cilia are either not formed or not maintained. TEM on coronal forebrain sections of E12.5 *cbs/cbs* embryos showed primary cilia projecting into the ventricle that did not seem to be different from those of wild-type (Fig. 8E-G). The cilia originate from well defined basal bodies (Fig. 8F), showed a “9+0” morphology (Fig. 8G), and displayed a proximal-to-distal tapering (Fig. 8E, black arrow). SEM analysis could also reveal cilia projecting into the ventricle from the dorsolateral telencephalon (Fig. 9B) and the GEs of *cbs/cbs*

mutants. The cilia of the dorsolateral telenecephalon of the *cbs/cbs* mutant seemed to be of normal length (wild type: 973 +/- 160 nm (n = 26); *cbs/cbs*: 894 +/- 213 nm (n = 33); p = 0.25, Student´s *t* test). In conclusion, both TEM and SEM detected ultrastructurally normal cilia projecting into the ventricle of *cbs/cbs* mutant forebrain. Additionally ultrastructurally and morphologically normal cilia were also detected in the midbrain (Fig. 11 A/B) and bronchia (Fig. 11 C/D) of *cbs/cbs* mutants.

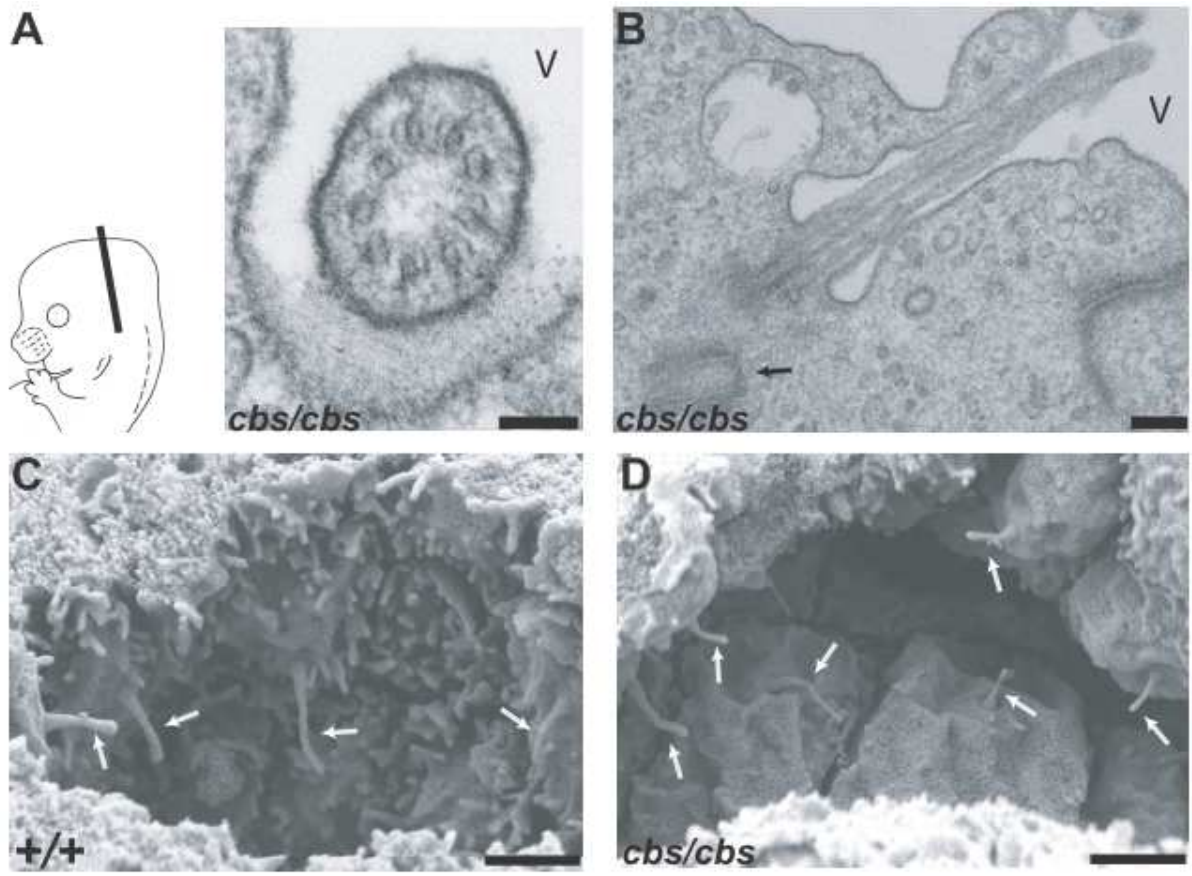

Fig. 11. Cilia are present in the midbrain and bronchia of *cbs/cbs* mutants. A/B. TEM of cilia projectiong into the dorsal mesencephalic ventricle (V) of E12.5 *cbs/cbs* embryos. **A.** Cross section of ventricular cilium, revealing the characteristic "9+0" morphology of primary cilia. Scheme (lower left) indicates the plane of section for (**A**, **B**). **B.** Cilium cut longitudinally. Arrow indicates a centriole adjacent to the basal body that forms the base of each cilium. **C/D.** SEM of epithelial cilia (white arrows) projecting into the bronchial lumen of E12.5 wild-type (+/+) (**C**) and *cbs/cbs* (**D**) embryos. Scalebar: 100 nm (**A**); 200 nm (**B**); 1 µm (**C**, **D**).

3.3 The *cbs/cbs* mutants exhibit a pronounced disorganization of the dorsal telencephalon

The forebrain of *cbs/cbs* mutants showed a major disorganization in dorsal telenecephalic morphology (Fig. 12A-G). The telencephalic midline of E12.5 wild-type littermates invaginated and exhibited development of the choroid plexus, cortical hem, and the hippocampal anlage (Fig. 12A). Invagination of the telencephalic midline did occur in *cbs/cbs* mutants, but the morphology of the dorsomedial telencephalon was profoundly affected and the hippocampal primordium and the cortical

hem could not be identified by morphology. The *cbs/cbs* mutants rather showed a kinked ventricular zone (VZ) that folded in upon itself (Fig. 12B, arrows) to form rosette-like heterotopias (Fig. 12H-J). The development of the medial and lateral GE seemed relatively normal in contrast (Fig. 12B). The diencephalon and the dorsal telencephalon show at caudal levels a clear separation in wild-type embryos at E12.5 (Fig. 12C), but this differentiation is lost in the *cbs/cbs* mutants. Here a continuous ventricular zone (VZ) runs from the dorsal diencephalon to the dorsolateral telencephalon (Fig. 12D). This phenotype was even more severe in E11.5 embryos having both the *cbs* and the *Ift88* knock-out allele (Fig. 7A). The dorsal telencephalic midline hardly invaginated, the cortical VZ was diminished to a very thin stripe, and the medial and lateral GE were also extremely reduced in size (Fig. 12F). Later developmental stages of this complementation analysis could not be examined because of an earlier lethality than that seen in *cbs/cbs* mutants. E11.5 *cbs/cbs* mutants showed a similar diminished invagination and disorganization of the dorsal midline, invaginations of the cortical VZ (Fig. 12G, arrowhead), and subpial heterotopias (Fig. 12G, arrow), when compared with E12.5 *cbs/cbs* mutants. In comparison both the cortex and the GEs were thicker than in the *cbs*/*Ift88*$^{tm1.1Bky}$ complementation mutants (Fig. 12F).

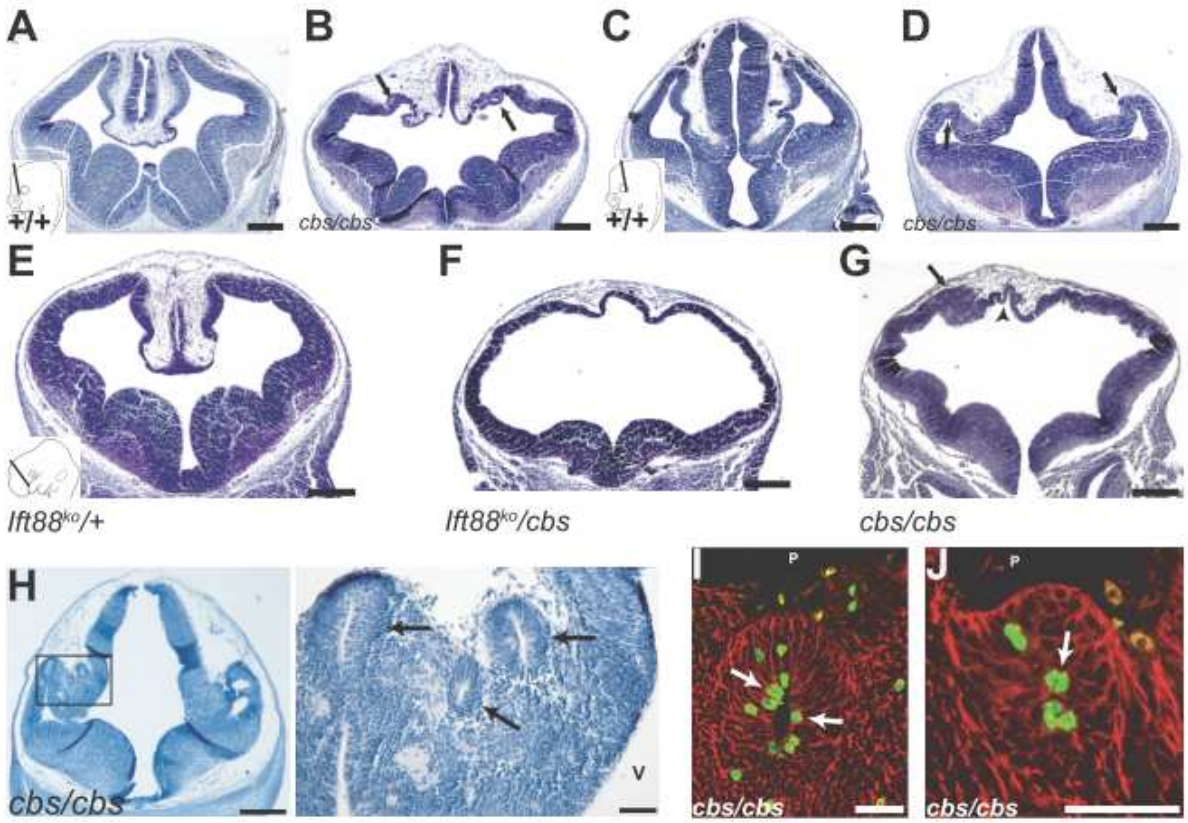

Fig. 12. The *cbs/cbs* mutant displays a pronounced disorganization of the dorsal telencephalon. A-D, H. Hematoxylin-stained coronal sections of E12.5 wilde-type (+/+) (**A**, **C**) and *cbs/cbs* (**B**, **D**, **H**) embryos. Hematoxylin-stained coronal sections of E11.5 *Ift88*$^{ko/+}$ embryo (**E**), a *Ift88*^{ko}*/cbs* compound heterozygote littermate (**F**), and a *cbs/cbs* embryo (**G**). Schematic insets (lower left) (**A**, **C**, **E**) indicate the plane of section for (**A**,**B**), (**C**, **D**), and (**E**-**G**), respectively. **H.** Caudal-most telencephalon depicting lateral heterotopias (left, boxed). Enlargement of the boxed area shows them to have a rosette-like morphology (right). **B, D, G, H.** Arrows indicate heterotopias. G. Arrowhead indicates VZ. **I/J.** Mitotic cells revealed with an anti-phosphorylated-histone H3 antibody (green, PH3) in subpial heterotopias of E12.5 *cbs/cbs* embryos. Red = anti-nestin antibody. Arrows indicate nestin/PH3-positive cells. **A-J:** Dorsal is to the top. **H-J:** Lateral is to the left. P = pial surface.; V = ventricle; (+/+) = wild-type. Scalebar: 300 µm (**A**-**G**, **H** (left)); 50 µm (**I**, **J**).

The number of mitotic cells at the VZ were not significantly altered in the cortex of E12.5 *cbs/cbs* mutants ($p = 0.06$, $n = 5$, Student´s *t* test) (Fig. 13C). A great number of the mitotic VZ cells were positive for the anti-nestin antibody, which indicates, that they are neural precursors (Fig. 13A/B, arrows; N). The GEs displayed instead a large increase in mitotic cells (Fig. 13C). The reason for this is the appearance of cells dividing 10-30 µm away from the VZ, many of which were nestin-negative (Fig. 13B, arrowheads; N). Similar results were seen at E11.5. Additionally mitotic cells at the lumen of heterotopias could also be identified as nestin-positive (Fig. 12I/J). No change was detectable for the number of mitotic cells located basally >30 µm from the ventricular zones of the cortex and GE (Fig. 13E).

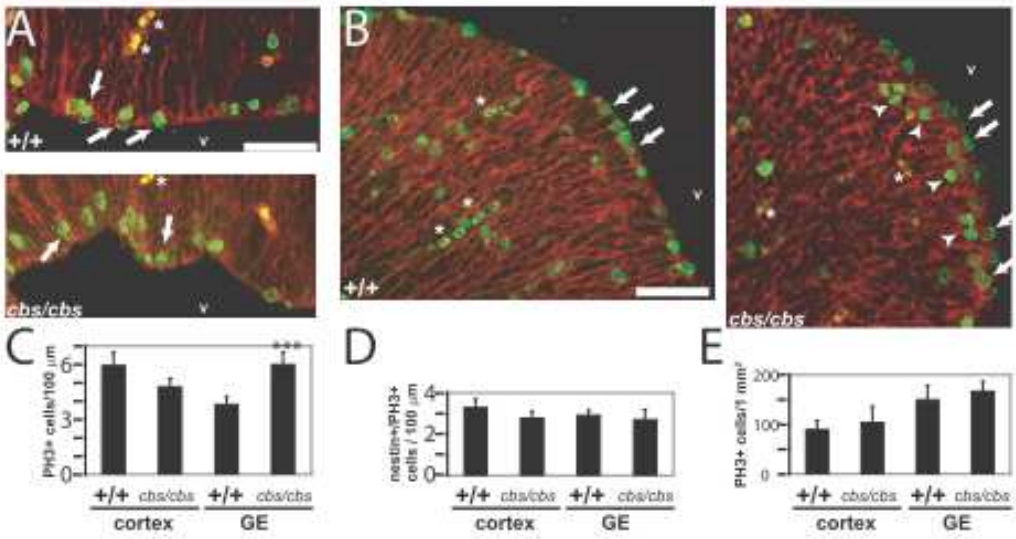

Fig. 13. Mitotic cells in the cortex and GEs of the *cbs/cbs* mutant. A/B. Mitotic cells revealed with an anti-phosphorylated-histone H3 antibody (green, PH3) in the VZ of the dorsolateral cortex (**A**) and the GRs (**B**) of E12.5 wild-type and *cbs/cbs* embtyos. Red = anti-nestin antibody. Arrows indicate nestin/PH3-positive cells. Arrowheads indicate sub-VZ mitoses. Asteriks indicate blodd cells. **C-E.** Quantitation of PH3 staining in the cortex (cortex) and GEs (GE), expressed as the number of PH3-positive (**C**) and double nestin/PH3-positive cells (**D**) per 100 µm of VZ, and in the number of basally located (i.e., >30 µm from the VZ) PH3-positive cells per 1 mm^2 (**E**). ***p<0.001, Student´s *t*-test. **A/B.** Dorsal is to the top, lateral is to the left. V = ventricle; (+/+) = wild-type; Scalebar: 50 µm (**A/B**).

3.4 Dorsomedial telencephalic cell types are specified but do not from morphological structures in *cbs/cbs* mutants

The dorsomedial telencephalon is the origin of several different cell types including choroid plexus, the cortical hem, the hippocampus and Cajal-Retzius cells. Because of severe disorganization of these structures in *cbs/cbs* mutants shown by histological examination, the determination of these structures was analyzed with appropriate tissue-specific markers. The choroid plexus origins from the dorsal midline and expresses *Ttr1* (Fig. 14A, arrow, left panel) (Duan *et al*, 1989). In *cbs/cbs* mutants, *Ttr1* was still expressed but in a irregular pattern and at a notedly lower expression level when compared to wild-type littermates (Fig. 14A, arrow, right panel). The cortical hem is located directly dorsal to the choroid plexus and is marked by the expression of several Wnt family genes including *Wnt2b* (Grove *et al*., 1998) (Fig. 14B, arrow, left panel). Analysis of *Wnt2b* expression in *cbs/cbs* mutants showed a domain of expression in the dorsal telencephalon (Fig. 14B, arrow, right panel) lateral to the *Ttr1* expression domain seen in an adjacent section (cf. Fig. 14A). Like to the *Ttr1* expression pattern, the expression of *Wnt2b* was considerably reduced and in scattered groups of cells (Fig. 14B, arrow, right panel).

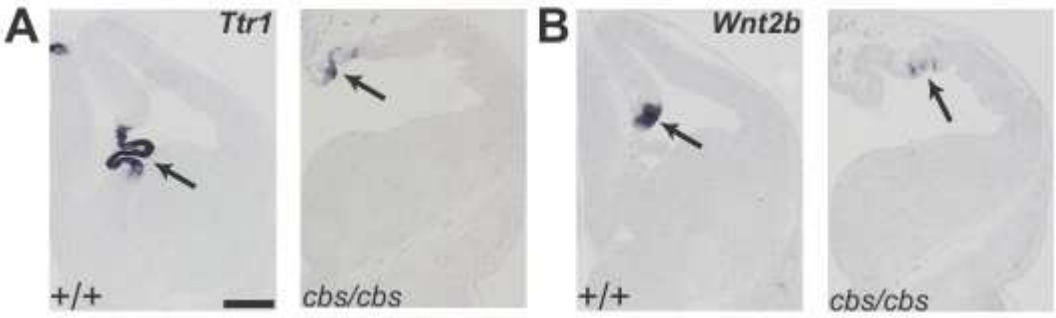

Fig. 14. Dorsomedial telencephaloc cell types are specified but do not form morphological structures. A/B. *In situ* hybridization analysis of E12.5 wild-type (+/+) and *cbs/cbs* embryos. For each coronal section, one telencephalic half is shown, with dorsal to the top, lateral to the right. **A.** *Ttr1 in situ* hybridization. Arrows indicate *Ttr1* expression in the choroid plexus. **B.** *Wnt2b in situ* hybridization. Arrows indicate *Wnt2b* expression in the cortical hem. Scalebar: 300 µm.

The hippocampal anlage lies adjacent to the cortical hem and expresses *EphB1* (Tole *et al.*, 2000) (Fig. 15A, arrow, left panel). In *cbs/cbs* mutants the expression of *EphB1* was not detected in the dorsal telencephalon, whereas its expression in the ventral telencephalon was not affected (Fig. 15A, right panel). The hippocampus is also characterized by the expression of the *Lhx2* homeodomain gene at high levels (Fig. 15B, left panel), which is needed for normal hippocampal development (Porter *et al*., 1997; Bulchand *et al*., 2001; Monuki *et al*., 2001; Mangale *et al*., 2008), but in *cbs/cbs* mutants the high level expression of *Lhx2* was reduced (Fig. 15B, left panel). This suggest that the hippocampus was not specified correctly in *cbs/cbs* mutants. The cortical hem is an important source of Cajal-Retzius (CR) cells, the earliest born cortical neurons, which are marked by the expression of *reelin* (Meyer *et al*., 2002; Takiguchi-Hayashi *et al*., 2004) (Fig. 15C, arrow, left panel). A single layer of *reelin*- expressing cells at the cortical marginal zone of E12.5 wild-type and *cbs/cbs* mutant embryos was revealed (Fig. 15C, arrow, both panels). In summary, the data indicates that cells of dorsomedial telencephalic character are formed in *cbs/cbs* mutants but they fail to form morphologically distinct structures.

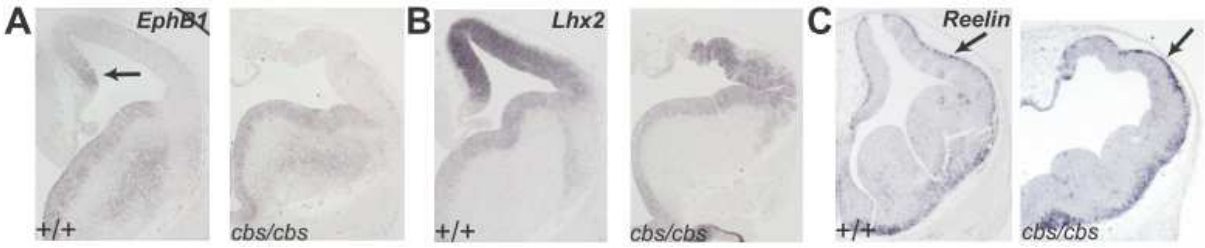

Fig. 15. Dorsomedial telencephaloc cell types are specified but do not form morphological structures. A-C. *In situ* hybridization analysis of E12.5 wild-type (+/+) and *cbs/cbs* embryos. For each coronal section, one telencephalic half is shown, with dorsal to the top, lateral to the right. **A.** *EphB1 in situ* hybridization. Arrow indicate *EphB1* expression in the hippocampal anlage. **B.** *Lhx2 in situ* hybridization. *Lhx2* expression in the hippocampus and neocortex. **C.** *Reelin in situ* hybridization. Arrows indicate *Reelin* expression in the Cajal-

Retzius cells. Scalebar: 300 µm.

3.5 The pallial-subpallial boundary fails to form correctly in *cbs/cbs* mutants

It was of interest, if the dorsal-ventral subdivisions of the telencephalon in *cbs/cbs* mutants formed properly. *Pax6* (Fig. 16A, left panel) and *Ngn2* (Fig. 16B, left panel) exhibit a lateral-high to medial-low expression gradient in the wild-type developing cortex, with a sharp expression boundary at the pallial-subpallial boundary (PSPB) of the telencephalon (Walther and Gruss, 1991; Gradwohl *et al*., 1996). In *cbs/cbs* mutant telencephalon the graded expression of both genes was lost, and their ventral expression domains were not as sharply defined when compared to wild-type embryos (Fig. 16A/B, right panel).

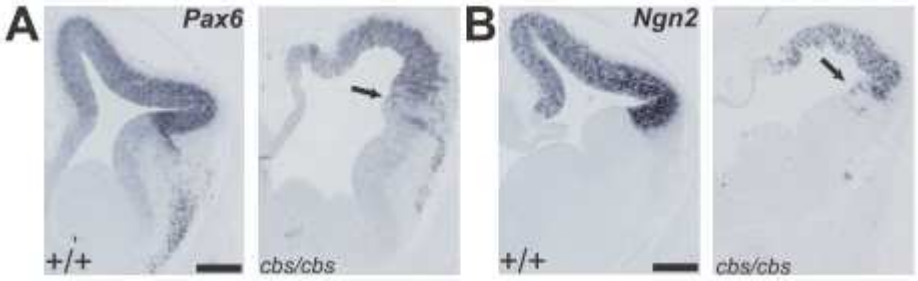

Fig. 16. Relaxation of the pallial-subpallial boundary (PSBP) in cbs/cbs mutants. *In situ* hybridization analysis of E12.5 wild-type (+/+) and *cbs/cbs* embryos. For each coronal section, one telencephalic half is shown, with dorsal to the top, lateral to the right. **A.** *Pax6 in situ* hybridization; Arrow in the right panel indicates the PSBP. **B.** *Ngn2 in situ* hybridization. Arrow in the right panel indicates the PSBP. (+/+) = wild-type. Scalebar: 300 µm.

Analysis for *Pax6* by immunofluorescence showed also widespread Pax6-positive cells at the boundary region (Fig. 17).

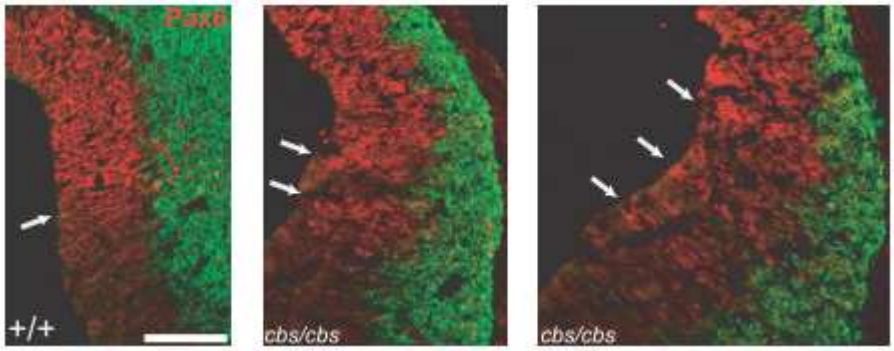

Fig. 17. Relaxation of the pallial-subpallial boundary (PSBP) in cbs/cbs mutants. Immunohistofluorescence analysis of E12.5 wild-type (+/+) and *cbs/cbs* embryos. For each coronal section, one telencephalic half is shown, with dorsal to the top, lateral to the right. **A.** Red, Anti-Pax6 antibody; Green, TuJ1 antibody, recognizing newborn neurons. Left panel, arrow indicates the PSBP. Middle and right panel, arrows indicate

radial stripes of Pax6 expression at the PSBP in *cbs/cbs* mutants. (+/+) = wild-type. Scalebar: 300 µm.

Dlx2 is a marker for the medial and lateral GEs (Bulfone *et al*., 1993), and *in situ* hybridization analysis on adjacent sections indicated that scattered *Pax6* and *Ngn2* expressing cells were located within the ventral telencephalic area of *cbs/cbs* mutants (Fig. 18A, right panel). *Dlx2* showed as well a diffuse border of expression, and scattered *Dlx2*-expressing cells were found in neocortical territory (Fig. 18A, right panel). The expression of *Dlx2* in the GEs was substantially similar compared to wild-type littermates (Fig. 18A), which is consistent with the histological analysis. To define the formation of the PSPB in *cbs/cbs* mutants in more detail, the expression of the *Dbx1* homeobox gene in the ventral pallium, located just dorsally to the PSPB (Medina *et al*., 2004), was examined. The *Dbx1*-expressing cells were more widely distributed in *cbs/cbs* mutants, in particular in the neocortex (Fig. 18B, right panel). This data indicates, that the PSPB does not correctly develop in *cbs/cbs* mutants and that cells expressing dorsal or ventral markers intermingle at the boundary.

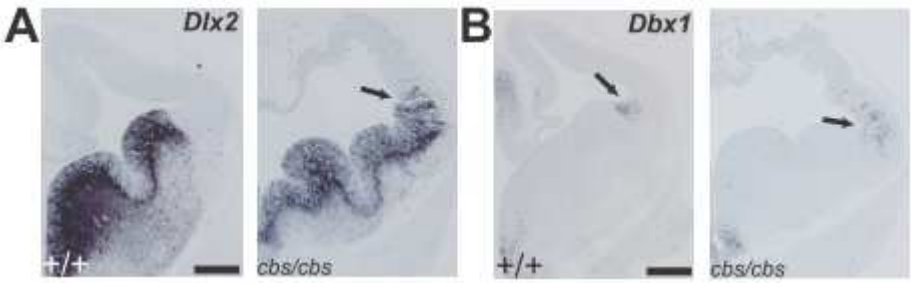

Fig. 18. Relaxation of the pallial-subpallial boundary (PSBP) in cbs/cbs mutants. A/B. *In situ* hybridization analysis of E12.5 wild-type (+/+) and *cbs/cbs* embryos. For each coronal section, one telencephalic half is shown, with dorsal to the top, lateral to the right. **A.** *Dlx2 in situ* hybridization; Arrow in the right panel indicates the PSBP. **B.** *Dbx2 in situ* hybridization. Arrows indicate the PSBP. (+/+) = wild-type. Scalebar: 300 µm.

3.6 The dorsal telencephalic-diencephalic boundary in *cbs/cbs* mutants is weakened

It was of interest to see, if the telencephalic-diencephalic boundary also did not from properly in the *cbs/cbs* mutants. Histological analysis had showed highly abnormal structure in this region containing many of the rosettes (Fig. 12D, H-J). This region we named caudal rosette-rich area (CRA). On the basis of the severity of these deformations, morphological landmarks could not be used. Because of this reason developmental marker analysis was used to elucidate the cellular composition of this area. Apart from the cortical hem and CR neurons *Foxg1* is expressed by all telencephalic cells, and exhibits an expression gradient in the hippocampus with lower expression levels medially (Fig. 19A, left panel) (Tao and Lai, 1992; Hanashima *et al*., 2002). *In situ* hybridization for *Foxg1* showed a likewise pattern in *cbs/cbs* mutant neocortex, with higher expression levels laterally and weak expression medially, but revealed an absence of *Foxg1* expression in the CRA except for a small patch

of cells located at its lateral margin (Fig. 19A, right panel). Due to lower *Foxg1* expression levels in developing hippocampus of wild-type embryos analysis of the expression patterns of *Lhx2* and *Emx2*, which show both an opposite expression gradient to *Foxg1* in the cortex (Fig. 19B/C, left panels), was done. Additionally to their expression in the *cbs/cbs* neocortex (*Lhx2:* Fig. 15B; *Emx2:* Fig. 24B) both *Lhx2* and *Emx2* exhibited a widespread expression within the CRA (Fig. 19B/C, right panels). The examination of *Wnt2b* and *Ttr1* expression, which mark the choroid plexus and cortical hem in wild-type embryos, showed likewise the presence of scattered *Wnt2b*- (Fig. 19D, right panel) and *Ttr1*- (Fig. 20A, right panel) positive cells in the lateral-most part of the CRA. These data lets assume that telencephalic cells contribute to the CRA.

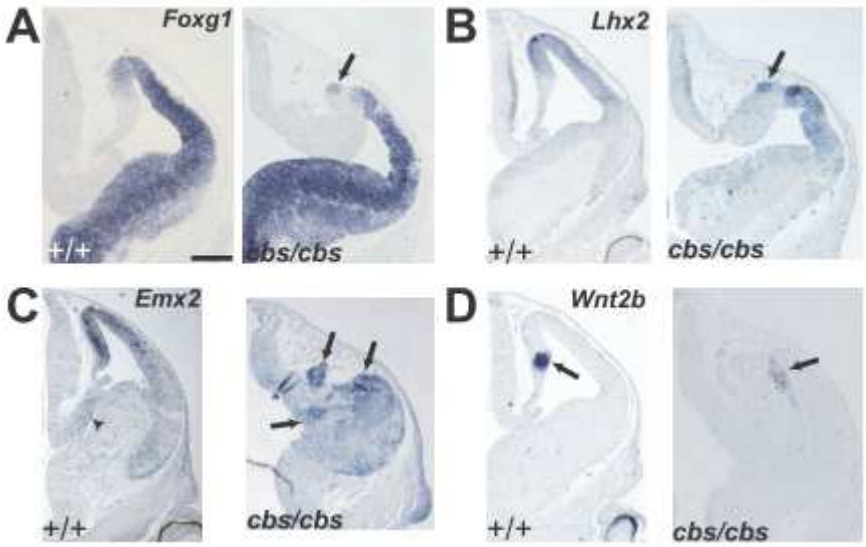

Fig. 19. The dorsal telencephalic-diencephalic boundary in the *cbs/cbs* mutant. A-D. *in situ* hybridization analysis of E12.5 wild-type (+/+) and cbs/cbs embryos. For each coronal section, only one telencephalic half is shown, with dorsal to the top, lateral to the right. **A.** *FoxG1*. **B.** *Lhx2*. **C.** *Emx2*. Asterisk indicates fold in the tissue. **D.** *Wnt2b*. Scalebar: 300 µm.

Emx2 and *Lhx2* are also expressed in the eminentia thalami (ET) and in the dorsal diencephalon, respectively. Therefore the possibility was investigated, if the CRA also contains diencephalic cell types. The dorsal and the ventral thalamus are separated from each other by the expression of *Shh* in the zona limitans in trathalamica (ZLI), which is the case in both wild-type and *cbs/cbs* mutant forebrain (Fig. 20B). This indicates that the dorsal thalamus in the *cbs/cbs* mutants do not extend into the CRA. The expression of *Dlx2*, which marks the ventral thalamus (VT) of wild-type embryos (Bulfone *et al*., 1993), is found in the CRA of *cbs/cbs* mutants, although in a highly disorganized and irregular manner (Fig. 20C, right panel). *Foxd1* is expressed in the ventral diencephalon of wild-type embryos (Fig. 20D, left panel). A group of *Foxd1*-expressing is located within the CRA of *cbs/cbs* mutants (Fig. 20D, right panel), which is similar to *Dlx2*. However, neither *Dlx2* (Fig. 20C) nor *Foxd1* (Fig. 20D) expressions were seen in the dorsal telencephalon. Taken together these data suggest that

the CRA is primarily composed of VT and ET cells, but also contains some scattered telencephalic cells.

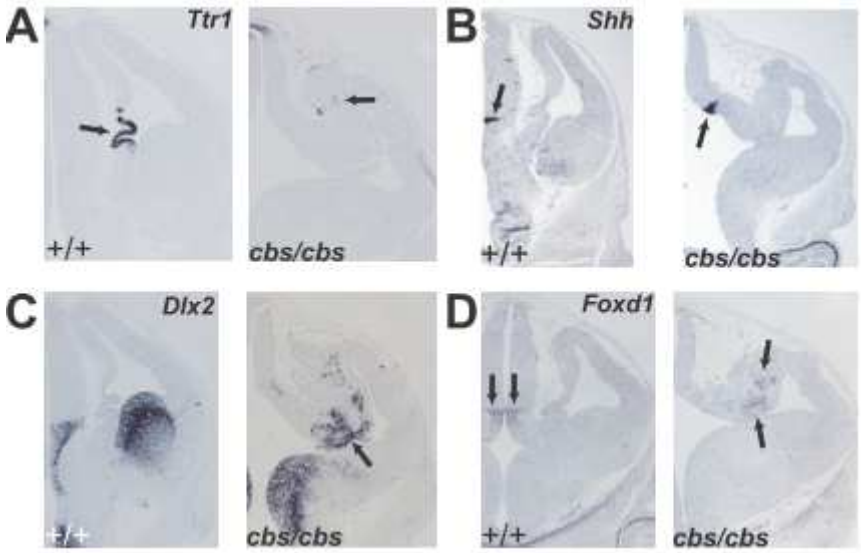

Fig. 20. The dorsal telencephalic-diencephalic boundary in the *cbs/cbs* mutant. A-D. *in situ* hybridization analysis of E12.5 wild-type (+/+) and cbs/cbs embryos. For each coronal section, only one telencephalic half is shown, with dorsal to the top, lateral to the right. **A.** *Ttr1*. **B.** *Shh*. **C.** *Dlx2*. **D.** *FoxD2*. Scalebar: 300 µm.

3.7 Wnt expression and signaling is upregulated in *cbs/cbs* mutants

Mutations in ciliary and basal body proteins have lately been shown to result in an upregulation of canonical Wnt signaling (Gerdes *et al*., 2007; Corbit *et al*. 2008). The expression of several *Wnt* genes was analyzed to determine, if Wnt signaling may play a role in the morphological deformations seen in the *cbs/cbs* mutants. In the neocortex of E12.5 wild-type embryos *Wnt7b* expression can be seen in the cortical hem and hippocampal VZ, and in cortical neurons, but it is absent in from the neocortical VZ (Fig. 21A, left panel). In *cbs/cbs* mutants the expression of *Wnt7b* was normal in cortical neurons, but they displayed ectopic expression in isolated neocortical progenitor cells, similar to *Gli3* mutants (Fig. 21A, right panel) (Theil *et al*., 2005). Strong expression of *Wnt7b* ,at caudal levels of the *cbs/cbs* forebrain, could also be seen in the CRA, which probably is consistent with its expression in the wild-type VT and ET (Fig. 21B, right panel).

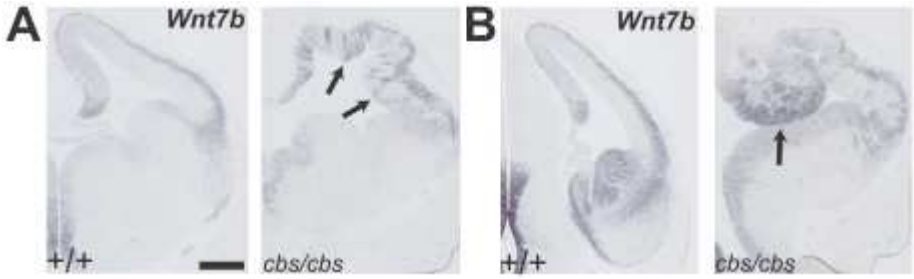

Fig. 21. Canonical Wnt signalling in the *cbs/cbs* mutant. A/B. *in situ* hybridization analysis of E12.5 wild-type (+/+) and cbs/cbs embryos. For each coronal section, only one telencephalic half is shown, with dorsal to the top, lateral to the right. **A.** *Wnt7b* expression in the rostral part of the telencephalon. **B.** *Wnt7b* expression in the caudal part of the telencephalon. Arrows indicate signal described in the text. Scalebar: 300 µm

An upregulation of *Wnt8b* similar to *Wnt7b* was also observed in the CRA (Fig. 22B, right panel), although the upregulation was not as extensive.

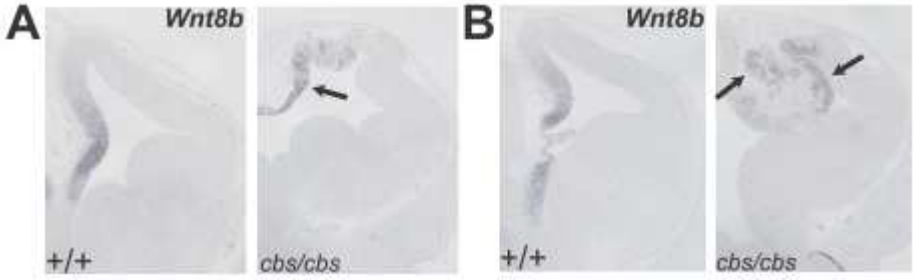

Fig. 22. Canonical Wnt signalling in the *cbs/cbs* mutant. A/B. *in situ* hybridization analysis of E12.5 wild-type (+/+) and cbs/cbs embryos. For each coronal section, only one telencephalic half is shown, with dorsal to the top, lateral to the right. **A.** *Wnt8b* expression in the rostral part of the telencephalon. **B.** *Wnt8b* expression in the caudal part of the telencephalon. Arrows indicate signal described in the text. Scalebar: 300 µm

The upregulated *Wnt* gene expression in the CRA brought me to check for activation of canonical Wnt signaling. *Axin2* is a direct target of the canonical Wnt signaling pathway (Jho *et al*., 2002; Lustig *et al.*, 2002) and exhibits a graded expression in wild-type dorsomedial telencephalon (Fig. 23A, left panel). *cbs/cbs* mutants otherwise displayed a patchy *Axin2* activation dorsomedially (Fig. 23A, right panel). In contrast, *Axin2* was strongly expressed in the CRA of *cbs/cbs* mutants, in particular within heterotopias (Fig. 23B, right panel). *Axin2* expression was also detected in the dorsal thalamus of both genotypes at this level (Fig. 23B, both panels).

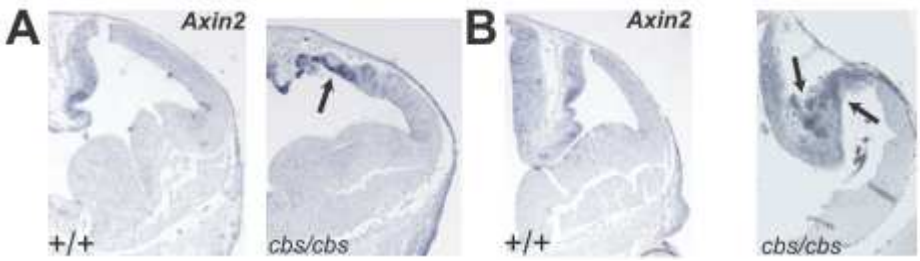

Fig. 23. Canonical Wnt signalling in the *cbs/cbs* mutant. A/B. *in situ* hybridization analysis of E12.5 wild-type (+/+) and cbs/cbs embryos. For each coronal section, only one telencephalic half is shown, with dorsal to the top, lateral to the right. **A.** *Axin2* expression in the rostral part of the telencephalon. **B.** *Axin2* expression in the caudal part of the telencephalon. Arrows indicate signal described in the text. Scalebar: 300 µm

To quantitate this increases in Wnt signaling, I performed quantitavie, quantitative RT-PCR upon mRNA extracted from E12.5 *cbs/cbs* mutant telencephalon, comparing gene expression levels to wild-type littermates. A 1.54 +/- 0.25-fold increase in the expression of *Axin2* ($p < 0.05$, $n = 5$, Student´s *t* test) but interestingly not that of *Wnt7b* (1.25 +/- 0.24-fold increase, $p = 0.37$, $n = 6$) was observed, indicating that the heterotopic expression of *Wnt7b* is in aggregate not reflective of an increase in total mRNA levels. Taken together this data indicates that an ectopic activation of canonical Wnt signaling in the CRA occurs, but it cannot be directly connected to an upregulation of *Wnt7b* expression.

3.8 Targets of Shh signaling and Gli3 protein processing are disturbed in the forebrain of *cbs/cbs* mutants

Several phenotypes seen in *cbs/cbs* mutants resemble that detected in the *Gli3* deletion mutant Xt^J, including polydactyly, defects in the determination of dorsal telencephalic tissue, the formation of rosette-shaped heterotopias in the dorsal cortex, and the relaxation of the telencephalic-diencephalic boundary (Johnson, 1967; Theil *et al*., 1999; Tole *et al*., 2000; Fotaki *et al*., 2006). Because of these similarities in phenotypes I examined *Gli3* expression patterns in the *cbs/cbs* mutant. High levels of *Gli3* expression were maintained in the telencephalon of *cbs/cbs* mutants (Fig. 24A, right panel).
A complete abolition and a strong downregulation, respectively, of the transcription factors *Emx1* and *Emx2* is one of the hallmarks of the Xt^J mutant (Theil *et al*., 1999; Tole *et al*., 2000). This is not he case in *cbs/cbs* mutants, where analysis of both of these markers showed no downregulation in their expression (Fig. 24B/C, right panels), rather, a patchy *Emx1* expression pattern.

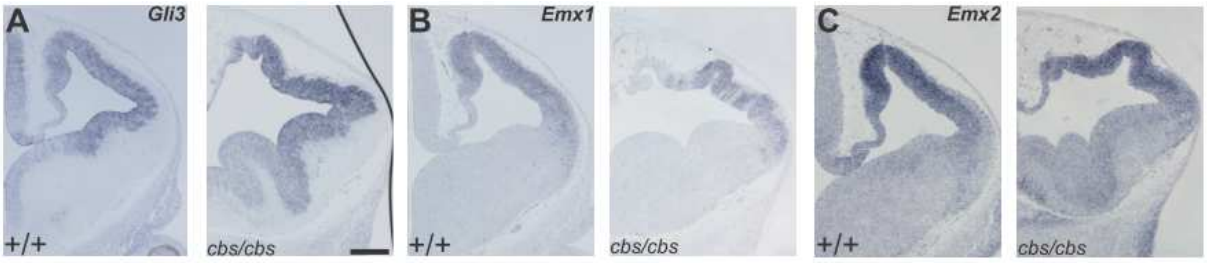

Fig. 24. Shh signalling in the forebrain of *cbs/cbs* mutant. A-C. *In situ* hybridization analysis of E12.5 wild-type (+/+) and cbs/cbs embryos. For each coronal section, only one telencephalic half is shown, with dorsal to the top, lateral to the right. **A.** *Gli3* expression **B.** *Emx1* expression **C**. *Emx2* expression. Scalebar: 300 µm

Defects in the proteolytic processing of Gli3 in a number of IFT mutants was reported by several laboratories (Haycraft *et al*., 2005; Huangfu and Anderson, 2005; Liu *et al*., 2005; May *et al*., 2005; Tran *et al*., 2008). Western blotting upon protein extracted from E12.5 forebrain tissue was performed to analyze the effect upon Gli3 processing in *cbs/cbs* mutants. The production of both the full-length, 190 kDa activator (Fig. 25B, arrows) form of Gli3 and the truncated, 90 kDa repressor (Fig. 25B, arrowheads) form of Gli3 could be detected by using an anti-N-terminal-Gli3 antibody. In *cbs/cbs* mutants, no change in the amount of the cleaved isoform (Fig. 25B, arrowheads) was detectable, but a strong increase was observed in the amount of the full-length isoform (Fig. 25B, arrows). Quantitation showed a 5.6-fold increase in the amount of the full-length Gli3-isoform in *cbs/cbs* mutant forebrain, compared with wild-type, whereas the amount of the processed Gli3-isoform in the *cbs/cbs* mutants did not change significantly (Fig. 25C). Together, the total amount of Gli3 protein increases by 67.2% in *cbs/cbs* mutant forebrain (Fig. 25C). These changes are not clarified at the level of transcription, as Northern blot analysis of mRNA isolated from the forebrain exhibited neither a change in the quantity of *Gli3* mRNA nor in transcript size (Fig. 25A).

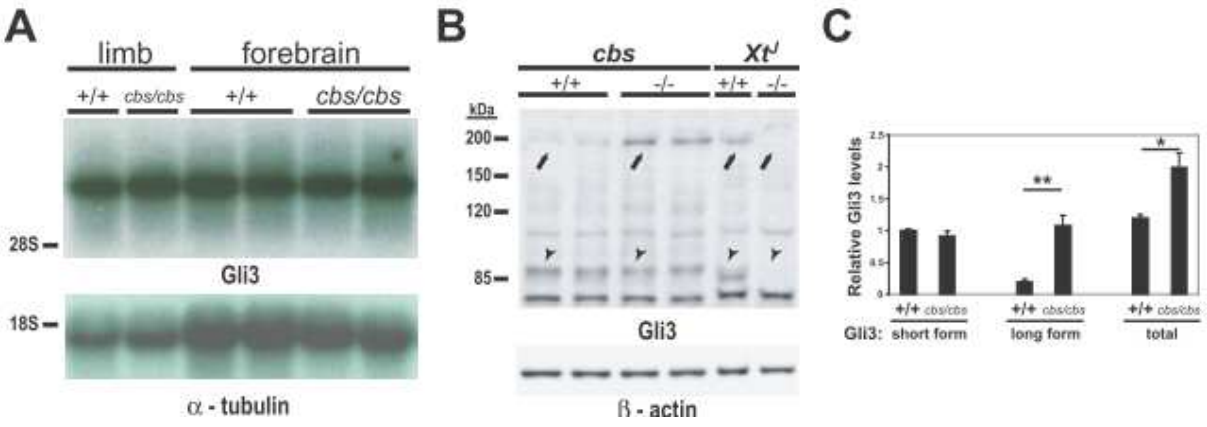

Fig. 25. Gli3 protein processing is disturbed in the forebrain of *cbs/cbs* mutant. A. Northern blots of whole RNA from forebrain of E12.5 wild-type (+/+) and *cbs/cbs* embryos. Full-length *Gli3* (top) and α-tubulin (bottom) cDNAs were used as probes. Ribosomal markers are to the left. **B.** Western blots from protein lysates from forebrain of E12.5 *cbs/cbs* and Xt^J and wild-type (+/+) and homozygous mutant (-/-) embryos. An anti-N-terminal-Gli3 antibody (top) and an anti-β-actin (bottom) antibody were used. Specific bands corresponding to

the 190 kDa full-length Gli3 isoforms (arrows) and the 80 kDa proteolytically processed Gli3 isoform (arrowheads) are indicated. The specificity of the antibody was shown by examining homozygous *Gli3* deletion mutants (Xt^J), in which neither full-length nor processed Gli3 isoforms are detectable. Protein markers (kDa) are to the left. **C.** Quantitation of Gli3 Western blots seen in (B), first indicating the amount of the 90 kDa (short form) Gli3 isoform, setting levels in +/+ to 1.0. A quantitation comparison of the 190 kDa (long form) isoform shows 19.4% levels in +/+ embryos, compared with the short form. *cbs/cbs* mutants show a 5.6-fold increase in the amount of the long form, compared with +/+ embryos, to levels greater than that of the short form in *cbs/cbs* embryos. The combined amount of short and long isoforms is also indicated (total). Mean values+/- SEM (n = 4 – 8). **p < 0.01, *p < 0.05, Student´s t test.

To examine the potential effect of an overproduction of the full-length Gli3 isoform in *cbs/cbs* mutant forebrain, *in situ* hybridization analysis of *Ptch1*, a downstream target of Shh signaling (Goodrich *et al*., 1996; Marigo *et al*., 1996; Platt *et al*., 1997; Agren *et al*., 2004) was performed. The expression of *Ptch1* seemed to increase in the GEs of *cbs/cbs* mutants (Fig. 26A, right panel), but no expression was detected in the dorsal telencephalon. To quantitate these evidently increase in *Ptch1* expression, I performed quantative, real-time RT-PCR upon mRNA extracted from E12.5 *cbs/cbs* mutant telencephalon, comparing gene expression levels to wild-type littermates. A clear increase in the expression of both *Ptch1* and *Gli1* (Fig. 26B), another downstream target of Shh signaling (Lee *et al*., 1997) could be detected.

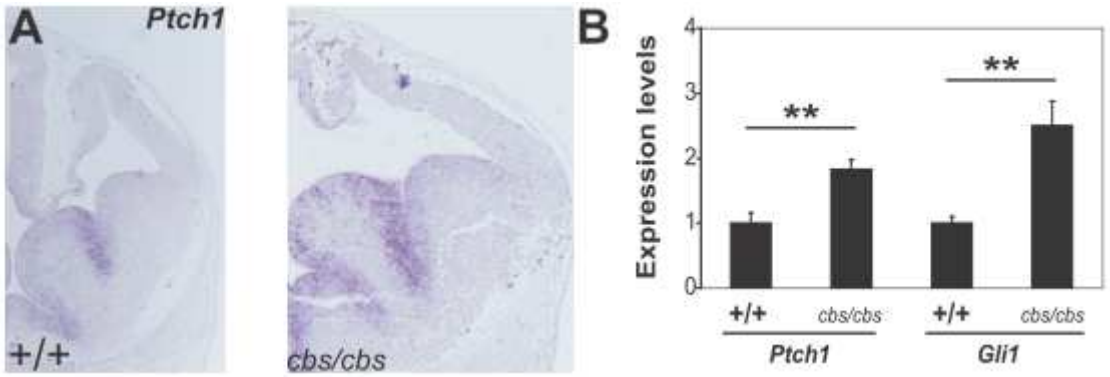

Fig. 26. Effect of an overproduction of the full-length Gli3 isoform in *cbs/cbs* mutant forebrain. A. *Ptch1 in situ* hybridization analysis of E12.5 wild-type (+/+) and *cbs/cbs* embryos. For each coronal section, only one telencephalic half is shown, with dorsal to the top, lateral to the right. Scale bar: 300 µm. **B.** Quantitative real time RT-PCR was performed upon total mRNA isolated from E12.5 telencephalon. Reverse-transcribed cDNA was analyzed using TaqMan probes recognizing *Ptch1* and *Gli1*. cDNA was normalized using probes for GAPDH. Mean values+/- SEM (n = 4 – 8). **p < 0.01, *p < 0.05, Student´s t test.

It was of interest then to check, whether cells in *cbs/cbs* mutants lost their competence to respond to Shh signaling. To test this, fibroblast cultures were prepared from decapitated, eviscerated E12.5 wild-type and *cbs/cbs* mutant embryos. Fibroblasts were electroporated with a Shh-responsive plasmid, which expresses the firefly luciferase gene under the control of a minimal promoter and 8 tandem

copies of a Gli binding site (Sasaki *et al*., 1997), using a plasmid expressing Renilla luciferase to control for transfection efficiency. Cells were permitted to grow till they reached confluency and the production of cilia was promoted by switching to a low-serum medium (Ocbina and Anderson, 2008), followed by treatment for 12 h with Shh at 1µg/ml and lysis for quantitation of luciferase activity. Shh was able to induce a sevenfold increase in luciferase expression from the Gli-responsive reporter plasmid in wild-type fibroblasts (Fig. 27), but both basal and Shh-induced luciferase expression levels were greatly reduced in *cbs/cbs* mutant fibroblasts (Fig. 27).

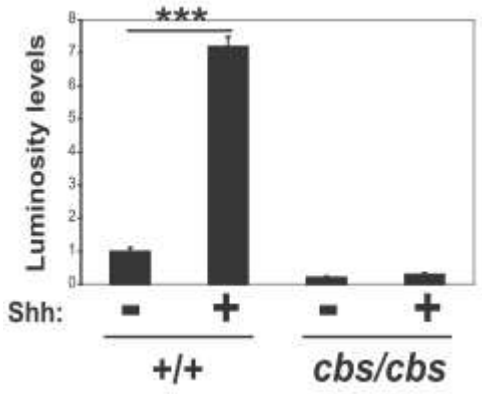

Fig. 27 Luciferase assay analyzing the competence of fibroblast cells to respond to Shh signaling. A. Luciferase assay using a Gli-responsive luciferase plasmid transiently transfected into fibroblasts prepared from wild-type (+/+) and cbs/cbs embryos and allowed to reach confluency. Sonic hedgehog (Shh, 1 µg/ml) was added to the cultures for 12 h before lysis and analysis of luciferase levels. Relative luminosity levels relative to Shh-untreated wild-type cells are indicated. Mean values+/- SEM (n = 4 – 8). ***p < 0.001, Student´s *t* test.

4 Discussion

The *cobblestone* (*cbs*) mouse mutant was generated in an ENU screen undertaken by my supervisor Dr. Kerry L. Tucker to uncover deformations in the developing central and peripheral nervous systems. In the course of the characterization of the *cbs/cbs* mouse mutant I was able to reveal that the *cbs* mutation is a hypomorphic allele of the gene encoding intraflagellar transport (IFT) protein Ift88. By further investigation of the *cbs/cbs* forebrain phenotype I could show that primary cilia are important for the normal development of the dorsal telencephalon.

4.1 Evidence for *Ift88* to be the defective gene in the *cbs/cbs* mutants

Several results allow me to conclude that *Ift88* is the defective gene in the *cbs/cbs* mutants: First, fine mapping indicated it to lie in a 0.5 cM interval containing *Ift88.* Second, the Ift88 mRNA and protein are expressed at only around 25% of the levels of wild-type embryos. Third, compound *cbs/Ift88*$^{tm1.1Bky}$ embryos show a very similar phenotype in the forebrain when compared to *cbs/cbs* mutant embryos of the same age. The phenotype of the compound *cbs/Ift88*$^{tm1.1Bky}$ embryos is even more severe than in the *cbs/cbs* mutant embryos. The reason for the more severe phenotype could be that in the compound embryos the levels of Ift88 protein is even more reduced when compared to *cbs/cbs* mutant embryos. The further reduced Ift88 protein levels in the compound embryos results from the complete deletion of one allele of the *Ift88* gene, whereas this is not the case in the *cbs/cbs* mutant embryos.

The results of a reduced expression and lack of a mutation in the *Ift88* mRNA of the *cbs/cbs* mutant leads to the assumption of a new hypomorphic allele that enables the embryos to live long enough to exhibit significant defects in dorsal telencephalic development, whereas the full knock-out is not suitable for this investigation because of its embryonic lethality at already E10.5 (Murcia *et al*., 2000).

Ultrastructural normal primary cilia projecting into the ventricle of the forebrain are still to be seen in the *cbs/cbs* mutant embryos, whereas this is not the case in other *Ift88* mutations (Murcia *et al*. 2000; Haycraft *et al*., 2001; Kramer-Zucker *et al*., 2005; Banizs *et al*., 2005). My hypothesis is that the observed Ift88 protein levels in the *cbs/cbs* mutant embryos, which refers to 25% of wild-type levels, are still sufficient for the assembly and maintaining of primary cilia, as shown by TEM and SEM in the developing forebrain (Fig. 8; Fig. 9; Fig. 11). However, they seem not adequate enough to support the levels of signal transduction/ protein processing needed for a proper development, as demonstrated by a reduction of Gli3 processing, as has been reported for a number of IFT mutants (Haycraft *et al*., 2005; Huangfu and Anderson, 2005; Liu *et al*., 2005; May *et al*., 2005; Tran *et al*., 2008). Furthermore, in knock-out mutations of IFT genes (Murcia *et al*., 2000; Liu *et al*., 2005), *situs inversus* has been connected with a loss of cilia at the embryonic node (Murcia *et al*., 2000; Huangfu *et al*., 2003; Houde *et al*., 2006). *cbs/cbs* mutant embryos never showed *situs inversus*, whereas

compound heterozygotes of the *cbs* and *Ift88* knock-out alleles, in which the protein levels of Ift88 are expected to be reduced further than in *cbs/cbs* mutant embryos, did display *situs inversus*. This observation leads to the suggestion that the level of Ift88 protein in *cbs/cbs* mutant embryos lies just above the limit for the formation of functional cilia in early development, but is not high enough to enable a proper signal transduction. Taken together the results imply that IFT is potentially impaired in the *cbs/cbs* mutant embryos.

The levels of Ift88 protein are also reduced in the *Ift88* hypomorph *Tg737orkp*, and analysis of brain ventricles of this mutant postnatally indicated that cilia were still present, but they were sparser, shorter and displayed altered morphology (Banizs *et al*., 2005). It is to be expected that *cbs/cbs* mutants would also display morphological defects in primary cilia over time, but because of the early lethality of the *cbs/cbs* mutant embryos it is not possible to do this analysis.

I can draw the conclusion that the reduction of Ift88 protein levels displayed by *cbs/cbs* mutant embryos results mainly in a defect in ciliary function connected to a defective IFT by the following results:

First, a large number of studies have reported the Ift88 protein to be localized only at the base and tips of primary cilia, in a wide range of tissues (Taulman *et al*., 2001; Pazour *et al*., 2002; Haycradft *et al*., 2005, 2007). Second, it is well recorded for Ift88 to be involved in IFT (Rosenbaum and Witman, 2002). Third, the changes of the Gli3 processing revealed in *cbs/cbs* mutant embryos (Fig. 25B; Fig. 25C) have also been seen in a number of mutants in IFT proteins that are documented to be localized to primary cilia (Haycraft *et al*., 2005; Huangfu and Anderson, 2005; Liu *et al*., 2005; May *et al*., 2005; Tran *et al*., 2008). Fourth, two other IFT proteins have been reported to exhibit deformations during telencephalic development. *Dnch2*, a gene encoding the retrograde IFT motor, displays a breakdown of the pallial-subpallial boundary when knocked out (May *et al*.., 2005). A null mutation of *Thm1*, a novel protein that is localized to cilia and is involved in the regulation of retrograde IFT, displays exencephaly and heterotopia-like structures in the cerebral cortex (Herron *et al*., 2002; Tran *et al*., 2008).

In summary the combined results indicate clearly that *cbs* is a novel mutation of *Ift88*, because it shows no morphological ciliary defect but does suggest a reduction in ciliary function based on a possible defective IFT, through its altered processing of Gli3, when compared with *Ift88* deletion mutants and other IFT mutants (Huangfu *et al*., 2003; May *et al*., 2005; Houde *et al*., 2006; Tran *et al*., 2008).

4.2 Impaired Hh signalling in the *cbs/cbs* mutant

4.2.1 The forebrain phenotype of the *cbs/cbs* mutant is similar to defects in the Gli3 mutant *Xt^J*

The defects displayed by the *cbs/cbs* mutants in the developing telencephalon include severe disorganization of structures of the dorsomedial telencephalon (Fig. 12) such as the choroid plexus (Fig. 14A), the cortical hem (Fig. 14B), and the hippocampus (Fig. 15). The mutation also affects the pallial-subpallial (Fig. 16; Fig. 17; Fig. 18) as well as the telenecphalic-diencephalic (Fig. 19; Fig. 20) boundary. These are the major borders confining the dorsal telencephalon. The *Gli3* mouse mutant *Xt^J* displays, when compared to *cbs/cbs* mutant embryos, a strikingly similar forebrain phenotype. Both mutants exhibit abnormal development of the dorsomedial telencephalon and of the boundaries that separate the dorsal from the ventral telencephalon (Tole *et al*., 2000; Kuschel *et al*., 2003) and from the diencephalon (Theil *et al*., 1999; Fotaki *et al*., 2006). Both mutants are also distinguished by ectopic *Wnt7b* expression in cortical progenitors (Theil, 2005). A further characterization of both mutants is as well the formation of heterotopias with a rosette-like structure (Theil *et al*., 1999; Fotaki *et al*., 2006). The similarities shared by both mouse mutants lead to the suggestion that the displayed phenotypes have a related origin, but noticeable phenotypic distinctions between the two mutations exist, which would argue against this simple assumption. A closer examination indicated that the processing of Gli3 is defective in *cbs/cbs* mutants. Thus, there is a link confirming the related origin of the similar forebrain phenotypes.

4.2.2 Different phenotypes between *cbs/cbs* and *Xt^J*

Beside the similarities there are also important phenotypic differences between the two mutations. Invagination and specification of dorsomedial structures (e.g. choroid plexus, cortical hem) (Fig. 12A-D; Fig. 14-20), similar to *Gli3* hypomorphic mutants (Kuschel *et al*., 2003; Friedrichs *et al*., 2008), still occurs to some extent in the *cbs/cbs* mutants. *Xt^J* mutants do not exhibit any invagination or specification of this dorsomedial structures (Johnson, 1967; Theil *et al*., 1999). *Emx1* and *Emx2*, which are downregulated in the *Xt^J* mouse mutant (Theil *et al*., 1999; Tole *et al*., 2000), are still expressed in the developing forebrain of *cbs/cbs* mutant embryos (Fig. 24B/C). This is a possible indication of a weaker *Gli3* mutant phenotype. The formation of rosettes, however, starts at an earlier time point and is in addition considerably expanded in *cbs/cbs* mutant embryos. This result can be a sign of a stronger phenotype in *cbs/cbs* mutant embryos when compared to *Gli3* mutants.

4.2.3 Defective proteolytic processing of the Gli3 protein in the *cbs/cbs* mutant

A possible explanation for the uncovered differences could be the nature of the Xt^J mutation. It is a genomic deletion of Gli3 in which both the full-length transcriptional activator as well as the processed transcriptional repressor isoform of Gli3 are absent (Maynard *et al*., 2002). This is not the case in the *cbs/cbs* mutants.

Both of the Gli3 protein isoforms are still present, but in the *cbs/cbs* mouse mutant the proteolytic processing of Gli3 protein is clearly altered, shifting the relative ratio of Gli3 activator and repressor form. The *cbs/cbs* mutants exhibit an increase of the full-length, unprocessed isoform of Gli3 by a factor of five (Fig. 25C), whereas the amount of the cleaved isoform is unchanged. Because of this the total amount of Gli3 protein is increased by 67%. At the level of the Gli3 mRNA no increase occurs in the *cbs/cbs* mutants (Fig. 25A). This indicates that the expression of the *Gli3* gene is not defective in the *cbs/cbs* mutants. The observed shift of the relative ratio of Gli3 activator and repressor form has to take place on the level of proteolytic processing level of Gli3.

A simple explanation of this result is that the full-length isoform may be stabler within the mutant cells than the processed isoform. All three Gli family members (Gli1, Gli2 and Gli3) can be targeted for rapid degradation by two conserved sequences in their C-terminus (Huntzicker *et al*., 2006). The full-length isoform would also possess this sequences, which makes the reasons for its potential enhanced stability unclear. One possibility could be that motifs in the N terminus may protect the protein from degradation. Recent studies may give another possible explanation for this phenotype.

The formation of the two different isoforms of Gli3 is dependent on the interaction between Gli3 and SuFu (Humke *et al*., 2010). SuFu is an important negative regulator of the Hh signalling pathway. The result of the loss of SuFu is the destabilization of the full-length form of Gli3, whereas the processed form of Gli3 is unaffected (Wang *et al*., 2010). Full-length Gli3 associates together with SuFu in the cytoplasm, which is independent of primary cilia (Chen *et al*., 2009; Jia *et al*., 2009). The full-length Gli3-SuFu-complex promotes the primary cilia dependent (Huangfu and Anderson, 2005) proteolytic processing of full-length Gli3. At the same time full-length Gli3 is also protected from degradation through Spop in the cytoplasm as long as it is bound by SuFu (Chen *et al*., 2009). Spop seems not to need primary cilia for the degradation of full-length Gli3 (Chen *et al*., 2009). A possible explanation for the increased level of full-length Gli3 in the *cbs/cbs* mutants could be that the proteolytic processing of Gli3, which requires primary cilia, is impaired. The Gli3-SuFu-complex can still enter the primary cilium of *cbs/cbs* mutants, but SuFu can no longer dissociate from full-length Gli3, a process depending on Kif3a (Humke *et al*., 2010). Kif3a is, like Ift88, a component of IFT, and *Ift88* is the defective gene in *cbs/cbs* mutants. Perhaps Ift88 is also in the context of IFT, together with Kif3a, required for the dissociation of SuFu from full-length Gli3. Thus, SuFu may fail to dissociate from full-length Gli3, which is then at the same also protected by degradation through Spop. This

could then result in the observed increase of full-length Gli3 protein levels. However, the problem with this explanation is that full-length Gli3 needs to dissociate from SuFu to enter the nucleus and become a transcriptional activator. The nature of the *cbs/cbs* mutant itself could give the solution for this discrepancy. *cbs* is a hypomorphic allele of *Ift88*, and the observed Ift88 protein levels in the *cbs/cbs* mutant embryos, 25% of wild-type levels, may at least be sufficient for the formation and maintenance of primary cilia. The remaining 25% of Ift88 protein levels could also still be enough for some of the full-length Gli3 to dissociate from SuFu upon Hh signalling activation, enter the nucleus and act there as a transcriptional activator. At the same time the levels of Ift88 protein are as well sufficient for the processing of Gli3 to its cleaved repressor isoform, which is unaffected by SuFu and the degradation through Spop (Wang et al., 2010).

The competition between the two isoform in *cbs/cbs* mutants could be a reason for a further decrease of the effective concentration of the Gli3 repressor. As a possible result target genes of Gli3, which would usually be repressed in wild-type embryos, would be activated in the forebrain of *cbs/cbs* mutants in an abnormally fashion. The identity of the target genes of Gli3 in the developing cortex are unfortunately not well understood. *Emx1* as well as *Emx2*, as an example, are downregulated in the Xt^J mutant (Theil *et al*., 1999; Tole *et al*., 2000), but *Emx2* seems not to be a direct transcription target of Gli3 (Theil *et al*., 2002). Because of this observation the overproduction of the Gli3 activator isoform in *cbs/cbs* mutants is likely not directly linked to the expression of *Emx2* in *cbs/cbs* mutant embryos.

However, it has been reported that the Wnt signalling pathway directly regulates the transcriptional activation of *Emx2* (Theil et al., 2002). But the upregulation of *Wnt7b* and *Wnt8b* that was discovered in *cbs/cb* mutants, was most pronounced in the caudal-most telencephalon, some distance away from the more rostral cortex where *Emx1* and *Emx2* are expressed. But there is the possibility that diffusion of these growth factors could induce *Emx1* and *Emx2* transcription. Regardless of their transcriptional control, the maintenance of the expression of *Emx1* and *Emx2* in *cbs/cbs* mutants, and the similarities in the *cbs* and Xt^J forebrain phenotypes, leads to the assumption that reduced expression of *Emx1* and *Emx2* do not mainly affect the telencephalic defects of the Xt^J mutants. This is consistent with the analysis of a *Emx1/Emx2* double knock-out, which did not reproduce many aspects of the Xt^J phenotype (Shinozaki et al., 2004).

4.2.4 Defective Hh signalling response in the *cbs/cbs* mutant

I observed an upregulation of the Shh-responsive genes *Ptch1* and *Gli1* in the ventral telencephalon of *cbs/cbs* mutants (Fig. 26), which is not the case in several mouse mutants with defective IFT proteins. A reduction of *Ptch1* and *Gli1* expression was discovered in the forelimb (Haycraft *et al*., 2005; Liu *et al*., 2005), hippocampus (Han *et al*., 2008), and cerebellum (Spassky *et al*., 2008). The reason for this contradiction could be the fact that cortical cilia are still present in the *cbs/cbs* mutants, whereas they are absent in the brain (Han *et al*., 2008; Spassky *et al*., 2008) or the forelimb (Haycraft

et al., 2005) of the mutants analysed in three of the studies mentioned above. Transcriptionally active Gli3 is not made in IFT mutants lacking cilia (Haycraft *et al*., 2005; Huangfu and Anderson, 2005; Liu *et al*., 2005). It seems that cilia are really required for the production and release of the transcriptionally activating, full-length Gli3 isoform (Caspary *et al*., 2007; Chen *et al*., 2009; Humke *et al*., 2010; Wen *et al*., 2010). The mutation of the gene that encodes for the ciliary protein Arl13b leads also to an upregulation of *Ptch1* in the spinal cord, which is similar to the *Ptch1* upregulation seen in the GEs of the *cbs/cbs* mutant (Fig. 26). As a hypothesis it is possible that the low level of Ift88 protein in *cbs/cbs* mutant embryos is sufficient for the formation and maintenance of morphologically normal cilia as well as for the production and aggregation of the full-length isoform of Gli3 that acts as an activator for transcription as seen for the revealed upregulation of *Ptch1* and *Gli1*. Another possibility could be that Gli2 may take over this function. It has been reported to be localized to cilia and it has been shown that it needs cilia for its function as a transcriptional activator (Haycraft *et al*., 2005; Chen *et al*., 2009). Because of the 75% decrease of Ift88 protein levels in *cbs/cbs* mutant embryos, a disfunction in IFT is to be anticipated. This is the case for the *cbs/cbs* mutant embryos, where it prevents an acute response to Shh treatment *in vitro*, as revealed in the luciferase experiments on fibroblast cultures (Fig. 27). That was also observed in other mutants for IFT (Ocbina and Anderson, 2008). The inconsistency between this result and the upregulation of the expression of Hh signalling targets may be explained by the fact that the formation of the Gli3 transcriptional activator is independent of primary cilia (Chen *et al*., 2009; Jia *et al*., 2009).

Nonetheless, it is unlikely for an altered Shh signalling to be also responsible for the phenotype in the dorsal forebrain of *cbs/cbs* mutant embryos, as seen by comparison with the situation in the Xt^J mutant. Shh signalling is in the homozygous Xt^J mutant embryos, as in *cbs/cbs* mutant embryos, not ectopically activated in the dorsal telencephalon (Theil et al., 1999). The dorsal phenotype of the telencephalon of Xt^J mutant embryos is not rescued in Shh/Xt^J double mutant embryos (Rash and Grove, 2007), which also speaks against an involvement of Shh signalling in the dorsal telencephalic phenotype.

On the other hand the subdivision of the telencephalon into a dorsal and a ventral domain is controlled by the dorsalizing effect of *Gli3* expression and the ventralizing effect of *sonic hedgehog* (*Shh*) expression. At the beginning, *Gli3* is expressed in the whole telencephalon (Fig. 7B, Introduction) and is then gradually downregulated in the ventral part of the telencephalon (Aoto *et al*., 2002; Corbin *et al*., 2003). The elimination of *Gli3* expression results in a lack of the choroid plexus, cortical hem, the hippocampus and the neocortex (Grove *et al*., 1998; Theil *et al*., 1999; Tole *et al*., 2000; Kuschel *et al*., 2003). The dorsalizing effect of *Gli3* expression is achieved by the cleaved Gli3 repressor isoform. The *cbs/cbs* mutants exhibit a large increase in the full-length, unprocessed isoform of Gli3, whereas the amount of the cleaved isoform is unchanged. The competition between the two isoforms in

cbs/cbs mutants could be a reason for a further decrease of the effective concentration of the Gli3 repressor, resulting in the loss the choroid plexus, cortical hem, and the hippocampus

4.3 Wnt signalling in the *cbs/cbs* mutant

4.3.1 Canonical Wnt signalling in the *cbs/cbs* mutant

Other proteins important for development also have been localized to cilia, such as Wnt signalling proteins (Corbit *et al*., 2007). While some studies claim that that primary cilia are not involved in the regulation of the canonical Wnt signaling pathway (Huang and Schier, 2009; Ocbina *et al*., 2009), several other studies indicate and support the possibility that canonical Wnt signalling is constrained instead of potentiated by primary cilia (Takemaru *et al*., 2003; Simons *et al*., 2005; Gerdes *et al*., 2007; Corbit *et al*., 2008; Voronina *et al*., 2009; McDermott *et al*., 2010). These contradictory findings suggest that primary cilia are perhaps not as important for canonical Wnt signalling as they are for the Hedgehog signalling pathway and that the constraining influence of primary cilia on the canonical Wnt signalling pathway may be cell type-specific and subtle. I could reveal a clear upregulation of *Axin2*, a target of canonical Wnt signalling (Fig. 23), in the caudal rosette-rich area (CRA) of *cbs/cbs* mutant embryos, especially in the heterotopias. An ectopic expression of *Wnt7b* (Fig. 21) and *Wnt8b* (Fig. 22) was also observed in the same region, which could be responsible for the *Axin2* upregulation. The area specific increase of canonical Wnt signalling in *cbs/cbs* mutant embryos seems to be consistent with the idea that the canonical Wnt signalling pathway may be cell type-specific and subtle. An upregulation of *Wnt7b* and *Wnt8b* are also observed in the Xt^J mutant (Theil, 2005), but the upregulation of *Wnt7b* and *Wnt8b* in the CRA of *cbs/cbs* mutant embryos is much more pronounced than observed in the similar brain region of Xt^J mutant embryos, suggesting that it may be a direct consequence of ciliary misfunction.

An earlier hypothesis suggested that β-catenin, a component of the canonical Wnt signalling pathway, is degraded at the basal body and the lack of primary cilia leads to an accumulation of cytoplasmatic β-catenin resulting in an elevated canonical Wnt response (Gerdes *et al*., 2007). A recent study has revealed that β-catenin is accumulated at the basal body of primary cilia by the Wnt signalling modulator Jouberin (Jbn) (Lancaster *et al*., 2009) to constrain the pathway (Lancaster *et al*., 2011). Jbn normally alleviates the nuclear translocation of β-catenin and thus affects positively the canonical Wnt signalling (Lancaster *et al*., 2009). The results of the recent study of Lancaster and colleagues suggests that the otherwise positive effect of Jbn is inhibited by the presence of primary cilia. The localization of Jbn to primary cilia is dependent on both anterograde and retrograde IFT, however it appears to be independent of Wnt ligands (Lancaster *et al*., 2009; Lancaster *et al*., 2011). Thus it could be possible that impaired IFT in the *cbs/cbs* mutant embryos may result in an accumulation of Jbn in the cytosol. An increased amount of β-catenin would be then translocated to

the nucleus upon a canonical Wnt response, resulting in the observed upregulation of the canonical Wnt signalling in *cbs/cbs* mutant embryos.

4.3.2 Non-canonical Wnt signalling in the *cbs/cbs* mutant

Several observations reported in this study speak against an impairment of the planar cell polarity (PCP) pathway, a non-canonical branch of the Wnt signalling, in *cbs/cbs* mutant embryos. PCP controls the coordinated, polarized orientation of cells within epithelial tissues, thus establishing cellular asymmetries within the tissue plane. It is necessary for several cellular processes in vertebrates such as convergent extension (CE) (Sokol, 1996; Heisenberg *et al*., 2000; Tada and Smith, 2000; Wallingford *et al*., 2000) and ciliogenesis (Gray *et al*., 2009; Kim *et al*., 2010; Dai *et al*., 2011). The PCP signalling pathway is also necessary for the polarized beating of motile cilia in the epidermis (Park *et al*., 2008; Mitchell *et al*., 2009) and in the ependyma (Borovina *et al*., 2010; Guirao *et al*., 2010; Tissir *et al*., 2010). Thus, it is not surprising that it is also involved in left-right patterning because it is required for the planar positioning of the motile primary cilia in the node of mice, the gastrocoel roof of *Xenopus*, and the Kupffer´s vesicle of zebrafish (Antic *et al*., 2010; Borovina *et al*., 2010; Hashimoto *et al*., 2010; Song *et al*., 2010). A crucial hallmark for a defective left-right patterning is the defect called *situs inversus*, and *cbs/cbs* mutant embryos (n = 61) never displayed it, which points to a possible normal PCP signalling in *cbs/cbs*.

PCP mutant mice exhibit a specific type of neural tube defects (NTD) called craniorachischisis, and this defect has an impact to the whole hindbrain and spinal cord in such that the vertebrate neural tube fails to close at the level of the neural tube (Kibar *et al*., 2001; Hamblet *et al*., 2002; Curtin *et al*., 2003; Y Wang *et al*., 2006) as a result of impairment in CE cell movements (Wallingford and Harland, 2002; J Wang *et al*., 2006; Ybot-Gonzalez *et al*., 2007). This type of NTD, however, is not highly specific for mutations involved in severe defects of ciliogenesis, because the initial closure of the hindbrain still occurs (Huangfu *et al*., 2003; Huangfu and Anderson, 2005; Liu *et al*., 2005; Caspary *et al*., 2007). 10% of the *cbs/cbs* mutant embryos display, similar to other mice mutant for genes engaged in ciliogenesis, at E12.5 a NTD called exencephaly (Fig. 3A), in which the closure fails to occur at the level of the forebrain. Exencephaly appears very rarely in mice mutant for core PCP genes, which again leads to the assumption of normal PCP signalling in *cbs/cbs*.

5 Future aspects

Even though several results allow me to conclude that *Ift88* is the defective gene in the *cbs/cbs* mutants, the mutation itself is still unknown. Sequencing of the mRNA transcript in the *cbs/cbs* mutant revealed no changes in the ORF or the 5´ and 3´ UTRs. This result indicates a mutation in an intron or a regulatory region, which should be identified by applying the technique of deep sequencing.

By the approach of luciferase assay I was able to show that cells in the *cbs/cbs* mutant have lost their competence to respond to Hh signalling. However, the analysis was only performed with fibroblast cultures. It would be highly informative to repeat the experiment by using neurosphere cultures to test, if neurons also do not respond anymore to Hh signalling.

The *cbs/cbs* mutant exhibits a five-fold increase of the full-length isoform of Gli3, the main mediator of the Hh signalling pathway. The reason for this increase is still unclear, but the analysis of the interaction between Gli3 and SuFu as well as Spop in the *cbs/cbs* mutant first by immunohistochemistry, followed by immunoprecipitation and western blots could give an answer to this question. An approach of subcellular fractionation would be informative to define the localization of Gli3 and SuFu in *cbs/cbs* mutant cells. To test if the full-length isoform of Gli3 is still able to enter the nucleus to act as a transcriptional activator, *cbs/cbs* mutant and wt control cells could be treated with the direct Smo activator SAG (Chen *et al*., 2002) followed by subcellular fractionation analysis. The full-length Gli3 isoform is converted into a transcriptional activator by phosphorylation (Humke *et al*., 2010). An additional analysis by phosphate affinity SDS-PAGE (Kinoshita *et al*., 2009) would maybe give further insight, if the five-fold increase of the full-length isoform of Gli3 is reflected by a change of its phosphorylation in *cbs/cbs* mutant cells. Finally, it would also be of highly interest to investigate, if Ift88, like Kif3a, is also necessary for the dissociation of SuFu from full-length Gli3. This could be done by using $Ift88^{-/-}$ and $Ift88^{+/+}$ MEF cells analysing their steady-state levels of both isoforms of Gli3 as well as the phosphorylation state of full-length Gli3 after treatment or without treatment with SAG. At the same time the interaction between Gli3 and SuFu in $Ift88^{-/-}$ and $Ift88^{+/+}$ MEF cells with and without Hh pathway activation should be investigated by immunoprecipitation

An area-specific increase of canonical Wnt signalling in the *cbs/cbs* mutant could be confirmed. A luciferase assay should be done to test if the cells in the *cbs/cbs* mutant have changed their competence to respond to Wnt signalling using fibroblast as well as neurosphere cultures. The main mediator of the canonical Wnt pathway is β-catenin, and the identification of its subcellular localization in *cbs/cbs* mutant cells by immunohistochemistry and nuclear extraction would be very informative. The same approach should then also be performed for Jbn, which normally facilitates the nuclear translocation of β-catenin to positively adjust canonical Wnt signalling. Another possibility would be to investigate the activity of the canonical Wnt pathway in *cbs/cbs* mutant and wt cells overexpressing Jbn by a luciferase assay.

The *cbs/cbs* mutant embryos (n = 61) never displayed *sizus inversus*, which can be explained by normal functioning primary cilia in the node. Thus far, the primary cilia in the node of *cbs/cbs* mutant embryos were not investigated, but it should be performed by SEM and/or TEM. If the primary cilia in the node of *cbs/cbs* mutant embryos are still normal in morphology and ultrastructure, it would further confirm my hypothesis that the remaining protein levels of Ift88 are sufficient for the formation and maintenance of the cilia but not any more for a proper function of signal transduction.

Abbreviations

Anatomical terms

A-P	Anterior - posterior
ANR	Anterior neural ridge
AVE	Anterior visceral endoderm
CGNP	Cerebellar granule neuron precursors
CNCC	Cardiac neural crest cells
CGA	caudal ganglionic eminences
CNS	Central nervous system
CR	Cajal-Retzius cells
CRA	Caudal rosette-rich area
D-V	Dorsal – ventral
DG	Dentate gyrus
DT	Dorsal thalamus
ES cell	Embryonic stem cell
ET	Eminentia thalami
GE	Ganglionic eminences
GNP	Granule neuron precursors
IFT	Intraflagellar transport
LGE	Lateral ganglionic eminences
MGE	Medial ganglionic eminences
NCC	Neural crest cells
NTD	Neural tube defect
PSPB	Pallial-subpallial boundary
PNS	Peripheral nervous system
S	Septum
VT	Ventral thalamus
VZ	Ventricular zone
ZLI	Zona limitans trathalamica

Genes, proteins, signalling pathways

aln	alien
APC	Adenomatous polyposis coli
Arl13b	ADP-ribosylation factor-like 13B
BBS	Biedl-Bardet syndrome

Bmp	Bone morphogenetic protein
Cbs	cobblestone
cDNA	copy DNA
Cul1	Cullin
Dbx 1	developing brain homeobox 1
Dkk 1	Dickkopf 1
Dlx 2	Distal-less homeobox 2
DNA	Deoxyribonucleic acid
dNTP	Deoxyribonucleotide-triphosphate
Dvl	Dishevelled
EGFP	Enhanced green fluorescent protein
Emx 1/2	Empty spiracles homolog 1/2
EphB 1	Eph receptor B1
Foxd 1	Forkhead box G1
FoxG1	Forkhead box D1
GAPDH	Glyceraldehyde-3-phosphate dehydrogenase
GFP	Green fluorescent protein
Gli 1/2/3	Gli-Kruppel family member Gli 1/2/3
Gsh2	GS homeobox 2
GSK3β	Glycogen synthase kinase 3β
Hesx 1	Homeobox gene expressed in ES cells
Hh	Hedgehog
HRP	Horse raddish peroxidase
Fgf	Fibroblast growth factor
Fz	Frizzled
IFT	Intraflagellar transport
Ift 88	Intraflagellar transport 88 homolog
Inv	Inversin
Jbn	Jouberin
Jnk kinase	c-Jun N-terminal kinase
Kif3a	Kinesin-like protein Kif3a
lacZ	Gene encoding for β-Galactosidase
Lhx2	LIM homeobox protein 2
LRP 5/6	Low-density lipoprotein receptor 5/6
Ngn 2	Neurogenin 2
Nkx2.1	Nk homeobox 1
mRNA	messenger RNA

Odf1	oral-facial-digital syndrome 1 gene homolog
	paired box gene 6
ORF	open reading frame
orpk	oak ridge polycystic kidney
Pax6	Paired box gene 6
PCP	Planar cell polarity
PDD	Processing determinant domain
PKA	Protein kinase A
Ptch 1	Patched 1
RA	Retinoic acid
RhoA	Ras homolog gene family, member A
RNA	Ribonucleic acid
Rock	Rho-associated coiled-coin containing protein
	kinase 1
SAG	Smo activator
SCF	Skp1-Cul1-F-box multi-protein E3 ubiquitin
	ligase complex
Sfrp 2	Secreted frizzled-protein related protein 2
Shh	Sonic hedgehog
Six3	Sine oculis-related homeobox 3 homolog
Skp1	S-phase kinase-associated protein 1
Slb	Selective LIM-domain binding
Smo	Smoothed
SNP	Single nucleotide polymorphism
SPOP	Speckle-type Pot protein
SSLP	Simple sequence length polymorphism
SuFu	Suppressor of Fused
TCF	T-cell factor
TGFβ	Transforming growth factor β
TLE	Transducin-like enhancer of split 1
Ttc21b	Tetratricopeptide repeat domain 21B
Ttr1	Thioltransferase 1
UTR	Untranslated region
Wnt	Wingless/Integrated
Wnt 2b/3a/7b/8b	Wingless-related MMTV integration site
	2b/3a/7b/8b
Xt^J	extratoes

Xvin	Xenopus inversin

Materials and Methods

APS	Ammoniumpersulfate
BSA	Bovine serum albumin
BCIP	5-Bromo-4-chloro-3-indolyl phosphate
Ca^{2+}	Calcium^{2+} ion
CHAPS	3-[(3Chloamidopropyl)dimethylammonio]-1-propanesulfonate
DAB	3,3´-Diaminobenzidine
DAPI	4´,6´-diamidino-2-phenylindol
DEPC	Diethyl dicarbonate
DMEM	Dulbecco´s modified Eagle´s medium
DMSO	Dimethylsulfoxide
ECL	Enhanced Chemiluminescence
EM	Electron microscopy
ENU	N-ethyl-N-nitrosourea
EDTA	Ethylendiamine-tetraacetate
EtBr	Ethidiumbromide
EtOH	Ethanol
FBS	Fetal bovine serum
FCS	Fetal calf serum
IHC	Immunohistochemistry
ISH	*in situ* hybridization
LB	Luria-Bertani
MeO	Methanol
$MgCl_2$	Magnesiumdichloride
MOPS	3-(N-morpholino)propanesulfonic acid
MP-H_2O	Double distilled water
NB	Northern blot
NBT	Nitro blue tetrazolium chloride
NGS	Native goat serum
OsO_4	Osmiumtetraoxide
PBS	Phosphate buffered saline
PBST	Phosphate buffered saline + Tween-20
PCR	Poly chain reaction
PFA	Paraformaldehyde

PIPES	Piperazine-N,N´-bis(2-ethanesulfonic acid)
PMSF	Phenylmethanesulfonylfluoride
PVP	Polyninylpyrrolidone
RT-PCR	Reverse Transcriptase PCR
RTq-PC	Real Time quantitative PCR
SDS	Sodiumdodecylsulfate
SEM	Scanning EM
SOB	Super optimal broth
SSC	Saline sodium citrate
TAE	Tris-acetic acid-EDTA-buffer
TBE	Tris-borate-EDTA-buffer
TBS	Tris-buffered saline
TBS-T	Tris-buffered saline + Tween-20
TEM	Transmission EM
TEMED	N,N,N',N'-Tetramethylethylenediamine
Tris	Trimethylsilylsilan
TritonX-100	Polyethylene glycol p-(1,1,3,3-tetramethyl-butyl)-phenyl-ether
Tween-20	Polyoxyethylen(20)-sorbitan-monolaurate
WB	Western blot

Others

AB	Antibody
Bp	Basepairs
cM	centi Morgan
Ct	Treshold cycle
E	Embryonic day
ES cell	Embryonic stem cell
et al.	et alteri
G 1	Generation 1
h	hour
kDa	kilo Dalton
ko	knock out
M	Mol pro litre
MEF	Mouse embryonic fibroblasts
mg	miligram
ml	Milliliter

ms	Mouse
n	Number (of samples)
n.s.	Not significant
o/N	Over night
p	Probability-value (statistical significance)
pH	Potentia hydrogenii (cologarithm of the activity of dissolved hydrogen ions)
rb	Rabbit
RE	Relative expression
rpm	Rounds per minute
SEM	Standard error of the mean
UV	ultraviolet

References

Agren M, Kogerman P, Kleman MI, Wessling M, Toftgard R (2004) Expression of the PTCH1 tumor suppressor gene is regulated by alternative promoters and a single functional Gli-binding site. Gene 330:101-114.

Altman J, and Bayer SA (1990) Migration and distribution of two populations of hippocampal granule precursors during the perinatal and postnatal periods. J Comp Neurol 301:365-381.

Antic D, Stubbs JL, Suyama K, Kintner C, Scott MP, Axelrod JD (2010) Planar cell polarity enables posterior localization of nodal cilia and left-right axis determination during mouse and *Xenopus* embryogenesis. PLoS One 5:e8999. doi:10.1371/journal.pone.008999.

Aoto K, Nishimura T, Eto K, and Motoyama J (2002) Mouse GLI3 regulates Fgf8 expression and apoptosis in the developing neural tube, face, and limb bud. Dev Biol 251:320-332.

Axelrod JD, Miller JR, Shulman JM, Moon RT, and Perrimon, N (1998) Differential recruitment of Dishevelled provides signaling specificity in the planar cell polarity and Wingless signaling pathways. Genes Dev 12:2610-2622.

Bachiller D, Klingensmith J, Kemp C, Belo JA, Anderson RM, May SR, McMahon JA, McMahon AP, Harland RM, Rossant J, De Robertis EM (2000) The organizer factors Chordin and Noggin are required for mouse forebrain development. Nature 403:658-661.

Bai CB, Joyner AL (2000) Gli1 can rescue the in vivo function of Gli2. Development 128:5161-5172.

Banizs B, Pike MM, Millican CL, Ferguson WB, Komlosi P, Sheetz J, Bell PD, Schwiebert EM, Yoder BK (2005) Dysfunctional cilia lead to altered ependyma and choroid plexus function, and result in the formation of hydrocephalus. Development 132:5329-5339.

Belo JA, Bachiller D, Agius E, Kemp C, Borges AC, Marques S, Piccolo S, De Robertis EM (2000) Cerberus-like is a secreted BMP and nodal antagonist not essential for mouse development. Genesis 26:265-270.

Bisgrove BW, Yost HJ (2006) The roles of cilia in developmental disorders and disease. Development 133:4131-4143.

Bishop GA, Berbari NF, Lewis J, Mykytyn K (2007) Type III adenylyl cyclase localizes to primary cilia throughout the adult mouse brain. J Comp Neurol 505:562-571.

Bitgood MJ, Shen L, McMahon AP (1996) Sertoli cell signaling by Desert hedgehog regulates the male germline. Curr Biol 6:298-304.

Borovina A, Superina S, Voskas D, Ciruna B (2010) Vangl2 directs the posterior tilting and asymmetric localization of motile primary cilia. Nat Cell Biol 12:407-412.

Bouwmeester T, Kim S, Sasai Y, lu B, De Robertis EM (1996) Cerberus is a head-inducing secreted factor expressed in the anterior endoderm of Spemann´s organizer. Nature 382:595-601.

Brachmann I, Jakubick VC, Shaked M, Unsicker K, Tucker KL (2007) A simple slice culture system for the imaging of nerve development in embryonic mouse. Dev Dyn 236:3514-3523.

Breunig JJ, Sarkisian MR, Arellano JJ, Morozov YM, Ayoub AE, Sojitra S, Wang B, Flavell RA, Rakic P, Town T (2008) Primary cilia regulate hippocampal neurogenesis by mediating sonic hedgehog signaling. Proc Natl Acad Sci USA 105:13127-13132.

Bulchand S, Grove EA, Porter FD, Tole S (2001) LIM-homeodomain gene Lhx2 regulates the formation of the cortical hem. Mech Dev 100:165-175.

Bulfone A, Puelles L, Porteus MH, Frohman MA, Martin GR, Rubenstein JL (1993) Spatially restricted expression of Dlx-1, Dlx-2 (Tes-1), Gbx-2, and Wnt-3 in the embryonic day 12.5 mouse forebrain defines potential transverse and longitudinal segmental boundaries. J Neurosci 13:3155-3172.

Camus A, Davidson BP, Billiards S, Khoo P, Rivera-Perez JA, Wakamiya M, Begringer RR, Tam PP (2000) The morphogenetic role of midline mesendoderm and ectoderm in the development of the forebrain and the midbrain of the mouse embryo. Development 127:1799-1813.

Caspary T, Larkins CE, Anderson KV (2007) The graded response to Sonic Hedgehog depends on cilia architecture. Dev Cell 12:767-778.

Chang C, Hemmati-Brivanlou A (1998) Neural crest induction by Xwnt7b in Xenopus. Dev Biol 194:129-134.

Chen JK, Taipale J, Young KE, Maiti T, Beachy PA (2002) Small molecule modulation of Smoothened activity. Proc Natl Acad Sci 99:14071-14076.

Chiang C, Litingtung Y, Lee E, Young KE, Cordon JL, Westphal H, Beachy PA (1996) Cyclopia and defective axial patterning in mice lacking Sonic hedgehog gene function. Nature 383:407-413.

Chizhikov VV, Davenport J, Zhang Q, Shih EK, Cabello OA, Fuchs JL, Yoder BK, Millen KJ (2007) Cilia proteins control cerebellar morphogenesis by promoting expansion of the granule progenitor pool. J Neurosci 27:9780-9789.

Cohen E, Meininger V (1987) Ultrastructural analysis of primary cilium in the embryonic nervous tissue of mouse. Int J Dev Neurosci 5:43-51

Cole DG, Diener DR, Himelblau AL, Beech PL, Fuster JC, and Rosenbaum JL (1998) Chlamydomonas kinesin-II-dependent intraflagellar transport (IFT): IFT particles contain proteins required for ciliary assembly in Caenorhabditis elegans sensory neurons. J Cell Biol 141:993-1008.

Corbin JG, Gaiano N, Machold RP, Langston A, and Fishell G (2000) The Gsh2 homeodomain protein controls multiple aspects of telencephalic development. Development 127:5007-5020.

Corbin JG, Rutlin M, Gaiano N, and Fishell G (2003) Combinatorial function of the homeodomain proteins Nkx2.1 and Gsh2 in ventral telencephalic patterning. Development 130:4895-4906.

Corbit KC, Aanstad P, Singla V, Norman AR, Stainier DY, Reiter JF (2005) Vertebrate Smoothened functions at the primary cilium. Nature 437:1018-1021.

Corbit KC, Shyer AE, Dowdle WE, Gaulden J, Singla V, Reiter JF (2008) Kif3a constrains beta-catenin-dependent Wnt signalling through dual ciliary and non-ciliary mechanisms. Nat Cell Biol 10:70-76.

Curtin JA, Quint E, Tsipouri V, Arkell RM, Cattanach B, Copp AJ, Henderson DJ, Spurr N, Stanier P, Fisher EM, *et al.* (2003) Mutation of Celsr1 disrupts planar polarity of inner ear hair cells and causes severe neural tube defects in mouse. Curr Biol 13:1129-1133.

Dahmane N, Ruiz i Altaba A (1999) Sonic hedgehog regulates the growth and patterning of the cerebellum. Development 126: 3089-3100.

Dai D, Zhu H, Wlodarczyk B, Zhang L, Li L, Li AG, Finnell RH, Roop DR, Chen J (2011) Fuz controls the morphogenesis and differentiation of hair follicles through the formation of primary cilia. J Invest Dermatol 131(2):302-310.

Dai P, Akimaru H, Tanaka Y, Maekawa T, Nakafuku M, Ishii S (1999) Sonic Hedgehog-induced activation of the Gli1 promoter is mediated by GLI3. J Biol Chem 274:8143-8152.

Davenport JR, and Yoder BK (2005) An incredible decade for the primary cilium: a look at a once-forgotten organelle. Am J Physiol Renal Physiol 289:F1159-F1169.

Davis EE, Brueckner M, Katsanis N (2006) The emerging complexity of the vertebrate cilium: new functional roles for an ancient organelle. Dev Cell 11:9-19.

Delaune E, Lemaire P, Kodjabachian L (2005) Neural induction in Xenopus requires early FGF signaling in addition to BMP inhibition. Development 132:299-310.

Delous M, Baala L, Salomon R, Laclef C, Vierkotten J, Tory K, Golzio K, Lacoste T, Besse L, Ozilou C, *et al.* (2007) The ciliary gene RPGRIP1L is mutated in cerebello-oculo-renal syndrome (Joubert syndrome type B and Meckel syndrome. Nat Genet 39:875-881.

Dietrich WF, Miller JC, Steen RG, Merchant M, Damron D, Nahf R, Gross A, Joyce DC, Wessel M, Dredge RD, et al. (1994) A genetic map of the mouse with 4,006 simple sequence length polymorphisms. Nat Genet 7:220-245.

Doetsch F, Garcia-Verdugo JM, Alvarez-Buylla A (1999) Regernation of a germinal layer in the adult mammalian brain. Proc Natl Acad Sci USA 96:11619-11624.

Dou CL, Li S, and Lai E (1999) Dual role of brain factor-1 in regulating growth and patterning of the cerebral hemispheres. Cereb Cortex 9:543-550.

Duan W, Cole T, Schreiber G (1989) Cloning and nucleotide sequencing of transthyretin (prealbumin) cDNA from rat choroid plexus and liver. Nucleic Acids Res 17:3979.

Dubreuil V, Marzesco AM, Corbeil D, Huttner WB, Wilsch-Brauninger M (2007) Midbody and primary cilium of neural progenitors release extracellular membrane particles enriched in the stem cell marker prominin-1. J Cell Biol 176:483-495.

Echelard Y, Epstein DJ, St-Jacques B, Shen L, Mohler J, McMahon JA, McMahon AP (1993) Sonic hedgehog, a member of a family of putative signaling molecules, is implicated in the regulation of CNS polarity. Cell 75:1417-1430.

Eggenschwiler JT, Anderson KV (2007) Cilia and developmental signaling. Annu Rev Cell Dev Biol 23:345-373.

Ericson J, Muhr J, Placzek M, Lints T, Jessell TM, Edlund T (1995) Sonic hedgehog induces the differentiation of ventral forebrain neurons: a common signal for ventral patterning within the neural tube. Cell 81:747-756.

Essner JJ, Vogan KJ, Wagner MK, Tabin CJ, Yost HJ, and Bruechner M (2002) Conserved function for embryonic nodal cilia. Nature 418:37-38.

Essner JJ, Amack JD, Nyholm MK, Harris EB, and Yost HJ (2005) Kupffer´s vesicle is a ciliated organ of asymmetry in the zebrafish embryo that initiates left-right development of the brain, heart and gut. Development 132:1247-1260.

Fainsod A, Deissler K, Yelin R, Marom K, Epstein M, Pillemer G, Steinbeisser H, Blum M. (1997) The dorsalizing and neural inducing gene follistatin is an antagonist of BMP-4. Mech Dev 63:39-50.

Fernandes M, Gitin G, Alcorn H, McConnell SK, and Hebert JM (2007) Mutations in the BMP pathway in mice support the existence of two molecular classes of holoprosencephaly. Development 134:3789-3794.

Ferrante MI, Zullo A, Barra A, Bimonte S, Messaddeq N, Studer M, Dolle P, Franco P (2006) Oral-facial-digital type I protein is required for primary cilia formation and left-right axis specification. Nat Genet 38:112-117.

Fliegauf M, and Omran H (2006) Novel tools to unravel molecular mechanisms in cilia-related disorders. Trends Genet 22:241-245.

Foley AC, Skromne I, and Stern CD (2000) Reconciling different models of forebrain induction and patterning: a dual role for the hypoblast. Development 127:3839-3854.

Fotaki V, Yu T, Zaki PA, Mason JO, Price DJ (2006) Abnormal positioning of diencephalic cell types in neocortical tissue in the dorsal telencephalon of mice lacking functional Gli3. J Neurosci 26:9282-9292.

Friedrichs M, Larralde O, Skutella T, Theil T (2008) Lamination of the cerebral cortex is disturbed in *Gli3* mutant mice. Dev Biol in press.

Fuccillo M, Rutlin M, and Fischell G (2006) Removal of Pax6 partially rescues the loss of ventral structures in Shh null mice. Cereb Cortex 16 (Suppl.1) i96-i102.

Fuchs JL, Schwark HD (2004) Neuronal primary cilia: a review. Cell Biol Int 28:111-118.

Fukuchi-Shimogori T, Grove EA (2001) Neocortex patterning by the secreted signaling molecule FGF8. Science 294:1071-1074.

Furuta Y, Piston DW, and Hogan BLM (1997) Bone morphogenetic proteins (BMPs) are regulators of dorsal forebrain development. Development 124:2203-2212.

Gerdes JM, Liu Y, Zaghloul NA, Leitch CC, Lawson SS, Kato M, Beachy PA, Beales PL, DeMartino GN, Fisher S, *et a.* (2007) Disruption of the basal body compromises proteasomal function and perturbs intracellular Wnt response. Nat Genet 39:1350-1360.

Gerdes JM, Katsanis N (2008) Ciliary function and Wnt signal modulation. Curr Top Dev Biol 85:175-195.

Gerdes JM, Davis EE, Katsanis N (2009) The vertebrate primary cilium in development, homeostasis, and disease. Cell 137:32-45.

Gilbertson RJ, and Ellison DW (2008) The origins of medulloblastoma subtypes. Annu Rec Pathol 3:341-365.

Goodrich LV, Johnson RL, Milenkovic L, McMahon JA, Scott MP (1996) Conservation of the hedgehog/patched signaling pathway from flies to mice: induction of a mouse patched gene by Hedgehog. Genes Dev 10:301-312.

Gorgas K (1984) Peroxisomes in sebaceous glands. V. Complex peroxisomes in the mouse preputial gland: serial sectioning and three-dimensional reconstruction studies. Anat Embryol (Berl) 169:261-270.

Gorivodsky M, Mukhopadhyay M, Wilsch-Braeuninger M, Phillips M, Teufel C, Kim C, Malik N, Huttner W, Westphal H (2009) Intraflagellar transport protein 172 is essential for primary cilia formation and plays a vital role in patterning the mammalian brain. Dev Biol 325:24-32.

Gradwohl G, Fode C, Guillemot F (1996) Restricted expression of a novel murine atonal-related bHLH protein in undifferentiated neural precursors. Dev Biol 180:227-241.

Gray RS, Abitua PB, Wlodarczyk BJ, Szabo-Rogers HL, Blanchard O, Lee I, Weiss GS, Liu KJ, Marcotte EM, Wallingford JB, Finnell RH (2009) The planar cell polarity effector Fuz is essential for targeted membrane trafficking, ciliogenesis and mouse embryonic development. Nat Cell Biol 11(10):1225-1232.

Grove EA, Tole S, Limon J, Yip L, Ragsdale CW (1998) The hem of the embryonic cerebral cortex is defined by the expression of multiple Wnt genes and is compromised in Gli3-deficient mice. Development 125:2315-2325.

Guirao B, Meunier A, Mortaud S, Aguilar A, Corsi JM, Strehl L, Hirota Y, Desoeuvre A, Boutin C, Han YG, *et al*. (2010) Coupling between hydrodynamic forces and planar cell polarity orientates mammalian motile cilia. Nat Cell Biol 12:341-350.

Gutin G, Fernandes M, Palazzolo L, Paek H, Yu K, Ornitz DM, McConnell SK, Hebert JM (2006) FGF acts independently of SHH to generate ventral telencephalic cells. Development 133:2937-2946.

Hamblet NS, Lijam N, Ruiz-Lozano P, Wang J, Yang Y, Luo Z, Mei L, Chien KR, Sussman DJ, Wynshaw-Boris A (2002) Dishevelled 2 is essential for cardiac outflow tract development, somite segmentation and neural tube closure. Development 129:5827-5838.

Han YG, Spassky N, Romaguera-Ros M, Garcia-Verdugo JM, Aguilar A, Schneider-Maunoury S, Alvarez-Buylla A (2008) Hedgehog signaling and primary cilia are required for the formation of adult neural stem cells. Nat Neurosci 11:277-284.

Han YG, Kim HJ, Dlugosz AA, Ellison DW, Gilbertson RJ, Alvarez-Buylla (2009) Dual and opposing roles of primary cilia in medulloblastoma development. Nat Med 15(9):1062-1065.

Hanashima C, Shen L, Li SC, Lai E (2002) Brain factor-1 controls the proliferation and differentiation of neocortical progenitor cells through independent mechanisms. J Neurosci 22:6526-6536.

Hanashima C, Fernandes M, Hebert JM, and Fishell G (2007) The role of FoxG1 and dorsal midline signaling in the generation of Cajal-Retzius subtypes. J Neurosci 27:11103-11111.

Haremaki T, Tanaka Y, Hongo I, Yuge M, and Okamoto H (2003) Integration of multiple signal transduction pathways on Fgf response elements of the *Xenopus caudal homologue Xcad3*. Development 130:4907-4917.

Hashimoto H, Itoh M, Yamanaka Y, Yamashita S, Shimizu T, Solnoca-Krezel L, Hibi M, and Hirano T (2000) Zebrafish Dkk1 functions in forebrain specification and axial mesendoderm formation. Dev Biol 217: 138-152.

Hashimoto M, Shinohara K, Wang J, Ikeuchi S, Yoshiba S, Meno C, Nonaka S, Takada S, Hatta K, Wynshaw-Boris A, *et al*. (2010) Planar polarization of node cells determines the rotational axis of node cilia. Nat Cell Biol 12:170-176.

Hatini V, Huh SO, Herzlinger D, Soares VC, Lai E (1996) Essential role of stromal mesenchyme in kidney morphogenesis revealed by targeted disruption of Winged Helix transcription factor BF-2. Genes Dev 10:1467-1478.

Haycraft CJ, Swoboda P, Taulman PD, Thomas JH, Yoder BK (2001) The C. elegans homolog of the murine cystic kidney disease gene Tg737 functions in a ciliogenic pathway and is disrupted in osm-5 mutant worms. Development 128:1493-1505.

Haycraft CJ, Banizs B, Aydin-Son Y, Zhang Q, Michaud EJ, Yoder BK (2005) Gli2 and Gli3 localize to cilia and require the intraflagellar transport protein polaris for processing and function. PLoS Genet 1:e53.

Haycraft CJ, Zhang Q, Song B, Jackson WS, Detloff PJ, Serra R, Yoder BK (2007) Intraflagellar transport is essential for endochondral bone formation. Development 134:307-316.

Hebert JM, and McConnell SK (2000) Targeting of *cre* to *FoxG1* (*BF-1*) locus mediates *loxP* recombination in the telencephalon and other developing head structures. Dev Biol 222:296-306.

Heeg-Truesdell E, Labonne C (2006) Neural induction in *Xenopus* requires inhibition of Wnt-beta-catenin signaling. Dev Biol 298:71-86.

Heisenberg CP, Tada M, Rauch GJ, Saude L, Concha ML, Geisler R, Stemple DL, Smith JC, Wilson SW (2000) Silberblick/Wnt11 mediates convergent extension movements during zebrafish gastrulation. Nature 405:76-81.

Herron BJ, Lu W, Rao C, Liu S, Peters H, Bronson RT, Justice MJ, McDonald JD, Beier DR (2002) Efficient generation and mapping of recessive developmental mutations using ENU mutagenesis. Nat Genet 30:185-189.

Hongo I, Kengaku M, Okamoto F (1999) FGF signaling and the anterior neural induction in *Xenopus*. Dev Biol 216:561-581.

Houde C, Dickinson RJ, Houtzager VM, Cullum R, Montpetit R, Metzler M, Simpson EM, Roy S, Hayden MR, Hoodless PA, Nicholson DW (2006) Hippi is essential for node cilia assembly and Sonic hedgehog signaling. Dev Biol 300:523-533.

Huang P, Schier AF (2009) Dampened Hedgehog signaling but normal Wnt signaling in zebrafish without cilia. Development 136:3089-3098

Huangfu D, Anderson KV (2005) Cilia and Hedgehog responsiveness in the mouse. Proc Natl Acad Sci U S A 102:11325-11330.

Huangfu D, Liu A, Rakeman AS, Murcia NS, Niswander L, Anderson KV (2003) Hedgehog signalling in the mouse requires intraflagellar transport proteins. Nature 426:83-87.

Hui CC, Joyner AL (1993) A mouse model of greig cephalopolysyndactyly syndrome: the extra-toesJ mutation contains an intragenic deletion of the Gli3 gene. Nat Genet 3:241-246.

Huntzicker EG, Estay IS, Zhen H, Lokteva LA, Jackson PK, Oro AE (2006) Dual degradation signals control Gli protein stability and tumor formation. Genes Dev 20:276-281.

Hynes M, Stone DM, Dowd M, Pitts-Meek S, Goddard A, Gurney A, Rosenthal A (1997) Control of cell pattern in the neural tube by the zinc finger transcription factor and oncogene Gli-1. Neuron 19:15-26.

Inoue T, Nakamura S, and Osumi N (2000) Fate mapping of the mouse prosencephalic neural plate. Dev Biol 219:373-383.

Ishimura A, Maeda R, Takeda M, Kikkawa M, Daar IO, Maeno M (2000) Involvement of BMP-4/msx-1 and FGF pathways in neural induction in the *Xenopus* embryo. Dev Growth Differ 42:307-316.

Jenkins PM, McEwen DP, Martens JR (2009) Olfactory cilia: linking sensory cilia function and human disease. Chem Senses 4(5):451-464.

Jho EH, Zhang T, Domon C, Joo CK, Freund JN, Costantini F (2002) Wnt/beta-catenin/Tcf signaling induces the transcription of Axin2, a negative regulator of the signaling pathway. Mol Cell Biol 22:1172-1183.

Jiang J, and Hui CC (2008) Hedgehog signaling in development and cancer. Dev Cell 15:801-812.

Johnson DR (1967) Extra-toes: a new mutant gene causing multiple abnormalities in the mouse. J Embryol Exp Morphol 17:543-581.

Karlstrom RO, Tyurina OV, Kawakami A, Nishioka N, Talbot WS, Sasaki H, Scjier AF (2003) Genetic analysis of zebrafish gli1 and gli2 reveals divergent requirement for gli genes in vertebrate development. Development 130:1549-1564.

Kazanskaya O, Glinka A, and Niehrs C (2000) The role of Xenopus dickkopf1 in prechordal plate specification and neural patterning. Development 127:4981-4992.

Keller R, Shih J, Sater K, Moreno C (1992) Planar induction of convergence and extension of the neural plate by the organizer of *Xenopus*. Dev. Dyn. 193:218-234.

Kibar Z, Vogan KJ, Goulx N, Justice MJ, Underhill DA, Gros P (2001) Ltap, a mammalian homolog of *Drosophila* Strabismus/Van Gogh, is altered in the mouse neural tube mutant Loop-tail. Nat Genet 28:251-255.

Kikuchi A, and Yamamoto H (2008) Tumor formation due to abnormalities in the beta-catenin-independent pathway of Wnt signaling. Cancer Sci 99:202-208.

Kinoshita E, Kinoshita-Kikuta E, Koike T (2009) Separation and detection of large phosphoproteins using Phos-tag SDS-PAGE. Nat Protoc 4:1513-1521.

Kim SK, Shindo A, Park TJ, Oh EC, Ghosh S, Gray RS, Lewis RA, Johnson CA, Attie-Bittach T, Katsanis N, Eallingford JB (2010) Planar cell polarity acts through septins to control collective cell movement and ciliogenesis. Science 329(5997):1337-1340.

Kimura C, Yoshinaga K, Tian E, Suzuki M, Aizawa S, and Matsuo I (2000) Visceral endoderm mediates forebrain development by suppressing posteriorizing signal. Dev Biol 225:304-321.

Kiprilov EN, Awan A, Desprat R, Velho M, Clement CA, Byskov AG, Anderson CY, Satir P, Bouhassira EE, Christensen ST, *et al* (2008) Human embryonic stem cells in culture possess primary cilia with hedgehog signaling machinery. J Cell Biol 180:897-904.

Knoetgen H, Teichmann U, and Kessel M (1999) Head-organizing activities of endodermal tissues in vertebrates. Cell Mol Biol 45:481-492.

Kozminski KG, Johnson KA, Forscher P, and Rosenbaum JL (1993) A motility in the eukaryotic flagellum unrelated to flagellar beating. Proc Natl Acad Sci USA 90:5519-5523.

Kramer-Zucker AG, Olale F, Haycraft CJ, Yoder BK, Schier AF, Drummond IA (2005) Cilia-driven fluid flow in the zebrafish pronephros, brain and Kupffer's vesicle is required for normal organogenesis. Development 132:1907-1921.

Kudoh T, Wilson SW, and Dawid IB (2002) Distinct roles for Fgf, Wnt and retinoic acid in posteriorizing the neural ectoderm. Development 129:4335-4346.

Kuschel S, Ruther U, Theil T (2003) A disrupted balance between Bmp/Wnt and Fgf signaling underlies the ventralization of the Gli3 mutant telencephalon. Dev Biol 260:484-495.

Lancaster MA, Louie CM, Silhavy JL, Sintasath L, Decambre M, Nigam SK, Willert K, Gleeson JG (2009) Impaired Wnt-beta-catenin signaling disrupts adult renal homeostasis and leads to cystic kidney ciliopathy. Nat Med 15(9):1046-1054.

Lancaster MA, Schroth J, Gleeson JG (2011) Subcellular spatial regulation of canonical Wnt signalling at the primary cilium. Nat Cell Biol 13(6):700-707.

Lee J, Platt KA, Censullo P, Ruiz i Altaba A (1997) Gli1 is a target of Sonic hedgehog that induces ventral neural tube development. Development 124:2537-2552.

Lee SM, Tole S, Grove E, and McMahon AP (2000) A local Wnt3a signal is required for development of the mammalian hippocampus. Development 127:457-467.

Lemischka IR, Farmer S, Racaniello VR, Sharp PA (1981) Nucleotide sequence and evolution of a mammalian alpha-tubulin messenger RNA. J Mol Biol 151:101-120.

Linker C, Stern CD (2004) Neural induction requires BMP inhibition only as a late step, and involves signals other than FGF and Wnt antagonists. Development 131:5671-5681.

Litingtung Y, Dahn RD, Li Y, Fallon JF, Chiang C (2002) Shh and Gli3 are dispensable for limb skeleton formation but regulate digit number and identity. Nature 418:979-983.

Liu A, Wang B, Niswander LA (2005) Mouse intraflagellar transport proteins regulate both the activator and repressor functions of Gli transcription factors. Development 132:3103-3111.

Lustig B, Jerchow B, Sachs M, Weiler S, Pietsch T, Karsten U, van de Wetering M, Clevers H, Schlag PM, Birchmeier W, Behrens J (2002) Negative feedback loop of Wnt signaling through upregulation of conductin/axin2 in colorectal and liver tumors. Mol Cell Biol 22:1184-1193.

McDermott KM, Liu BY, Tlsty TD, Pazour GJ (2010) Primary cilia regulate branching morphogenesis during mammary gland development. Curr Biol 20:731-737.

Mangale VS, Hirokawa KE, Satyaki PR, Gokulchandran N, Chikbire S, Subramanian L, Shetty AS, Martynoga B, Paul J, Mai MV, Li Y, Flanagan LA, Tole S, Monuki ES (2008) Lhx2 selector activity specifies cortical identity and suppresses hippocampal organizer fate. Science 319:304-309.

Marigo V, Davey RA, Zuo Y, Cunningham JM, Tabin CJ (1996) Biochemical evidence that patched is the Hedgehog receptor. Nature 384:176-179.

Marshall WF, and Kintner C (2008) Cilia orientation and the fluid mechanics of development. Curr Opin Cell Biol 20:48-52.

Marshall WF (2008) Chapter 1 Basal bodies platforms for building cilia. Curr Top Dev Biol 85:1-22.

Martynoga B, Morrison H, Price DJ, and Mason JO (2005) FoxG1 is required for specification of ventral telencephalon and region-specific regulation of dorsal telencephalic precursor proliferation and apoptosis. Dev Biol 283:113-127.

May SR, Ashique AM, Karlen M, Wang B, Shen Y, Zarbalis K, Reiter J, Ericson J, Peterson AS (2005) Loss of the retrograde motor for IFT disrupts localization of Smo to cilia and prevents the expression of both activator and repressor functions of Gli. Dev Biol 287:378-389.

Maynard TM, Jain MD, Balmer CW, LaMantia AS (2002) High-resolution mapping of the Gli3 mutation extra-toes reveals a 51.5-kb deletion. Mamm Genome 13:58-61.

McEwen DP, Jenkins PM, and Martens JR (2008) Chapter 12 Olfactory cilia: our direct neuronal connection to the external world. Curr Top Dev Biol 85:333-370.

McGarth J, Somlo S, Makova S, Tian X, and Brueckner M (2003) Two populations of node monocilia initiate left-right asymmetry in the mouse. Cell 114:61-73.

McMahon JA, Takada S, Zimmermann LB, Fan CM, Harland RM, McMahon AP (1998) Noggin-mediated antagonism of BMP signaling is required for growth and patterning of the neural tube and somite. Genes Dev 12:1438-1452.

Meinhardt H (2001) Organizer and axes formation as a self-organizing process. Int J Dev Biol 45:177-188.

Meyer G, Perez-Garcia CG, Abraham H, Caput D (2002) Expression of p73 and Reelin in the developing human cortex. J Neurosci 22:4973-4986.

Mitchell B, Stubbs JL, Huisman F, Tobrek P, Yu C, Kintner C (2009) The PCP pathway instructs the planar orientation of ciliated cells in the *Xenopus* larval skin. Curr Biol 19:924-929.

Monuki ES, Porter FD, Walsh CA (2001) Patterning of the dorsal telencephalon and cerebral cortex by a roof plate-Lhx2 pathway. Neuron 32:591-604.

Moody SA, Quigg MS, Frankfurter A (1989) Development of the peripheral trigeminal system in the chick revealed by an isotype-specific anti-beta-tubulin monoclonal antibody. J Comp Neurol 279:567-580.

Mukhopadhyay M, Shtrom S, Rodriguez-Esteban C, Chen L, Tsukui T, Gomer L, Dorward DW, Glinka A, Grinberg A, Huang SP, Niehrs C, Izpisua Belmonte JC, Westphal H (2001) Dickkopf1 is required for embryonic head induction and limb morphogenesi in the mouse. Dev Cell 3:323-434

Munoz-Sanjuan I, and Brivanlou AH (2002) Neural induction, the default model and embryonic stem cells. Nat Rev Neurosci 3:271-280.

Murcia NS, Richards WG, Yoder BK, Mucenski ML, Dunlap JR, Woychik RP (2000) The Oak Ridge Polycystic Kidney (orpk) disease gene is required for left-right axis determination. Development 127:2347-2355.

Murdoch JN, Copp AJ (2010) The relationship between sonic Hedgehog signaling, cilia and neural tube defects. Birth Defects Res A Clin Mol Teratol 88:633-652.

Nagele RG, Lee HY (1979) Ultrastructural changes in cells associated with interkinetic nuclear migration in the developing chick neuroepithelium. J Exp Zool 210:89-106.

Niehrs C (1999) Head in the Wnt. Trends Genet 15:314-319.

Nielsen SK, Mollgard K, Clement CA, Veland IR, Awan A, Yoder BK, Novak I, and Christensen ST (2008) Characterization of primary cilia and Hedgehog signaling during development of the human pancreas and in human pancreatic duct cancer cell lines. Dev Dyn 237:2039-2052.

Nieuwkoop P, and Nigtevecht GV (1954) Neural activation and transformation in explants of competent ectoderm under the influence of fragments of anterior notochord in urodeles. J Embryol Exp Morphol 2:175-193.

Nusslein-Volhard C, Wieschaus E (1980) Mutations affecting segment number and polarity in *Drosophila*. Nature 287:795-801.

Ocbina PJ, Anderson KV (2008) Intraflagellar transport, cilia, and mammalian Hedgehog signaling: analysis in mouse embryonic fibroblasts. Dev Dyn 237:2030-2038.

Ocbina PJ, Tuson M, Anderson KV (2009) Primary cilia are not required for normal canonical Wnt signaling in the mouse embryo. PLoS ONE 4:e6839

Ohkubo Y, Chiang C, and Rubenstein JL (2002) Coordinate regulation and synergistic actions of BMP4, SHH and FGF8 in the rostral prosencephalon regulate morphogenesis of the telencephalic and optic vesicles. Neuroscience 111:1-17.

Pan J, and Snell W (2007) The primary cilium: keeper of the key to cell division. Cell 129:1255-1257.

Panchision DM, Pickel JM, Studer L, Lee SH, Turner PA, Hazel TG, McKay RD (2001) Sequential actions of BMP receptors control neural precursor cell production and fate. Genes Dev 15:2094-2110.

Park TJ, Mitchell BJ, Abitua PB, Kintner C, and Wallingford JB (2008) Dishevelled controls apical docking and planar cell polarization of basal bodies in ciliated epithelial cells. Nat Genet 40:871-879.

Pasca di Magliano M, Sekine S, Ermilov A, Ferris J, Dlugosz AA, Hebrok M (2006) Hedgehog/Ras interactions regulate early stages of pancreatic cancer. Genes Dev 20:3161-3173.

Pazour GJ, Wilkerson CG, and Witman GB (1998) A dynein light chain is essential for the retrograde particle movement of intraflagellar transport (IFT). J Cell Biol 141:979-992.

Pazour GJ, Baker SA, Deane JA, Cole DG, Dickert BL, Rosenbaum JL, Witman GB, Besharse JC (2002) The intraflagellar transport protein, IFT88, is essential for vertebrate photoreceptor assembly and maintenance. J Cell Biol 157:103-113.

Pazour GJ, and Witman GB (2003) The vertebrate primary cilium is a sensory organelle. Curr Opin Cell Biol 15:105-110.

Pazour GJ, and Bloodgood RA (2008) Chapter 5 Targeting proteins to the ciliary membrane. Crrr Top Dev Biol 85:115-149.

Pedersen LB, and Rosenbaum JL (2008) Chapter Two Intraflagellar Transport (IFT) role in ciliary assembly, resorption and signaling. Curr Top Dev Biol 85:23-61.

Perea-Gomez A, Lawson KA, Rhinn M, Zakin L, Brulet P, Mazan S, Ang SL (2001) Otx2 is required for visceral endoderm movement and for the restriction of posterior signals in the epiblast of the mouse embryo. Development 128:753-65.

Perea-Gomez A, Rhinn M, and Ang SL (2001) Role of the anterior visceral endoderm in restricting posterior signals in the mouse embryo. Int J Dev Biol 45:311-320.

Pera EM, Ikeda A, Eivers E, De Robertis EM (2003) Integration of IGF, FGF, and anti-BMP signals vis Smad1 phosphorylation in neural induction. Genes Dev 17:3023-3028.

Phillips CL, Miller KJ, Filson AJ, Nurnberger J, Clendenon JL, Cook G, Dunn KW, Overbeek PA, Gattone VH, Bacallao RL (2004) Renal cysts of inv/inv mice resemble early infantile nephronophthisis. J Am Soc Nephrol 15:1744-1755.

Piccolo S, Sasai Y, Lu B, De Robertis EM (1996) Dorsoventral patterning in *Xenopus*: inhibition of ventral signals by direct binding of chordin to BMP-4. Cell 86:589-598.

Piperno G, Siuda E, Henderson S, Segil M, Vaananen H, and Sassaroli M (1998) Distinct mutants of retrograde intraflagellar transport (IFT) share similar morphological and molecular defects. J Cell Biol 143:1591-1601.

Platt KA, Michaud J, Joyner AL (1997) Expression of the mouse Gli and Ptc genes is adjacent to embryonic sources of hedgehog signals suggesting a conservation of pathways between flies and mice. Mech Dev 62:121-135.

Porter FD, Drago J, Xu Y, Cheema SS, Wassif C, Huang SP, Lee E, Grinberg A, Massalas JS, Bodine D, Alt F, Westphal H (1997) Lhx2, a LIM homeobox gene, is required for eye, forebrain, and definitive erythrocyte development. Development 124:2935-2944.

Praetorius HA, Spring KR (2001) Bending the MDCK cell primary cilium increases intracellular calcium. J Membr Biol 184:71-79.

Praetorius HA, Spring KR (2003) The renal cell primary cilium functions as a flow sensor. Curr Opin Nephrol Hypertens 12:517-520.

Pugacheva EN, Jablonski SA, Hartman TR, Hesnke EP, Golemis EA (2007) HEF-1 dependent Aurora A activation induces disassembly of the primary cilium. Cell 129:1351-1363.

Rallu M, Machold R, Gaiano N, Corbin JG, McMahon AP, Fishell G (2002) Dorsoventral patterning is established in the telencephalon of mutants lacking both Gli3 and Hedgehog signaling. Development 129: 4963-4974.

Ramamurthy V, Cayouette M (2009) Development and disease of the photoreceptor cilium. Clin Genet 76:137-145.

Rash BG, Grove EA (2006) Area and layer patterning in the developing cerebral cortex. Curr Opin Neurobiol 16:25-34.

Rash BG, Grove EA (2007) Patterning the dorsal telencephalon: a role for Sonic hedgehog?. J Neurosci 27:11595-11603.

Reese TS (1965) Olfactory cilia in the frog. J Cell Biol 25:209-230.

Rentzsch F, Bakkers J, Kramer C, Hammerschmidt M (2004) Fgf signaling induces posterior neuroectoderm independently of Bmp signaling inhibition. Dev Dyn 231:750-757.

Reversade B, and De Robertis EM (2005) Regulation of ADMP and BMP2/4/7 at opposite embryonic poles generates a self-regulating morphogenetic field. Cell 123:1147-1160

Reversade B, Kuroda H, Lee H, Mays A, and De Robertis EM (2005) Depletion of Bmp2, Bamp4, Bmp7 and Spemann organizer signals induces massive brain formation in *Xenopus* embryos. Development 132:3381-3392.

Rohtagi R, Milenkovic L, Scott MP (2007) Patched1 regulates Hedgehog signaling at the primary cilium. Science 317:372-376.

Rosenbaum JL, Witman GB (2002) Intraflagellar transport. Nat Rev Mol Cell Biol 3:813-825.

Rothbacher U, Laurent MN, Deardorff MA, Klein PS, Cho KWY, and Fraser SE (2000) Dishevelled phosphorylation, subcellular localization and multimerization regulate its role in early embryogenesis. EMBO J 19:1010-1022.

Ruppert JM, Vogelstein M, Arheden K, Kinzler KW (1990) GLI3 encodes a 190-kilodalton protein with multiple regions of GLI similarity. Mol Cell Biol 10:5408-5415.

Sasaki H, Hui C, Nakafuku M, Kondoh H (1997) A binding site for Gli proteins is essential for HNF-3beta floor plate enhancer activity in transgenics and can respond to Shh in vitro. Development 124:1313-1322.

Rubenstein JLR, Shimamura K, Martinez S, and Puelles L (1998) Regionalization of the prosencephalic neural plate. Annu. Rev. Neurosci. 21:445-477.

Sawamoto K, Wichterle H, Gonzalez-Perez O, Cholfin JA, Yamada M, Spassky N, Murcia NS, Garcia-Verdugo JM, Marin O, Rubenstein JL *et al* (2006) New neurons follow the flow of cerebrospinal fluid in the adult brain. Science 311:629-632.

Saxen L (1989) Neural Induction. International Journal of Developmental Biology. 33:21-48.

Schier AF (2001) Axis formation and patterning in zebrafish. Curr Opin Genet Dev 11:393-404.

Scholey JM, Anderson KV (2006) Intraflagellar transport and cilium-based signaling. Cell 125:439-442.

Seto ES, and Bellen HJ (2004) The ins and outs of Wingless signaling. Trends Cell Biol 14:45-53.

Shah AS, Ben-Shahar Y, Moninger TO, Kline JN, Welsh MJ (2009) Motile cilia of human airway epithelia are chemosensory. Science 325:1131-1134.

Shanmugalingam S, Houart C, Picker A, Reifers F, Macdonald R, Barth A, et al. (2000) Ace/Fgf8 is required for forebrain commissure formation and patterning of the telencephalon. Development 127:2549-2561.

Sheng G, dos Reis M, Stern CD (2003) Churchill, a zinc finger transcriptional factor, regulates the transition between gastrulation and neurulation. Cell 115:603-613.

Shiba D, Yamaoka Y, Hagiwara H, Takamatsu T (2009) Localizsation of Inv in a distinctive intracillary compartment requires the C-terminal ninein-homolog-containing region. J Cell Sci 122 (Pt1):44.54.

Shimamura K, Hartigan DJ, Martinez S, Puelles L, and Rubenstein JL (1995) Longitudinal organization of the anterior neural plate and neural tube. Development 121:3923-3933.

Shimamura K, Rubenstein JL (1997) Inductive interactions direct early regionalization of the mouse forebrain. Development 124:2709-2718.

Shinozaki K, Yoshida M, Nakamura M, Aizawa S, and Suda Y (2004) Emx1 and Emx2 cooperate in initial phase of archipallium development. Mech Dev 121:475-489.

Shinya M, Koshida S, Sawada A, Kuroiwa A, and Takeda H (2001) Fgf signaling through MAPK cascade is required for development of the subpallial telencephalon in zebrafish embryos. Development 128:4153-4164.

Shinozaki K, Yoshida M, Nakamura M, Aizawa S, Suda Y (2004) Emx1 and Emx2 cooperate in initial phase of archipallium development. Mech Dev 121:475-489.

Simons M, Gloy J, Ganner A, Bullerkotte A, Bashkurov M, Kronig C, Schermer B, Benzing T, Cabello OA, Jenny A, Mlodzik M, Polok B, Driever W, Obara T, Walz G (2005) Inversin, the gene product mutated in nephronophthisi type II, functions as a molecular switch between Wnt signaling pathways. Nat Genet 37(5):537-543.

Smith JL, Schoenwolf GC (1989) Notochordal induction of cell wedging in the chick neural plate and its role in the neural tube formation. J Exp Zool 250:49-62.

Smith WC, Harland RM (1991) Injected Xwnt-8 RNA acts early in Xenopus embryos to promote formation of a vegetal dorsalizing center. Cell 67:753-765.

Sokol SY (1996) Analysis of Dishevelled signaling pathways during *Xenopus* development. Curr Biol 6:1456-1467.

Song H, Hu J, Chen W, Elliott G, Andre P, Gao B, Yang Y (2010) Planar cell polarity breaks bilateral symmetry by controlling ciliary positioning. Nature 466:378-382.

Spassky N, Han YG, Aguilar A, Strehl L, Besse L, Laclef C, Ros MR, Garcia-Verdugo JM, Alvarez-Buylla A (2008) Primary cilia are required for cerebellar development and Shh-dependent expansion of progenitor pool. Dev Biol 317:246-259.

Spektor A, Tsang WY, Khoo D, Dynlacht BD (2007) Cep97 and CP110 suppress a cilia assembly program. Cell 130:678-690.

St-Jacques B, Hammerschmidt M, McMahon AP (1999) Indian hedgehog signaling regulates proliferation and differentiation of chondrocytes and is essential for bone formation. Genes Dev 13:2072-2086.

Storm E (2006) Dosage dependent functions of *Fgf8* in regulating telencephalic patterning centers. Development 133:1831-1844.

Stottmann RW, Tran PV, Turbe-Doan A, Beier DR (2009) Tc21b is required to restrict sonic hedgehog activity in the developing mouse forebrain. Dev Biol 335(1):166-178.

Stoykova A, Treichel D, Hallonet M, and Gruss P (2000) *Pax6* modulates the dorsoventral patterning of mammalian telencephalon. J Neurosci 20:8042-8050.

Tada M, Smith JC (2000) Xwnt11 is a target of *Xenopus* Brachyury: Regulation of gastrulation movements via Dishevelled, but not through the canonical Wnt pathway. Development 127:2227-2238.

Takemaru T, Yamaguchi S, Lee YS, Zhang Y, Carthew RW, Moon RT (2003) Chibby, a nuclear β-catenin-associated antagonist of the Wnt/Wingless pathway. Nature 422:905-909.

Takiguchi-Hayashi K, Sekiguchi M, Ashigaki S, Takamatsu M, Hasegawa H, Suzuki-Migishima R, Yokoyama M, Nakanishi S, Tanabe Y (2004) Generation of reelin-positive marginal zone cells from the caudomedial wall of telencephalic vesicles. J Neurosci 24:2286-2295.

Tao W, Lai E (1992) Telencephalon-restricted expression of BF-1, a new member of the HNF-3/fork head gene family, in the developing rat brain. Neuron 8:957-966.

Taulman PD, Haycraft CJ, Balkovetz DF, Yoder BK (2001) Polaris, a protein involved in left-right axis patterning, localizes to basal bodies and cilia. Mol Biol Cell 12:589-599.

Te Welscher P, Zuniga A, Kujjper S, Drenth T, Goedemans HJ, Meijlink F, Zeller R (2002) Progression of vertebrate limb development through SHH-mediated counteraction of GLI3. Science 298:827-830.

Theil T, Alvarez-Bolado G, Walter A, Ruther U (1999) Gli3 is required for Emx gene expression during dorsal telencephalon development. Development 126:3561-3571.

Theil T, Aydin S, Koch S, Grotewold L, Ruther U (2002) Wnt and Bmp signalling cooperatively regulate graded Emx2 expression in the dorsal telencephalon. Development 129:3045-3054.

Theil T (2005) Gli3 is required for the specification and differentiation of preplate neurons. Dev Biol 286:559-571.

Thomas PQ, Brown A, and Beddington RS (1998) Hex. A homeobox gene revealing peri-implantation asymmetry in the mouse embryo and an early transient marker of endothelial cell precursors. Development 125:85-94.

Tissir F, Qu Y, Montcouquiol M, Zhou L, Komatsu K, Shi D, Fujimori T, Labeau J, Tyteca D, Courtoy P, *et al*. (2010) Lack of cadherins Celsr2 and Celsr3 impairs ependymal ciliogenesis, leading to fatal hydrocephalus. Nat Neurosci 13:700-707.

Tole S, Ragsdale CW, Grove EA (2000) Dorsoventral patterning of the telencephalon is disrupted in the mouse mutant *extra-toes*.Dev Biol 217:254-265.

Toresson H, Potter S, and Campbell K (2000) Genetic control of dorsal-ventral identity in the telencephalon: opposing roles of *Pax6* and *Gsh2*. Development 127:4361-4371.

Tran PV, Haycraft CJ, Besschetnova TY, Turbe-Doan A, Stottmann RW, Herron BJ, Chesebro AL, Qiu H, Scherz PJ, Shah JV, Yoder BK, Beier DR (2008) THM1 negatively modulates mouse sonic hedgehog signal transduction and affects retrograde intraflagellar transport in cilia. Nat Genet 40:403-410.

Tucker KL, Meyer M, Barde YA (2001) Neurotrophins are required for nerve growth during development. Nat Neurosci 4:29-37.

Tucker KL, Wang Y, Dausman J, Jaenisch R (1997) A transgenic mouse strain expressing four drug-selectable marker genes. Nucleic Acids Res 25:3745-3746.

Tucker KL, Beard C, Dausmann J, Jackson-Grusby L, Laird PW, Lei H, Li E, Jaenisch R (1996) Germ-line passage is required for establishment of methylation and expression patterns of imprinted but not of nonimprinted genes. Genes Dev 10:1008-1020.

Varga Z, Wegner J, and Westerfield M (1999) Anterior movement of ventral diencephalic precursors separates the primordial eye field in the neural plate and requires cyclops. Dedvelopment 126:5533-5564.

Vierkotten J, Dildrop R, Peters T, Wang B, Ruthers U (2007) Ftm is a novel basal body protein of cilia involved in Shh signalling. Development 134:2569-2577.

Vlad A, Rohrs S, Klein-Hitpass L, Muller O (2008) The first five years of the Wnt targetome. Cell Signal 20 (5):795-802.

Vonica A, Gumbiner BM (2007) The Xenopus Nieuwkoop center and Spemann-Mangold organizer share molecular components and a requirement for maternal Wnt activity. Dev Biol 312:90-102.

Voronina VA, Takemaru T, Treuting P, Love D, Grubb BR, Hajjar AM, Adams A, Li FQ, Moon RT (2009) Inactivation of Chibby affects function of motile airway cilia. J Cell Biol 185:225-233.

Vortkamp A, Lee K, Lanske B, Segre GV, Kronenberg HM, Tabin CJ (1996) Regulation of rate of cartilage differentiation by Indian hedgehog and PTH-related protein. Nature 273:613-622.

Wallace VA (1999) Purkinje-cell-derived Sonic hedgehog regulates granule neuron precursor cell proliferation in the developing mouse cerebellum. Curr Biol 9:445-448.

Wallingford JB, Rowning BA, Vogeli KM, Rothbacher U, Fraser SE, Harland RM (2000) Dishevelled controls cell polarity during *Xenopus* gastrulation. Nature 405:81-85.

Wallingford JB, Harland RM (2002) Neural tube closure requires Dishevelled-dependent convergent extension of the midline. Development 129:5815-5825.

Walshe J, and Mason I (2003) Unique and combinatorial functions of Fgf3 and Fgf8 during zebrafish forebrain development. Development 130:4337-4349.

Walther C, Gruss P (1991) Pax-6, a murine paired box gene, is expressed in the developing CNS. Development 113:1435-1449.

Wang B, Fallon JF, Beachy PA (2000) Hedgehog-regulated processing of Gli3 produces an anterior/posterior repressor gradient in the developing vertebrate limb. Cell 100:423-434.

Wang C, Ruther U, Wang B (2007) The Shh-independent activator function of the full-length Gli3 protein and its role in vertebrate limb digit patterning. Dev Biol 305:460-469.

Wang J, Hamblet NS, Mark S, Dickinson ME, Brinkman BC, Segil N, Fraser SE, Chen P, Wallingford JB, Wynshaw-Boris A (2006) Dishevelled genes mediate a conserved mammalian PCP pathway to regulate convergent extension during neurulation.

Wang Y, Guo N, Nathans J (2006) The role of Frizzled3 and Frizzled6 in neural tube closure and in the planar polarity of inner-ear sensory hair cells. J Neurosci 26:2147-2156.

Wawersik S, Evola C, Whitman M (2005) Conditional BMP inhibition in *Xenopus* reveals stage-specific roles for BMPs in neural and neural crest induction. Dev Biol 277:425-442.

Wechsler-Reya RJ, Scott MP (1999) Control of neuronal precursor proliferation in the cerebellum by Sonic hedgehog. Neuron 22-103-114.

Whitlock K, and Westerfield M (2000) The olfactory placodes of the zebrafish form by convergence of cellular fields at the edge of the neural plate. Development 127:3645-3653.

Wilson SI, Graziano E, Harland R, Jessel TM, Edlunf T (2000) An early requirement for FGF signaling in the acquisition of neural cell fate in the chick embryo. Curr Biol 10:421-429.

Wilson SI, Rydstrom, A, Timborn T, Willert K, Nusse R, Jessel TM, Edlund T (2001) The status of Wnt signaling regulates neural and epidermal fates in the chick embryo. Nature 411:325-303.

Wilson SI, Edlund T (2001) Neural induction: toward a unifying mechanism. Nat Neurosci, 4 Supp. 1:1161-1168.

Wolda SL, Moody CJ, Moon RT (1993) Overlapping expression of Xwant-3A and Xwnt-1 in neural tissue of Xenopus laevis embryos. Dev Biol 155:46-57.

Xuan S, Baptista CA, Balas G, Tao W, Soares VC, Lai E (1995) Winged helix transcription factor BF-1 is essential for the development of the cerebral hemispheres. Neuron 14:1141-1152.

Yamashita T, Tucker KL, Barde YA (1999) Neurotrophin binding to the p75 receptor modulates Rho activity and axonal outgrowth. Neuron 24:585-593.

Ybot-Gonzalez P, Savery D, Gerrelli D, Signore M, Mitchell CE, Faux CH, Greene ND, Cropp AJ (2007) Convergent extension, planar cell polarity signaling and initiation of mouse neural tube closure. Development 134:789-799.

Ye W, Shimamura K, Rubenstein JL, Heynes MA, Rosenthal A (1998) FGF and Shh signals control dopaminergic and serotonergic cell fate in the anterior neural plate. Cell 93:755-766.

Yun K, Potter S, Rubenstein JL (2001) Gsh2 and Pax6 play complementary roles in dorsoventral patterning of the mammalian telencephalon. Development 128:193-205.

Zhang Q, Murcia NS, Chittenden LR, Richards WG, Michaud EJ, Woychik RP, Yoder BK (2003) Loss of the Tg737 protein results in skeletal patterning defects. Dev Dyn 227:78-90.

Zimmermann LB, De Jesus-Escobar JM, Harland RM (1996) The Spemann organizer signal noggin binds and inactivates bone morphogenetic protein 4. Cell 86:599-606.

Eidesstattliche Erklärung

Hiermit erkläre ich an Eides statt, dass ich die vorliegende Dissertation selbstständig und ohne unerlaubte Hilfsmittel durchgeführt habe.

Heidelberg, den _____

Marc Willaredt